GEMINI

8-M Telescopes Project

RPT-I-G0044

Preliminary Design for the Cassegrain Assembly

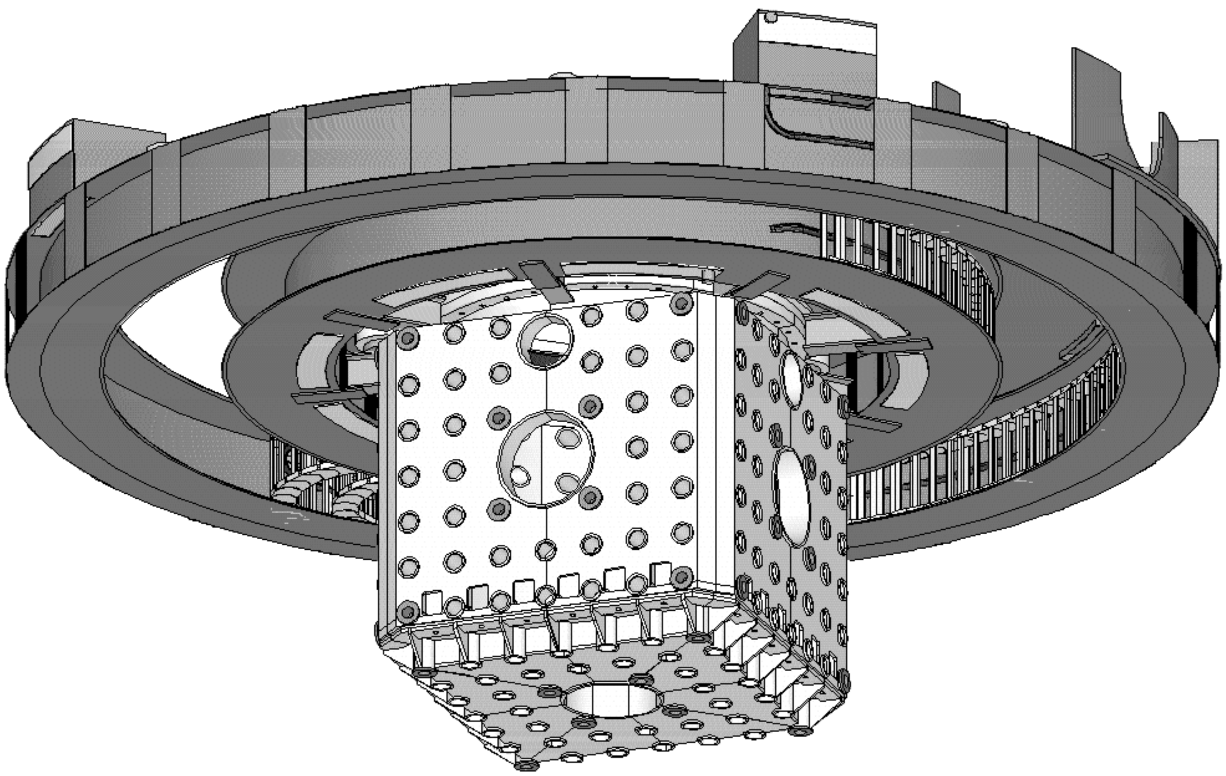

D. Montgomery, S. Wieland, D. Robertson
Instrumentation Group

6 June 1994

GEMINI PROJECT OFFICE 950 N. Cherry Ave. Tucson, Arizona 85719
Phone: (520) 318-8545 Fax: (520) 318-8590

TABLE OF CONTENTS

LIST OF FIGURES

LIST OF TABLES

1. INTRODUCTION

1.1 Introduction

The Gemini Project is an international collaboration to design, fabricate, assemble and commission two 8M telescopes, one on Mauna Kea in Hawaii, the other on Cerro Pachon in Chile. The telescopes will be International facilities designed to meet the Gemini Science Requirements, a document developed over the past 3 years by the Gemini Science Committee.

The Preliminary Design Review (PDR) for the Cassegrain cluster will be held in Tucson on June 15th and 16th 1994, and this document has been produced in support of this review.

The primary areas covered in this document are:

- Cassegrain Rotator
- Cassegrain Cable Wrap
- Instrument Support Structure

Other areas that are briefly covered are Instrument Handling, services for instruments and facilities (electrical. mechanical cryogenic, etc.), and Thermal Management.

Areas not covered in any detail except to show their relationship to the rest of the system are:

- Acquisition and Guiding System
- Adaptive Optics System
- Science Instruments

These will all be subject to their own separate reviews at various times during the project.

Following the PDR, work will continue on the detailed design of the Cassegrain Cluster Area leading to a Critical Design Review (CDR), presently scheduled for May 1995.

1.2 References

1. Gemini Science Requirements Document

2. Cassegrain Assembly Functional Requirements Document

3. Cassegrain Assembly Design Requirements Document

4. Preliminary Design Document

5. Gemini Systems Error Budget Plan

6. Instrument Interface Control Document, Draft Version, 1.0, S. Wieland, 25 March 1994.

7. Technical Report ”Primary Mirror Cell Deformation and Its Effect on Mirror Figure Assuming a 6 Zone Axial Defining System., RPT-O-G0030.

8. ANSI B4.2, 1978

9. ANSI-IT

10. BSS-436

11. Chironis

12. AGMA Standard 390-03

13. Kaydon, Inc. Large Bearing Selection Software

14. ANSI B4.1, 1967, R1979.

15. Telescope Enclosure Group Thermal Management Plan

16. Acquisition and Guidance Functional Specification.

2. CASSEGRAIN ASSEMBLY DESIGN DOCUMENTS

This chapter describes the various reference documents associated with this preliminary design report. They are listed in order of precedence, but all of the documents make some reference to the present Cassegrain area design. Figure 1 on page 103, shows the inter-relationships between the documents associated with Gemini subsystem designs.

2.1 Gemini Science Requirements Document

The Gemini Science Requirements Document was developed by the Gemini Project Scientist and the Gemini Science Committee. The current version is V2.0, dated 4 May, 1994. The purpose of this document is to establish the scientific priorities and requirements for the telescope systems.

2.2 Cassegrain Assembly Functional Requirements Document

This document has been developed by the Gemini Instrumentation Group and describes the functional requirements for the Cassegrain assembly consistent with the Gemini Science Requirements.

2.3 Cassegrain Assembly Design Requirements Document

This document, also developed by the Gemini Instrumentation Group, specifies the design requirements for the Cassegrain assembly design consistent with the Cassegrain assembly functional requirements document. It also establishes interface requirements with other major telescope systems and performance criteria consistent with the Gemini Error Budget Plan.

2.4 Preliminary Design Document

This document was developed by the Gemini Instrumentation Group as the preliminary design was developed. It describes the current preliminary design and illustrates how the design achieves the goals set out in the design requirements document. Furthermore, the preliminary design considers practical issues such as feasibility and cost.

2.5 Gemini Systems Error Budget Plan

This document was developed by the Gemini Systems Engineer. It apportions, in a top-down manner, errors to each of the telescope subsystems consistent with achieving the overall telescope performance goals stated in the Gemini Science Requirements document.

2.6 Instrumentation Interface Control Document

This document, developed by the Instrumentation Group, establishes the physical and functional interfaces for mounting instruments at the Cassegrain focus. It also contains requirements which instrument builders will be asked to comply with, but do not necessarily effect an instrument's scientific performance (e.g., use of closed cycle coolers). The document is currently in draft form.

3. CASSEGRAIN ASSEMBLY PRELIMINARY DESIGN

3.1 Description of Preliminary Design

The Cassegrain assembly consists of the Cassegrain rotator, Cassegrain cable wrap, and instrument support structure as shown in Figure 2 on page 104 and Figure 3 on page 105.

CASSEGRAIN ROTATOR. The design developed to meet the design requirements consists of an annular rotator mounted directly onto the bottom of the mirror cell. The upper surface of the rotator is static and forms the interface to the mirror cell, while the lower rotating surface forms the interface to the Instrument Support Structure. The rotator physically rotates the instrument support structure to position the field relative to the instruments and to track field rotation.

CASSEGRAIN CABLE WRAP. The cabling and services are connected through a cable / services wrap, which employs a rolling loop arrangement to allow a + 270 working rotation. The services are supported within flexible cable trunking which runs in two circular, concentric guide troughs. The inner guide trough is attached to the Cassegrain rotator, while the outer is static, fastened to the mirror cell. Break panels exist on the inner (rotating) guide trough above the side looking instruments and on extensions of the outer (static) guide trough which are re-entrant into the mirror cell.

INSTRUMENT SUPPORT STRUCTURE. The instrument support structure is cubic in shape, with a cylindrical flange which forms the interface to the rotator. The cube has five available planar faces, one upward looking and the remaining, sideward looking (telescope at zenith). These faces form the mechanical interfaces for instruments and the calibration and adaptive optics modules. There is a cylindrical cavity within the Instrument Support Structure which houses the science field fold mirror and associated articulating mechanisms used to fold the science beam out to any of the side looking instruments. The guidance and wavefront sensor assemblies are also located within the cylinder. Access is gained to the interior of the cube by removing the base. All of the side looking instrument support structure faces have a second port above the science beam port which is primarily used to feed the Adaptive Optics System. The return beam from the AO system uses the science field port and is directed to the instrument of choice by the science field fold mirror.

3.2 Meeting the Design Requirements

This section will describe how the design of the Cassegrain Assembly meets the interface and performance requirements specified in the Design Requirements Document. Tables are presented showing the overall performance in terms of mass moment, heat balance, pointing, tracking and image quality. The derivation of the figures in the tables is explained in more detail in the relevant sections.

3.2.1 Interface Requirements

This section will mirror the interface requirements laid out in the Design Requirements Document.

NOMINAL TELESCOPE TUBE BALANCE. Table 3 - 1 shows the mass and mass moment balance table for the telescope tube about the elevation axis in the z direction. In the table, the figure for the Cassegrain area is apportioned among the Cassegrain subsystems. The Cassegrain area refers to all of the subsystems which are the responsibility of the Gemini Instrumentation Group (i.e., instruments, acquisition and guidance, adaptive optics, and facility calibration). As the preliminary design is developed, the masses and mass moments of components will be compared with this allocation and conflicts resolved by design optimization. The mass and mass balance estimates for the current design exceed the requirements by <15 and 10%, respectively. Further optimization of the ISS cable wrap and rotator structure is required to meet the target budget. All efforts will be made to ensure that the present target masses for the instruments are maintained.

In Table 3 - 1, the column labeled "Balance Tolerance Addressed by Fixed Weights" assigns an allowable tolerance range for the mass and mass moment to the elements which are semi-permanent, i.e., Cassegrain rotator, cable wrap, ISS, and A&G Modules. This tolerance will determine the accuracy with which the mass and center of gravity of these elements have to be maintained prior to assembly on the telescope. A figure of 10% of the mass moment has been assumed. The residual out of balance will be trimmed as a one time balancing operation for the telescope tube by attaching or removing trim weights.

In the table, the column tabled "Balance Tolerance Addressed by Tube Balancing System" assigns an allowable tolerance range for the mass and mass moment to the elements which are reconfigurable (instruments). This tolerance will determine the accuracy with which the mass and center of gravity of these elements have to be maintained prior to assembly on the telescope. The tolerance assumed is 1 % of the mass moment after servicing or configuration.

BALANCE TOLERANCE DURING OPERATION. The nominal telescope tube balance will be achieved by changing fixed weights on the telescope tube and by the telescope tube balancing system. During operation, the mass distribution of elements within the Cassegrain area will change. They will change because of eccentricities of the c of g (displacements in x and y from the rotator axis) of rotating components w.r.t. the elevation axis, because of c of g changes during rotation, and because of moving elements within the modules. This change in balance will not be compensated for and must be within the capacity of the telescope tube drives. This figure has been set at 1000 Nm by the Gemini Telescope Group. Table 3 -2 shows the allowable out-of-balance apportioned to the individual subassemblies, consistent with this figure. As the design is developed, the out-of-balance terms will be compared with this allocation and any conflicts resolved.

SPACE ENVELOPE. Figure 4 on page 106 shows the current Cassegrain assembly within the available space envelope defined by the telescope structure and mirror cell. The dotted line represents a cylindrical volume with a domed end, available for instrumentation.

TABLE 3-1: Telescope Tube Balance

Item	Mass (tonnes)	C of G z-Distance from elevation axis (meters)	Nominal Mass Moment with respect to elevation axis (tonne meters)	Balance Tolerance Addressed by Fixed Weights (tonne meters)	Balance Tolerance Addressed by Tube Balancing System (tonne meters)
Main Truss[a]	9.253	5.4	49.653		
f/16 Top End[a]	6.783	13.8	93.416		
Center Section[a]	51.801	-0.06	-28975		
Mirror Cell Support Frame[a]	23.490	-1.7	-39.557		
Primary Mirror and Cell[a]	69.250	-0.5	-33.991		
Cassegrain Area[a]	13000	-3.1	-40.547		
Total	173.576	0	0		
Cassegrain Rotator	1.66	1.89	3.14	0.314	
Cable Wrap	1.2	2.1	2.41	0.241	
Instrument Support Structure	3.8	2.85	10.83	1.083	
Flip Mirror Assembly	0.3	3.25	0.98	0.098	
A&G/WFS Unit	0.25	2.32	0.58	0.058	
Total (rss)				1.11	
Mounting Face Loads					
Port 1	2	4.65	9.3		0.093
Port 2	2	2.85	5.7		0.057
Port 3 (facility)	0.8	2.85	2.28		0.023
Port 4	2	2.85	5.7		0.057
Port 5 (facility)	0.8	2.85	2.28		0.023
Total	14.8		43.3		0.127

[a] From ICD G 0001, Revision A, 2 Feb 1994

THERMAL MANAGEMENT. Table 3 -3 shows the allocation of allowable power dissipation (into the enclosed air). In this table, the figure for the Cassegrain area is apportioned among the Cassegrain area subsystems. As the designs for the respective subsystems are developed, the power dissipation from the components will be compared with this allocation and any conflicts resolved.

TABLE 3-2: Balance Tolerance During Operation

Item	Allowable Out-of-Balance Change (tonne meters [Nm])
CABLE WRAP	
Cable Wrap Structure	0.0042 [42]
Cable Chains and Services	0.06 [600]
ISS STRUCTURE	0.019 [190]
ROTATOR STRUCTURE	0.001 [10]
A&G	
Peripheral Guide Probes / WFS	0.005 [50]
AO Fold Mirror	0.005 [50]
Science Fold Mirror	0.01 [100]
Filters/Polarizers	0.005 [50]
High Order WFS	0.001 [10]
A&G Structure	0.001 [10]
INSTRUMENTS	
Side Looking Instruments (4)	0.0305 [305]
Upward Looking Instrument	0.01 [100]
Moving Elements In Instruments	0.00224[a] [22.4]
TOTAL (RSS)	**0.0721 [721]**
Allowable Apportioned to Cass Area	0.1 [1000]

[a] rss for 5 'instruments', each with 10 Nm allowable out of balance allocated for moving elements.

Further requirements for thermal management arise from considerations of thermal stability of the mirror cell. In the technical report, 'Primary Mirror Cell Deformation and Its Effect on Mirror Figure Assuming a Six-zone Axial Defining System,' RPT-O-G0030, produced by the Gemini Optics Group, two effects from the Cassegrain instruments are considered. These are heat input to the mirror cell in the vicinity of the rotator bearing (50 Watts) and heat generated within the mirror cell structure due to rotator electronics (30 Watts). The analysis estimates the transient deformations when these heat loads are applied.

In the preliminary design, the rotator motors are actively cooled by recirculating coolant within the motor mount subplate. This removes the majority of the heat generated by the motors. The residual is dissipated as a conductive load into the mirror cell structure or convected within the mirror cell cavity (the motors are largely reentrant into the mirror cell). With the motors at rated power, the conductive steady state heat load is estimated to be 8 Watts and the steady state convected heat load is estimated to be 0.16 Watts. The conductive heat load from the motors raise the temperature of the mirror bore in the vicinity of the motors by 0.2 C. The analysis carried out by the optics group indicates that the deformations induced in the mirror cell due to this are acceptable. The steady state convective heat load within the mirror cell is negligible.

CABLE / SERVICES ROUTING. Figure S on page 107 shows the route for Cassegrain cables and services through the primary mirror cell, including a suitable interface to this routing system.

TELESCOPE FOCUS. As specified by the Gemini Optics Group, the telescope focus is 4 meters behind the primary mirror vertex and 2.5 meters behind the mirror cell.

3.2.2 Performance Requirements

In the Gemini Systems Error Budget Plan, various engineering performance requirements have been allocated in a top-down error budget consistent with achieving telescope systems performance specified in the Gemini Science Requirements Document. The following sections will describe these performance requirements and how the Cassegrain assembly meets them. A more detailed explanation as to the derivation of the errors is given in later sections relevant to the component or subsystem. These performance requirements are for the IR-optimized (direct feed instrument) mode. For the non-IR-optimized mode (side looking instrument), there will be the additional effects caused by the folding flat and supporting structures. These effects have not yet been investigated, but the goal will be that they only marginally degrade the performance.

POINTING. Table 3 -5 shows the bottom-up pointing errors attributed to the Cassegrain cluster developed for the preliminary design. The last entry shows the requirements from the systems error budget plan, for comparison.

The geometric and flexural inaccuracies are translated into pointing errors by converting them to shifts of a hypothetical focal plane array. The plate scale of 620 1lm/arcsecond is used to convert translations in x and y into arcseconds on the sky. No other compensation of (or errors due to) the telescope optics or drives are taken into consideration.

Similar assumptions are made for the tracking performance table.

TRACKING. Table 3-6 shows the bottom-up tracking errors developed for the preliminary design. The last column shows the requirements from the systems error budget plan, for comparison.

TABLE 3-3: Nighttime Operational Power Dissipation Into Enclosure

Source	Power (kW)
Telescope Azimuth and Altitude Drives	4.0
Shutter Drives	0.0
Enclosure Drives	0.0
Telescope Control System Electronics (Bus Crates)	2.5
Instrumentation Allocation (Continuous Heat Sources)	2.0
Total	8.5

TABLE 3-4: Heat Output Estimate for Cassegrain

Source	Heat Generated (kW)	Heat Removal Method	Residual (kW)	Comments
Rotator Drive Electronic	2 (2 cabinets)	Air/Liquid Cooled Enclosure	0.1	Cabinets located on centre section
Rotator motors	0.124 (4 cabinets, rated output	Liquid cooled motor subplate	0.01	Residual dissipates into rotator structure / mirror cell
Bearing and Drive Friction	0.26 (at rate of 25 arcsec / sec)	Passive Dissipation	n/a	Dissipate into rotator structure
Guidance / WFS / Fold Mirror Electronics	1	Air/Liquid Cooled Enclosure	0.05	Cabinets mounted outside ISS
Guidance / WFS / Fold Mirror Mechanisms	0.05	Passive Dissipation into ISS/Cell Cavity	0.05	This is a goal for the A&G modules
Instrument / Calibration / AO / Electronics	5 (1 per instrument)	Air/Liquid Cooled Enclosure	0.250	Cabinets mounted with units
ISS ΔT	0.03	Passive Dissipation into ISS / Cell Cavity	0.03	ΔT assumed to be 1^{o}C
Heat Leakage from coolant return lines	0.041	n/a	0.041	
Total			0.53	

TABLE 3-5: Predicted Effects on Pointing Performance (Bottom-Up Error Budget Pointing)

Effect	Displacement / Tilt	Movement on Sky (f/16) - Uncorrected (arcsec)	Movement on Sky (f/16) - Residual (after pointing model correction) (arcsec)
Bearing clearance to rotator ring	50 µm	0.08	0.001 [a]
Rotator ring wedge	32 µ rad 61 µm at focus	0.098	0.0098 [a]
Rotator/ISS interface tolerance	101.6 µm	0.164	0.00164 [a]
ISS port eccentricity relative to rotator interface	50 µm	0.08	0.0008 [a]
Instrument Mount Tolerance	41 µm	0.066	0.00066 [a]
ISS Base Locating Tolerance	101.6 µm	0.164	0.00164
Geometric tolerance totals (rss)	176 µm	0.284	0.00284
Radial bearing runout	25 µm	0.04	0.008 [b]
Axial bearing runout	25 µm	defocus	defocus
Bearing tilt runout	25 µm at bearing radius, 67 µm at focus	0.1	0.02 [b]
Runout error totals (rss)	68 µm	0.108 (arscec on sky)	0.022 (arcsec on sky)
Lateral mirror cell to ISS interface flexure	10 µm	0.016	0.001 [c]
Mirror cell to ISS interface tilt flexure	13.3 µrad 26.6 µm at focus	0.043	0.0021 [c]
Bearing radial flexure	17.3 µm	0.028	0.001
Bearing tilt flexure	23.3 µrad 64.5 µm at focus	0.104	0.005
ISS lateral flexure	50 µm	0.081	0.004 [c]
ISS tilt flexure	10 µrad	0.000	0.000
Flexure error totals (additive)	168.5 µm	0.27	0.013
Total Cassegrain cluster f/16 pointing errors (rss)			0.026 arcsec
Systems Error Budget			1.39 arcseconds

a. Assumes pointing model corrects to 1%
b. Non-repeatable component of radial and axial runout assumed to be 15 µm
c. Flexural hysteresis assumed to be 5%

TABLE 3-6: Predicted Tracking Performance (Bottom-Up Tracking Error Budget)

Effect	Image Displacement / Rotation at Focal Plane	Movement on Sky - Uncorrected (arcsec)	Movement on Sky - Corrected (arcsec)
Encoder drive-train errors	159 μrad	0.057	0.001[a]
Servo system error	25 μrad	0.009	0.009
Total Drive Servo Rate Error (rss)			0.009
Calibration WFS module housing	8 μm[b]		
Fold mirror housing	4 μm		
Guide probe position flexure (relative to module interface)	4 μm		
Total guide probe position flexure (cumulative)	16 μm	0.026	0.005
Total Cassegrain guide tracking error (rss)			0.001[c]
Systems Error Budget			xxx

a. Encoder drive train errors are composite gear errors derived from AGMA standards. These errors are repeatable and can be linearized to 1%.
b. Flexure is referred to the guide probe position, i.e., includes the effects of tilts
c. This assumes that as pointing map can reduce this error by 5%

IMAGE QUALITY. Image quality is affected by the Cassegrain assembly through its contribution to telescope enclosure seeing, telescope seeing, and tracking effects. The contributions to enclosure seeing effects are dealt with in the interface requirements for the telescope enclosure and tracking effects are dealt with above. Table 3-7 shows the contribution of the Cassegrain area elements to the telescope thermal seeing. The derivation for the figures in the table are detailed in the section on Thermal Management (Chapter 12).

TABLE 3-7: Cassegrain Area Contributions to Thermal Seeing

Item	Heat convected into cavity (w)	Comment
Rotator Bearing (tracking speeds)	0	
Rotator Motors (rated load)	1.2	Local heating of cell
A&G Assembly	50	Design goal for A&G
Mirror Cell Structure ($\Delta T = 1^oC$)	34	Unconditioned cell
ISS Structure ($\Delta T = 1^oC$)	33	Unconditioned structure
Total	118	
Contribution to Thermal Seeing	0.004 arcseconds[a]	
Systems Error Budget (ISS ΔT)	0.015 arcseconds	

a. see Thermal Conditioning chapter. Effect on Image Quality

EMISSIVITY. From the GSRD, the requirement for the overall telescope emissivity is 4%, with a goal of 2%. Of this, the contribution from the Cassegrain area falls under the heading of "all other sources" which is apportioned 0.05%. The Cassegrain assembly preliminary design does not allow shadowing and vignetting of the science beam under any operational circumstances.

THROUGHPUT. In the Gemini Science Requirements, the throughput goals are defined for optical and IR configurations. These are considered separately below.

1. Optical. The optical throughput goals are not explicitly stated for the telescope system, but rather in terms of the performance of coatings and surfaces. In the optimized mode, with a direct beam feed, the Cassegrain assembly does not effect throughput.

2. IR. The throughput requirement is defined as 91% with 93% as the goal. In the direct feed mode the Cassegrain assembly has no effect on the throughout performance.

3.3 Instrument Support

Instruments will be rigidly attached to the instrument support structure. They can be configured in a variety of ways. There are five identical mechanical interfaces available. Up to three instruments can be mounted simultaneously in addition to the AO module and calibration module. This scheme allows the Cassegrain to be reconfigured with any instrument occupying the optimized (straight through mode) upward looking port. When configured, the telescope beam can be rapidly directed to any instrument by means of an automatically deployable steering mirror within the ISS. This fulfills a versatility goal of rapid instrument change as part of a scheduled observing run or in the event of rapid change of atmospheric conditions or instrument failure. The mounting scheme for instruments provides a standard mechanical interface which can be utilized by instruments of various sizes and configurations. Visitor instruments can be equipped with mechanical and electrical interface adapters to the standard interface.

3.4 Acquisition & Guidance Wavefront Sensing and Science Fold Mirror Support

These functions will be carried out by modules located within the Instrument Support Structure. They will also have the function of directing the telescope beam into the Adaptive Optics Module or alternately, into the science instruments. Two peripheral guiders / low resolution wavefront sensors will be provided within the A&G module. These can be positioned independently within the telescope guide field and have the capability of reaching the science field center for calibration purposes. A calibration high resolution wavefront sensor will be supplied for calibrating the primary mirror support system. The current preliminary design splits these functions among three modules, namely, the peripheral guider / low resolution wavefront sensor module, science fold mirror module, and the high resolution wavefront sensor module. These units occupy the space within the ISS and are mounted off the ISS base.

3.5 Adaptive Optics Support

The adaptive optics module can be attached to any side looking port but it is assigned to a 'facility port' with an 800kg payload. When in use, the AO feed mirror is deployed (within the peripheral guider module) and oriented to direct the telescope beam into the AO module. The corrected beam is fed back into the science port on the face where the AO unit is attached and directed to the required instrument by the science fold mirror located within the science fold mirror module. The deployment of the AO feed mirror will render one of the peripheral guiders inactive.

As the AO port is attached to a side looking port, it has the same mechanical and services interface as an instrument. The adaptive optics module can be rapidly switched in and out of the telescope beam and the corrected science beam can be rapidly directed to any instrument port.

3.6 Facility Calibration Support

The facility calibration will be supplied by a modular unit located on a 'facility' side looking port The mechanical and services interface are identical to a science instrument port, but with an allowable payload of 800 kg (See Table 3 -1). The articulated science fold mirror can direct the calibration source located at any port towards any other port.

3. 6.1 Instruments with Calibration Units

Instruments may have their own calibration units, particularly IR instruments. The ISS structure is sized such that the telescope focus is 300 mm beyond the mechanical interface. This space can accommodate a calibration beam feed from an instrument-mounted calibration unit. This space may also be utilized for baffling arrangements in the IR instruments if required.

4. *CASSEGRAIN ROTATOR*

This chapter describes the preliminary design of the Cassegrain rotator and how it meets the design requirements. The practical considerations of implementing the design are also discussed, where applicable.

4.1 Description of Preliminary Design

The Cassegrain rotator is an annular assembly consisting of an upper fixed ring which fastens onto the mirror cell mechanical interface, a large diameter crossed roller bearing, and a lower rotating ring which fastens onto the instrument support structure mechanical interface. The upper ring has locations for four motor assemblies which are servomotors coupled to planocentric speed reducers. Helical spur gear pinions are attached to the output shafts of the speed reducers. These drive a large ring gear attached to the lower, rotating ring. The pinions are spaced at 90º intervals and drive in opposing pairs to eliminate backlash, and preload the drive trains. The motors are recessed into clearance holes in the lower mirror cell surface, and the drive electronics are located on the telescope center section. This is shown in Figure 11 on page 113, Figure 13 on page 115, and Figure 14 on page 116.

On the upper fixed ring there are four locations for gear driven rotary encoders and one location for a gear driven multi- turn absolute encoder. These use anti-backlash pinions running on the ring gear. The lower ring has provision for an inductance tape encoder, should this be required. An electrically operated brake is supplied for safe parking of the rotator and for use during emergency stops. This brake operates on a normally free running pinion driven by the ring gear.

Mechanical end stops are provided to protect the cable wrap from overrun of the rotator. These are linear hydraulic bumpers, one for clockwise and one for the anti-clockwise direction.

4.2 Meeting the Design Requirements

This section will describe how the overall design of the Cassegrain rotator meets the design requirements.

4.2.1 Operational Range

The design of the rotator will allow continuous rotation in either direction. The limit to its range is determined by the range of the Cassegrain cable wrap and the absolute encoder. The normal operating range is ± 270º.

4.2.2 Maximum Feasible Range

A safe margin is allowed at each end of travel to allow the overrun limit switches and mechanical endswitches to operate. Extra travel is also required to allow for some misalignment of the cable wrap. The maximum range is ± 280 degrees.

4.2.3 Overrun Limit Switches and Mechanical Endstops

The rotator design has two overrun mechanical endstops, one for clockwise and one for anti-clockwise motion. These are progressive action hydraulic bumpers capable of safely stopping the fully laden rotator at maximum speed, with the motors running. The details of these mechanisms are described later when subassemblies of the rotator are described. They also supply an error signal prior to the engagement of the mechanical stop. The error signal will activate the rotator brake.

4.2.4 Zero Angle Definition and Sense of Rotation

When the telescope is parked facing east, the zero rotation angle is along the x-axis of the telescope coordinate system. Looking from the secondary to the primary, the rotation sense is clockwise positive. See Figure 12 on page 114.

4.2.5 Absolute Rotator Position

An absolute encoder in conjunction with several proximity switches will define a number of absolute reference datums. The number of these datums will depend on the maximum allowable time allowed for absolute re-datuming after an unscheduled power outage.

4.2.6 Design Loads and Service Factors

The bearing within the rotator has sufficient capacity for the expected loads with a safety factor greater than 5 times the capacity of static loading. The drive system has been designed to exceed the requirements in rotational inertia by a factor exceeding 5. The drive motor selection uses a service factor of 3 over the maximum calculated load torque to determine the continuous torque rating of the motor. Peak torque for the motor can exceed the continuous value by 50%.

4.2.7 Slew Rates and Tracking Rates

The drive unit specification requires a maximum allowable slew rate of 2º per second in either direction. The current design provides a slew speed of 0.9º per sec. Further investigations with the manufacturer of the motors and the speed reducers are expected to yield an increase in slewing speed which will meet the requirements. The encoding and servo system allow tracking rates to vary continuously from -0.5 degrees per second to +0.5 degrees per second during operation.

4.2.8 Overall Dimensions

The Cassegrain rotator assembly has overall dimensions of 1450 mm ID, 1750 mm OD, and 500 mm depth. The depth includes 200 mm for the rotator drive units which protrude 200 mm into the mirror cell.

4.3 Performance Estimate

This section outlines the performance estimate for the Cassegrain rotator assembly. Bottom up estimates are made for geometric accuracy, rotational accuracy, rigidity, mass and mass moment w.r.t. the telescope tube elevation axis.

4.3.1 Geometric Accuracy

Table 4 -1 shows the combined effects of geometric errors of the individual components of the Cass rotator on the accuracy of rotation. Errors are expressed in terms of decenter, piston and tilt.

TABLE 4-1: Geometric Accuracy

Component	Feature	Error Description	Value	Effect on Positional Accuracy of Component Attached to Rotator
Rotator Top Ring	Any	--	--	Top ring dimensional tolerances have no effect on accuracy as rotator axis defines telescope optical axis
Bearing	Bearing Radial Runout	Eccentricity	25 µm	25 µm radial excursion
	Bearing Axial Runout	Tilt (Runout / Bearing Radius)	32 µrad	tilt of 32 µrad and decenter. Decenter = tilt x (distance from rotator interface + 125 mm)
		Piston	25 µm	25 µm piston
	Bearing Pilot Diameter Eccentricity	Decenter	50 µm	50 µm decenter
Rotator Lower Ring	Bearing Location Diameter Clearance	Decenter	50 µm	50 µm decenter
	ISS Locating Diameter Clearance	Decenter	63 µm	63 µm decenter
	ISS Locating Diameter Eccentricity (Relative to bearing locating diameter)	Decenter	50 µm	50 µm decenter
	Wedge	Tilt	32 µrad	tilt of 32 µrad and decenter. Decenter = tilt x (distance from rotator interface + 43 mm)
Total (Rotator Interface, rss)				110 µm decenter, 25 µm piston, and 45.2 µrad tilt

4.3.2 Rotational Accuracy

The rotational accuracy is affected by many parameters including gear accuracy, gear noise, encoder resolution, friction, etc. All of these parameters are considered in the Cassegrain rotator servo system model. At this time, coarse estimates for these effects have been made and are included in the model. The results indicate that the performance is within 0.009 arcsec as specified for the rotator.

4.3.3 Mass

Table 4 -2 shows the mass and mass moment of the rotator based on the individual components. The mass of the rotator assembly, as presently shown, is in excess of our original mass budget requirement. This will be resolved in the critical design phase as part of the optimization of the Cassegrain area. Components will be lightweighted and the mass and mass moment for the Cassegrain area can be re-allocated among the other Cassegrain elements, consistent with performance goals.

TABLE 4-2: Rotator Components Masses and Mass Moments

Item	Mass (kg)	c of g Position w.r.t. Elevation Axis (-z, TTCS[a]) (m)	Mass Moment (kg-m)
Upper Fixed Ring	450	1.824	820.8
Motors	5.5 x 4	1.750	38.50
Encoders	(3.5 + 2.5) x 5	1.937	58.11
Speed Reducers	28 x 4	1.940	217.28
Motor Mount	2.7 x 4	1.720	15.57
Brakes	15.0	1.747	26.20
Pinions	5 x 6	2.00	60.00
Endstops	10 x 2	1.938	38.76
Bearing	450	1.941	873.45
Lower Rotating Ring	340	2.027	689.18
Ring Gear	150	2.001	300.15
Total	1658.0		3138.0

a. Telescope Tube Coordinate System

4.4 Description of Rotator Bearing

The bearing type selected is an internally preloaded crossed roller bearing with a nominal raceway diameter of 1.58 meters. This type of bearing is capable of handling combined thrust, radial, and moment loading. They can also be supplied with integral mounting holes for fasteners and locating pilot diameters on the rotating and non-rotating parts.

4.4.1 Bearing Dimensions

The bearing has an inner diameter of 1440 mm, outer diameter of 1724 mm, and is 101.6 mm deep. This size is matched to the dimensions of the instrument support structure for efficient coupling of structural loads. The bearing size will be specified to order, as this type of bearing is manufactured on a custom basis.

4.4.2 Service and Allowable Loads

During service, the bearing will see radial and thrust loads of approximately 12 tonnes and moment loads of 12 tonne meters in differing proportions depending upon telescope tube attitude. The static capacity of this type of bearing is quoted as thrust loads of 1300 tonnes, radial loads of 100 tonnes and moment loads of 380 tonne meters, satisfying the static load requirements with the service factor.

4.4.3 Bearing Preload

The bearing will be preloaded to eliminate internal clearance and increase rigidity. This preload will be sufficient to prevent unloading of the bearing elements under all operating conditions. The preload is determined by the manufacturer based on the service loads, accuracy and stiffness requirements. Increasing the preload will increase the bearing stiffness but incurs a penalty in bearing friction.

4.4.4 Rigidity

The bearing rigidity is largely determined by setting the preload. The bearing considered has the following properties:

1. Axial Stiffness = 1.38×10^{10} N/m
2. Radial Stiffness = 7.23×10^{9} N/m
3. Moment Stiffness = 4.31×10^{9} Nm/rad

These figures are estimates and are subject to varying preload and loads acting on the bearing (the stiffness is not linear over large load ranges).

4.4.5 Accuracy

These bearings can be made in precision grades with minimum quoted runouts between 5 and 25 µm depending on configuration and grade. For the development of the bottom up error budget, a conservative estimate of 25 µm is assumed which is split up, again conservatively, into 10 µm non-repeatable and 15 µm repeatable.

The run-out figures stated by the manufacturer are axial and radial. Radial run-out causes a rotational position dependent decenter (for the repeatable part). Axial run-out causes a rotational position dependent tilt (for the repeatable part) in addition to a rotational position dependent piston along the rotation axis. The tilt is determined by dividing the runout by the bearing radius. The non-repeatable components of these errors will, in effect, act like noise and will not be dependent on rotation angle.

For input into the bottom-up error budget, the effects of these errors must be translated to the focal plane. Decenters and pistons are mapped directly.

For a radial run-out of 25 µm, the shift in the focal plane will be 25 µm.

Tilts will cause additional decenters. The decenter at the focal plane caused by bearing tilt is obtained as follows:

$$D = \text{tilt} \times d = \frac{ro_a}{r_b} \times d \qquad \text{(EQ 4 - 1)}$$

where: D is the decenter at the focal plane in mm, tilt is the bearing tilt in radians (found by dividing axial run-out by the bearing radius), d is the distance from the focal plane to the plane of the bearing rotation in mm, ro_a *is the axial run-out, and* r_b *is the bearing radius.*

For an axial run-out of 25 µm at the bearing edge, a bearing radius of 750 mm and a distance from the bearing to the focal plane of 2000 mm: decenter = 0.067 mm. This figure is used in the bottom-up error budget.

4.4.6 Friction

The bearing will exhibit significant friction which will consist of a nominally constant component due to the internal preload and seal drag and also a varying component due to the changing ratios of thrust, radial and moment loads (these are dependent on the telescope tube altitude).

The estimated bearing friction due to internal preload (from the bearing manufacturer) is 350 ft lbs (520Nm). Seal drag is estimated to be 65 ft lbs (96Nm).

Load dependent friction is given by the following equation (from the bearing manufacturer)

$$\Gamma = \frac{\mu(4.4M + AD + 2.2RD)}{2} \qquad \text{(EQ 4 - 2)}$$

where: Γ *=torque (ft lb); M = moment load (ft lb); A = thrust (lb); R = radial load (lb); D = raceway diameter (ft); Coefficient of friction (*μ*) is 0.003 for three-row roller and 0.004 for other types.*

Substituting values in the above equation for zenith and horizon pointing yields friction of 298 ft lb (442 Nm) and 1412 ft lb (2095 Nm), respectively.

In addition to the nominal friction characteristics, the bearing will exhibit nonlinear friction effects at slow speed and on direction reversal. These effects are included in the servo control model.

Heat generated due to friction. Heat will be generated in overcoming the bearing friction, it will vary with the telescope tube altitude and rotation rate. The worst case is for slewing during horizon pointing which will generate heat according to the relationship:

$$Q_f = \omega\Gamma \qquad \text{(EQ 4 - 3)}$$

where ω is the rotator speed in rad/sec and Γ is the friction torque.

For w = 2º / second (0.0349 rad/sec), Q_f = 73 watts. This will be a transient heat load, lasting at most for 30 seconds. Under tracking conditions which may persist for much longer, the typical heat generated will be fractions of a watt.

4.4.7 Mass

The estimated mass of the Cassegrain rotator bearing is 450 kg.

4.4.8 Lubrication

The bearing manufacturer will recommend the type of lubricant given the operating loads and ambient conditions. This specification will include operating temperatures ranging from room temperature to expected conditions at the telescope sites (25 ºC to - 10 ºC). A remote lubrication line will be supplied within the mirror cell to allow an operator to lubricate the bearing in safety (the bearing must be rotated during lubrication).

4.4.9 Material

Consistent with the loads and performance requirements, the bearing steel should match, as closely as possible, the CTE for the rotator structure (8.3 x 10-6 / ºC).

4.5 Description of Rotator Structural Components

The structure of the rotator consists of an upper, fixed ring and a lower rotating ring, with the bearing sandwiched in between. The material will be steel. The alloy used will have a matching CTE with the mirror cell structure constructed from ASME A-36, CTE 8.3 x 10^{-6} / ºC. The components are machined from solid.

4.5.1 Upper Fixed Ring

The fixed ring acts as the bearing housing and is sandwiched between the mirror cell and the bearing. The upper surface has a locating spigot diameter for registration on the mirror cell and an annular land for the interface. A pitch circle diameter of clearance holes allows the fastening bolts to go through, from the mirror cell to the bearing. The fixed ring has four locations, nominally 90º apart for mounting the motor drive units and four similar mounting points for the rotary encoder units. Two additional mounting points are supplied for mounting a brake and a multi-turn absolute encoder. A locating diameter and land is provided for the bearing outer race.

4.5.1.1 Dimensional Accuracy

FLATNESS The bearing places requirements on this component of initial flatness and out-of-flatness deformation. This, in turn, sets the requirement on the flatness of the upper and lower surfaces which contact the mirror cell and bearing, respectively. The allowable tolerance for initial flatness is shared between these surfaces and the mirror cell interface. These surfaces are given 25% of the tolerance, the remaining 75% is apportioned to the mirror cell interface. The bearing requirements are 0.127 mm per 25 mm for radial flatness (dishing) and 0.038 mm per 90º segment for circumferential flatness (waviness). Thus, the radial flatness must be 0.022 mm per 25 mm or better and the circumferential flatness of these surfaces must be 0.0067 mm per 90º segment or better. This tolerance is achievable for a component of this size.

Out-of-flatness deformation is negligible for this component.

WEDGE The wedge between the top and bottom surfaces will tilt the Cassegrain assembly. It is, therefore, desirable to keep the parallelism within a reasonable tolerance. As the axis of the Cassegrain rotator defines the optical axis of the telescope, this tolerance will not effect the pointing other than a one time alignment of the telescope optics axis.

ECCENTRICITY The eccentricity of the locating diameter relative to the bearing location diameter will cause a decenter of the Cassegrain assembly. It is, therefore, desirable to keep the eccentricity within a reasonable tolerance. As the axis of the Cassegrain rotator defines the optical axis of the telescope, this tolerance will not effect the pointing. Other than a set up calibration, the initial alignment of the telescope optics will compensate for this error.

MIRROR CELL LOCATING DIAMETER The locating spigot diameter on the upper ring is 1774 mm with an H7h6 locating clearance fit (ANSI B4.2 - 1978). The tolerance width is +0.0, -0.102 mm.

BEARING LOCATING DIAMETER The bearing location diameter is 1724 mm. The recommended tolerance for the bearing locating diameter from the manufacturer is -0.0 +0.051 mm. This tolerance is on the limit for a turned component of this size according to ANSI IT number designation. This indicates that grinding may be required but this can be discussed with the manufacturer.

DRIVE UNIT LOCATIONS Center distance is 1005.8 mm ± 0.1 mm. The appropriate backlash allowance will ensure that there is no binding of the gears at the tightest position. This is commonly done by thinning the gear teeth, but the method used will be discussed with the manufacturer.

4.5.1.2 Mass Estimate

The rotator upper ring structure is solid steel. The mass is estimated at 450 kg.

4.5.2 Lower Rotating Ring

The lower ring has a locating diameter for the bearing inner and an annular land which acts as the bearing interface. 36 ϕ 19 clearance bolt holes allow fasteners to go through, from the instrument support structure to the bearing inner. Additional fasteners are supplied to hold the lower ring onto the bearing when the ISS is removed. The lower surface of the ring has a locating diameter for the instrument support structure and a flat annular area for the interface. Locating diameters and lands are also provided for the large ring gear with fastening detail of 36 M8 tapped holes on a 1644 PCD. A flange is provided for the cable wrap rotating cable chain guide mounting brackets. Provision is made for the addition of a track suitable for mounting an inductance tape encoder.

4.5.2.1 Dimensional Accuracy

FLATNESS. The bearing places requirements of initial flatness and out-of-flatness deformation on this component. This puts a requirement on the flatness of the upper and lower surfaces which contact the mirror cell and bearing, respectively. The allowable tolerance for initial flatness is shared between these surfaces and the mirror cell interface. These surfaces are given 25% of the tolerance, the balance is apportioned to the mirror cell interface. The bearing requirements are 0.127 mm per 25 mm for radial flatness (dishing) and 0.038 mm per 90º segment for circumferential flatness (waviness). Thus, the radial flatness must be 0.022 mm per 25 mm or better and the circumferential flatness of these surfaces must be 0.0067 mm per 90º segment or better. This tolerance is achievable for a component of this size. Out-of-flatness deformation will be negligible for this component.

WEDGE. The wedge between the top and bottom surfaces will tilt the Cassegrain assembly relative to the established rotation plane. This causes a shift of the instrument relative to the telescope focal plane and will effect the pointing. A reasonably achievable tolerance of 32 µradians is assumed for the bottom-up error table.

ECCENTRICITY. The eccentricity of the locating diameter relative to the bearing location diameter will cause a decenter of the Cassegrain assembly relative to the established rotation axis and will, therefore, effect the pointing. A reasonably achievable tolerance of 50 µm is assumed for the bottom-up error table.

INSTRUMENT SUPPORT STRUCTURE LOCATING DIAMETER. The locating diameter on the lower for the ISS spigot is 1394 mm with an H7h6 locating clearance fit (ANSI B4.2 - 1978). The tolerance width is -0.0 +0.127mm.

BEARING LOCATING DIAMETER. The bearing location diameter is 1440 mm. The recommended tolerance for the bearing locating diameter from the manufacturer is - 0.0 + 0.051 mm. See comments on this feature for the upper ring.

RING GEAR LOCATING DIAMETER. The ring gear locating diameter is a 1604 mm H7h6 fit. The locating land must have parallelism with the bearing surface and speed reducer locating surfaces of ± 0.012 mm. (That is, all points must fall within two parallel planes positioned 0.012 mm each side of the nominal.)

4.5.2.2 Mass Estimate

The lower rotating ring of the bearing is solid steel. The mass is estimated as 340 kg.

4.6 Description of Rotator Drive Units

The rotator drive units consist of commercially available shaftless AC servomotors. The motor chosen to meet the requirements is a Compumotor DM series 1015B. They drive a gear pinion through planocentric speed reducers. These are Teijin Seiki RV-A II Drives, Model RV-135A II. The output shaft is in the form of a face plate, to which the drive pinions are bolted, with a spigot pilot diameter location. The drive units are stood off the upper rotator ring locations by means of an annular interface plate. The drive ratio is 81:1.

4.6.1 Torque Capacity

The torque capacity of the actuators will exceed the maximum rotator torque under all operating conditions by a factor of 3. Table 4 -3 shows the load torque contributions from all the sources considered.

TABLE 4-3: Load Torque Contributions

Item	Load (Nm)
CABLE WRAP	
Cable Wrap Structure	10
Cable Wrap Friction	30[a]
Cable Chains and Services	300
ISS STRUCTURE	190
ROTATOR STRUCTURE	10
Bearing Friction (max)	2095[a]
Bearing Seal Drag	65[a]
A & G	
Peripheral Guide Probes / WFS	50
AO Fold Mirror	50
Science Fold Mirror	100
Filters / Polarizers	50
High Order WFS	10
A&G Structure	10
INSTRUMENTS	
Side Looking Instruments	305
Upward Looking Instrument	100
Moving Elements In Instruments	22.4[b]
Wind Loading	213
Total (rss)	2731

a. For total, friction is additive, eccentricities and wind drag are rss'd.
b. RSS for 5 instruments, each with 10 Nm allowable out of balance allocated for moving elements.

DETERMINING MOTOR TORQUE. There are four actuators operating in opposing pairs (two sets of two). The actuators will be preloaded to 50% of motor capacity. This will increase the stiffness and linearity of the drives. From table xxx the maximum estimated driving torque is taken to be 2800 Nm. A service factor of 3 indicates a required torque of 8400 Nm from the actuators with respect to the load. With a final drive gear ratio of 10:1, the total actuator torque must be 840 Nm. Split between four actuators in opposing pairs, each actuator must be capable of 420 Nm. The torque required from the drive motor is determined as follows:

$$\Gamma = \frac{\Gamma_{out}}{gear\ ratio} \qquad \text{(EQ 4 - 4)}$$

where: Γ = torque required from the motor, Γout = required actuator torque, and drive gear ratio = the speed reduction ratio.

For Γ_{out} = 420 Nm, and gear ratio = 81; Γ = 5.2 Nm. This figure is used to determine the minimum continuous output torque of the motor. The DM 1015B has a continuous torque rating of 10 Nm with a peak torque of 15 Nm. Losses in the gearing are expected to be of the order of a few percent and are accounted for by the service factor.

INERTIA MATCHING. It is important to match the inertia of the load reflected at the motor shaft to the motor inertia according to the application. The manufacturer recommends that for slow speed positioning this ratio should be less than 100:1.

The load inertia reflected at the motor shaft is determined as follows:

$$J_{Lm} = \frac{J_L}{gear\ ratio^2} \qquad \text{(EQ 4 - 5)}$$

where: J_{Lm} is the inertia reflected at the motor shaft, J_L is the load inertia, and gear ratio is the load to motor gear ratio.

For J_L = 20,000 kgm^2 and an overall drive gear ratio of 810:1, the reflected inertia at the motor shaft is 0.03 kgm^2.

In addition to the load inertia, the motor will also see the inertia of the speed reducer, Js. From the manufacturers, this is 0.0001744 kgm^2. The moment of inertia of the motor to speed reducer coupling is assumed to be insignificant.

The reflected inertia of the pinion at the motor shaft, J_{pm} is given by

$$\frac{J_{pm}}{acuator\ gear\ ratio^2} = \frac{0.5xmxr^2}{actuator\ gear\ ratio^2} = \frac{0.5x\rho\ \ xr^4xt}{actuator\ gear\ ratio^2} \quad \text{(EQ 4 - 6)}$$

Assuming the pinion gear is a solid disc and r is the material density, r is the radius, and t is the thickness.

For r = 6.7 x 103 kg/m^3, r = 0.0914 m, and t = 0.0287, J_{pm} = 3.21 x 10^{-6} kgm^2.

The total load inertia reflected at the motor, J_{mt} is given by

$$J_{mt} = J_{Lm} + J_s + J_{pm} \quad \text{(EQ 4 - 7)}$$

where J_{mt} *= 0.03 + 0.0001744 + 0.00000321 ~ 0.0302 kgm*^{2}*.*

The rotor inertia for DM 1015B is 0.012 kgm^2, giving a load to rotor inertial ratio of 2.5. This is well within the manufacturers specifications.

VELOCITY MATCHING. The overall motor to load drive ratio is 810:1 and the DM 1015B is rated at 2 rps. This gives an output velocity of 0.9 °/sec. This is approximately half of the target slewing velocity of 2° /sec. The RV-135A II speed reducer has a lowest standard reduction ratio of 81:1. It is possible to order non-standard ratios to give a higher output velocity. In addition, the motor speed can exceed the rated value, investigations with the manufacturers are ongoing.

4.6.2 Stiffness

The effective stiffness of the actuators will depend on the stiffness of the speed reducers, the structure to which they are attached, and the stiffness of the gear teeth.

SPEED REDUCER TORSIONAL STIFFNESS. The manufacturer quotes 1.21 x 10^6 Nm/rad for the RV-135A II speed reducer. For four actuators acting in two opposing pairs, their combined stiffness will be four times this figure (4.85 x 10^6 Nm/rad). The stiffness referred to the load will be magnified by the square of the final drive ratio of 10:1, giving a stiffness at the load, $S_{r\ l}$, of 48.5 x 108 .

SPEED REDUCER MOMENT STIFFNESS. Because the line of action of the gears is offset from the actuator bearings, the contact force will cause a moment on the actuator, causing a tilt. See Figure 16 on page 118. The manufacturer quotes a moment stiffness for the RV-135A II of 4.04 x 10^6 Nm/rad. For four actuators acting in two opposing pairs, their combined stiffness will be four times this figure (1.62 x 10^7 Nm/rad). The stiffness referred to the load will be magnified by the square of the ratio of the pitch line radius to the offset distance (0.914 / 0.065), giving a stiffness at the load, $S_{m\ l}$ = 3.2 x 10^9 Nm/rad.

MOUNT STIFFNESS. When the pinion gear is loaded against the ring gear, the resultant contact force will deform the actuator mount. As the line of action is offset from the actuator mount, there will also be a twisting moment. The effects on stiffness can be estimated as follows. The actuators are mounted on lugs which are part of the rotator upper fixed ring. The mount can be conservatively simplified as two cantilevered beams 150 mm long by 90 mm wide by 55 mm deep. Figure 15 on page 117.

From the engineer's theory of bending, direct tangential stiffness S_d is estimated as

$$\frac{W}{\delta} = \frac{2x3x(ExI)}{L^3} \qquad \text{(EQ 4 - 8)}$$

where W = tangential tooth load; L = length of the 'cantilever'; E = modulus of elasticity; and I = section second moment of area about the bending axis.

For W = 1 N; L= 150 mm; E = 210 x 10^3 N/mm^2; and I = 3.3 x 10^6 (section is 90 x 55 mm), W/δ = 1.25 x 10^6 N/mm. For four mounts acting in two opposing pairs, this converts to a radial stiffness at the load $S_{d\ l}$ of 1.25 x 106 x 1000 x 4 x $(0.9144)^2$ (pitch radius of ring gear) = 4.19 x 10^9 Nm/rad.

Because the line of action of the tooth force is offset from the plane of the motor mount, it will tend to bend the cantilevers out of plane, tilting the actuator. This tilt stiffness, S, can be estimated as before.

$$S_o = \frac{2x3x(ExI)}{L^3} x(1000xr^2) \qquad \text{(EQ 4 - 9)} .$$

In this case, the section is taken as 55 x 90 mm and the radius, r, is half the distance between the cantilevers (100 mm).

Thus, S_o = 4.67 x 10^6 Nm/rad. This tilt stiffness can be referenced to the load by multiplying by the square of the ratio of the pitch line radius to the offset distance . Because there are four mounts, stiffness at load, $S_{o\ l}$ = 4.67 x 106 x 4 x $(914.4 / 140)^2$ = 8.0 x 10^8 Nm/rad.

GEAR TOOTH STIFFNESS. The gear tooth flexure can be estimated by treating it as a cantilever beam and adding shear deflection. The tooth proportions must first be determined: Diametral Pitch, P = 5 /in; Dedendum = 1.2/P + 0.002 = 1.2/5 + 0.002 = 0.242 in (6.147 mm); Addendum = 1/P = 0.2 in (5.08 mm); and Face width = 25 mm.

Gear tooth stiffness in Nm/rad

$$S_t = \frac{1}{\dfrac{L}{AxG} + \dfrac{L^3}{3xExI}} \qquad \text{(EQ 4 - 10)}$$

where R = bearing radius, L = tooth length, A = tooth cross section area, G = shear modulus of elasticity, E = Young's modulus and I is the second moment of area for the tooth section about the bending axis.

$S_t = 3.73 \times 10^5$ N/mm. Referring this stiffness to angular stiffness at the load for four sets of opposing gear teeth (eight in all), $S_{tl} = S_t \times 1000 \times r^2 \times 2 = 6.23 \times 10^8$ Nm/rad.

Total drive stiffness in Nm/rad at the load is thus found to be:

$$S_{tot_l} = \frac{1}{\frac{1}{S_{ml}} + \frac{1}{S_{rl}} + \frac{1}{S_{dl}} + \frac{1}{S_{ol}} + \frac{1}{S_{tl}}} = 1.83x10^8 \text{ Nm/rad} \qquad \text{(EQ 4 - 11)}$$

The locked rotor natural frequency in Hz is

$$F_n = \frac{1}{2x} x \sqrt{\frac{S_t}{J}} = 15.2 \text{ Hz.} \qquad \text{(EQ 4 - 12)}$$

4.6.3 Motor Power Dissipation

The motors are rated at 125 watts continuous output. Assuming an efficiency of 80%, the heat generated in the motor will be 31 watts. This load will vary as the demands on the motors change due, for example, to an attitude change of the telescope, or a transient effect due to slewing. The majority of this heat will be actively removed. This is desirable as varying heat loads due to changing demands on the motors (with telescope tube altitude) will cause transient thermal effects in the actuator mounts which could, potentially, effect the calibration. The tubular motor mount forms a shroud around the motor. It is machined from aluminum to avoid differential contraction effects at the hot (motor) end and to act as a heat sink/convective radiator in the event that the water cooling system fails. The aluminum sub-plate to which the motor is attached has liquid circulating within and will be plumbed into the Cassegrain coolant circulation system. Figure 17 on page 119 shows the heat paths considered which are as follows.

1. Heat rejected to the water circulation system by conduction followed by surface to liquid convection. This is estimated by

$$Q_r = UA\Delta t = \frac{1}{\frac{1}{h} + \frac{x}{k}} (Ax\Delta t) \qquad \text{(EQ 4 - 13)}$$

where Q_r is the heat rejected in watts, A is the surface area of the heat exchanger in m^2, Δ t is the temperature difference between the motor subplate and the cooling fluid in ºC, h is the surface heat transfer coefficient to the fluid W/m^2 ºC, x is the characteristic thickness of the `tube wall' in meters and k is the thermal conductivity of the subplate material in W/m ºC.

For U = 0.00339, A = 0.0157, h = 4090, x =0.02, k = 200 and the temperature of the coolant is ambient, $Q_h = 45.8 (T_m - T_c)$, where T_m is the temperature of the motor and T_c is the average coolant temperature in the heat exchanger.

2. Heat rejected to the mirror cell interior by passive convection. This is estimated by

$$Q_c = hA_t \frac{(T_m - T_t) - T_a}{2} + hA_e(T_m - T_a) \qquad \text{(EQ 4 - 14)}$$

where h is the free convection coefficient in W /m² ºC, A_t is the outward looking area of the motor support tube in m², T_m is the motor mount temperature, T_t is the telescope structure temperature, A_e is the outward facing area of the motor subplate and T_a is the ambient temperature.

For h = 4 W/m ºC, A_t = 0.08m² , A_e =0.02 m² , Q_c = 0.17 (T_m -T_t -T_a) + 0.08 (T_m-T_a).

3. Conduction into the telescope structure. This is estimated by

$$Q_{con} = k\frac{A_c}{L}\left(\frac{T_m - T_t}{2}\right) \qquad \text{(EQ 4 - 15)}$$

where k is the thermal conductance of the motor mount in W/m² ºC, A_c is the conductive cross section area in m², L is the conductive path length in m (assumed to be half the motor mount length since the heat flux through the motor mount is assumed to be dominated by conduction).

For k = 200 W/m² ºC , A_c =0.00226, l = 0.07, Q_{con} = 3.02 (T_m -T_t), the total heat balance can be expressed as follows:

$$Q_{tot} = Q_r + Q_c + Q_{con} = 45.8(T_m\text{-}T_c) + 0.17(T_m\text{-}T_t\text{-}T_a) + 0.08(T_m\text{-}T_a) + 3.02(T_m\text{-}T_t) \qquad \text{(EQ 4 - 16)}$$

If we assume that the coolant temperature and telescope structure are at ambient 0 oc say, the motor temperature will be 0.63 ºC.

EFFECT ON TELESCOPE SEEING. A fraction of the heat generated in the motors will heat the surrounding telescope structure by conduction. Of particular interest is the heating of the internal wall of the mirror cell bore. This heat will be transferred to the air within the telescope bore by means of convection where it will rise, exit the primary mirror bore, mix with the flow of flushing air, and traverse the primary mirror. Figure 18 on page 120 and Figure 19 on page 121 shows a plot from an IDEAS FEA model of the motor and the immediate structure and the results. The model assumes 2W (a conservative estimate) to be generated in the vicinity of the motor. It includes passive convection from all free faces; the free convection coefficient is assumed to be 4W/ m² ºC. The model shows that the maximum increase in structure temperature over ambient within the bore of the mirror cell is 0.2ºC. Integrating the surrounding convected heat transfer into the mirror cell gives a figure of 1.2 W. This figure is input into the seeing calculations in the chapter on thermal management and is acceptable.

EFFECT ON TELESCOPE STRUCTURE. Actively cooling the motors will have a beneficial effect on the stability of the mirror cell. The maximum estimated heat load conducted into the mirror cell is 8 W for the four motors. The Gemini Optics group have investigated the transient effects of a 50 W heat input step in the vicinity of the rotator bearing. (RPT-O-G0030). The results show a maximum mirror deformation of 0.2 nm per minute (rms) which is acceptable.

EFFECT ON ENCLOSURE THERMAL BUDGET. The heat convected into the mirror cell is estimated as 0.16 W. This heat will eventually get into the enclosure air volume, but the amount is well within the allocation from the entire Cassegrain area.

COOLANT FAILURE. If the coolant system fails the motor temperature rise above ambient is estimated as 31/3.27 or 9.5 ^{o}C. This is well within the motor specifications and allows the rotator to be tested during commissioning without the cooling system.

4.6.4 Mass

Each actuator consists of the motor, motor mount, speed reducer and gear pinion. The masses are estimated in Table 4-4.

TABLE 4 -4: Actuator Masses

Item	Mass (Kg)	C of G Position in z direction w.r.t. cell interface (m)
Motor	5.5	+0.077
Motor Mount	2.7	+0.107
Speed Reducer (RV-135AII)	28.0	-0.109
Total (for one actuator of 4)	36.2	

4.7 Description of Rotator Drive Gearing

The drive train consists of a pinion and gear set. Pinions will operate in opposing pairs to eliminate backlash, increase drive stiffness and reduce hysteresis. The gear type will be helical spur gears which have a smoother operation than straight spur gears.

4.7.1 Drive Gear

The drive gear is a large ring gear 1828.8 mm PLD fastened to the rotator lower ring. This is driven by the pinions of the motor drive units. The tooth form is a helical spur gear for smooth operation. The gear ratio is 10:1. Gear quality shall be AGMA 12 and the diametral pitch is 5 /in.

4.7.2 Drive Pinions

The drive pinions are 182.88 mm PLD gears fastened to the actuator output. The tooth form is a helical spur gear. Gear quality shall be AGMA 14. The improvement in gear quality is allowable because of the smaller size of this gear.

4.7.3 Diametral Pitch

Our design is for the highest diametral pitch which can support the anticipated loads since this gives the smoothest operation and least error for a given gear class. The allowable diametral pitch is determined by using the Lewis formula, extracted from BSS 436. There are two relationships, one for strength, and one for wear.

$$\text{Strength:} \quad F = \frac{X_b Y S_b}{p} \qquad \text{(EQ 4 - 17)}$$

$$\text{Wear:} \quad F = \frac{X_c Z S_c}{K} \qquad \text{(EQ 4 - 18)}$$

where: F, the allowable tangential load, is the least for the above calculations on the pinion or gear. X_b and X_c are the speed factors for strength and wear respectively and are dependent on running times of the gear. For 12 hours running per day, X_b =X_c =0.48 for 40 rpm. (The slowest speed quoted in the reference.) Y is the strength factor given in graphical form in BSS 436, Z is the Zone factor, again, given in chart form in the reference. P is the diametral pitch in inches, K is the pitch factor = $P^{0.8}$, S_b is the bending stress factor and S_c is the surface stress factor.

The tooth load used is consistent with the design output torque of the actuators

$$F = \frac{TS_f}{PCR(2)} \qquad \text{(EQ 4 - 19)}$$

where: F is the tangential tooth load, T is the actuator output torque, S_f is the service factor and PCR is the pitch circle radius of the gear.

Summarizing the results:

TABLE 4 -5: Diametral Pitch

Item	**F (lbf)**	**X_b**	**S_b**	**Y**	**X_c**	**S_c**	**Z**	**DP (in)**
Pinion Strength	996.0	0.48	15,000	0.85	--	--	--	6.3
Gear Strength	996.0	0.48	15,000	0.73	--	--	--	5.3
Pinion Wear	996.0	--	--	--	0.48	3,000	5	11.8
Gear Wear	996.0	--	--	--	0.48	3,000	5	11.8
Selected DP								5

4.7.4 Gear Indexing Errors

Table 4-6 shows gear indexing errors. For a gear diameter of 72 inches and a pinion of 7.2 inches, the total indexing error is given by:

$$\text{Indexing error} = \left(\left(\frac{26.1}{72}\right)^2 + \left(\frac{13.9}{72}\right)^2\right)^2 = 40 \text{ arcminutes or 24.4 arcseconds} \qquad \text{(EQ 4 - 20)}$$

TABLE 4 -6: Gear Indexing Errors

Effect	Indexing Error (arcmin) Gear	Indexing Error (arcmin) Pinion
Center Distance Variation	0	0
Tooth Thickness Variation	2.2/D	1.34/D
Pitch Error	5.3/D	0.88/D
Profile Error	4.0/D	1.46/D
Pitch Diameter Runout	13.5/D	4.95/D
Lead Angle Error	1.38/D	1.38/D
Lateral Runout	1.38/D	1.38/D
Bearing Tolerance	21.1/D	12.1/D
Total Indexing Error (rss)	26.1/D	13.39/D

converting to microradians = 24.4 x 10^6 / (3600 * 57.3) = 118.5 microradians

The derivation of the table entries are taken from Chironis and AGMA standard 390.03 and are detailed below:

CENTER DISTANCE VARIATION. A property of involute tooth forms is that center distance variations do not effect indexing accuracy of gears but do effect backlash. Backlash is very important in the free running of gears, however, and will effect the center distance tolerance of the gear and pinion. AGMA recommendations for course pitch gearing (DP 5) are 0.04 -0.06 inches (1.02 - 1.5 mm).

TOOTH THICKNESS VARIATION. This is self explanatory and the figures used here were derived by taking the total composite error and subtracting pitch and runout errors (no specific table was found for tooth to tooth thickness variation). The indexing error is given by

$$e_{tooth} = 3438\left(\frac{\Delta B_o - \Delta B_i}{D}\right) \qquad \text{(EQ 4 - 21)}$$

where ΔB_o and ΔB_i are the tooth thickness variations.

From the reference, these are 6.4 x 10^{-4} in. and 3.9 x 10^{-4} in. for gear and pinion respectively.

PITCH ERROR. Pitch error is the difference in tooth spacing along the pitch line. The indexing error in arcmin is given by

$$e_{pe} = 6875\left(\frac{\Delta p_o - \Delta p_i}{D}\right) \qquad \text{(EQ 4 - 22)}$$

where: ΔP_o and ΔP_i are pitch errors of adjacent gear teeth.

From the AGMA standard for a quality 12 gear of DP5 max ($\Delta P_o - \Delta P_i$)= 7.74×10^{-4} in. for the gear and 1.28×10^{-4} in. for the pinion of quality 14.

INVOLUTE PROFILE ERROR. Involute profile error is the deviation of the tooth form from the true involute. Indexing error is given by

$$e_{ip} = 6875\frac{\Delta a1 - \Delta a2}{Dx\cos\varnothing} \qquad \text{(EQ 4 - 23)}$$

where: $\Delta a1$ and $\Delta a2$ are the profile errors between any two teeth, and ϕ is the pressure angle.

From the AGMA specification ($\Delta a1 - \Delta a2$)is 5.48×10^{-4} in. for the gear and 1.99×10^{-4} in. for the pinion.

PITCH DIAMETER ECCENTRICITY. This effect is eccentricity of the pitch line of the gear, its effect on indexing errors is given by

$$e_{pd} = 3438\left(\frac{e}{R}x\sin\theta_e\right) \qquad \text{(EQ 4 - 24)}$$

where: e is the eccentricity, R is the pitch circle radius, and Θ_e is the rotation angle about the rotation axis.

From the AGMA specification, e is taken as the runout tolerance of 19.6×10^{-4} in. for the gear and 7.18×10^{-4} in. for the pinion.

LEAD ANGLE ERROR. A varying lead angle from tooth to tooth will cause an indexing error of

$$e_{la} = \left(\frac{F}{D}\right)(\tan\lambda_e)(6875) \qquad \text{(EQ 4 - 25)}$$

where: F is the face width of the gear and λ_e is the lead angle error.

From the AGMA standard λ_e is 2×10^{-4} in. per inch of gear face width.

LATERAL RUNOUT. This is caused by misalignment of the gear teeth to the axis of rotation. The effect on indexing accuracy is given by

$$e_{lr} = 6875\left(\frac{F}{D}\sin\lambda\right) \qquad \text{(EQ 4 - 26)}$$

Runout is assumed to be 2×10^{-4} /in. rad.

BEARING AND GEAR ASSEMBLY TOLERANCE. Bearing errors will result in pitch diameter eccentricity, and a lateral runout. For the gear, these effects are estimated as 3×10^{-3} in. and 0.0043º. The first of these will cause indexing errors similar to pitch diameter eccentricity errors, the second is a lateral runout. The pinion and its mount have estimated tolerances for eccentricity and tilts of 0.0017 in. and tilts of 0.004º.

FLEXURE INDUCED INDEXING ERRORS. The flexure of the bearing will produce systematic errors, varying with telescope tube attitude. These can be split into eccentricities and misalignment tilt errors, dealt with previously. However, As the gears and encoders are at the compass points of the rotator, there is compensation if the positions are averaged.

4.7.4.1 Effect of Gear Indexing Errors on Rotator Drive

The gear errors will appear as torque ripple on the load. However, the repeatable nature will allow look-up calibration, if required. The estimated non-repeatable component of these errors is used in the Cassegrain servo control model.

4.7.4.2 Effect of Gear Indexing Errors on Position Feedback System

The gear errors will appear as position errors for the encoding system. The repeatable nature of these errors will allow the use of error compensating look-up tables. In addition, the configuration of having 4 diametrically opposite encoders allows the position to be averaged, eliminating the effects of decenter and eccentricity, major components of the indexing errors of the gear.

4.7.5 Backlash

A minimum backlash in the assembled gear train of 570 microradians is required for smooth gear operation (Kaydon, Inc. Software). The effect of backlash is eliminated by loading the gear pinions in opposing pairs, eliminating tooth to tooth clearance.

4.8 Description of Position Feedback System

The position feedback system consists of four rotary encoders positioned evenly at 90º intervals on the rotator. These are driven by anti-backlash gear pinions running on the rotator drive gear. The ratio of load to encoder is 1:10.

4.8.1 Encoders

There are four incremental encoders with 16 bit resolution. Readout rates (4 KHz for 2º per second) will allow position tracking during maximum slew speeds.

In addition, a multi turn absolute encoder is provided, driven by a pinion running on the ring gear.

4.8.2 Encoder Drive Gear Indexing Errors

These errors are identical to the drive errors developed in the previous section.

By taking differences between diametrically opposite encoders and averaging for the two sets, some of the larger components of the gear indexing errors will be automatically compensated. A portion of the remaining errors can be calibrated by comparing encoder readings for a full revolution of the rotator and correlating the results with a shift and add process. Further error correction can be achieved through calibration of sky objects as a reference source and the telescope azimuth drive.

The various components of the errors have different magnitudes and frequencies which are multiples of the rotator speed. The effects of these errors will be modeled using the servo system computer model.

4.8.3 Description of Servo System

The servo system is designed around a commercial PID controller board, hosted in a VME crate. This board receives demanded position information from the telescope control system. The position of the rotator relative to the telescope tube is supplied as position feedback. Both position and velocity information will be corrected by a look-up table. The look-up table will be determined during calibration and characterization of the drives. A tunable lead-lag filter conditions the analog input to the motors. The motors operate the drive gear train, which cause the rotator to move. Position feedback is available at the rotator and velocity feedback is available at the motor shafts. Since the Cassegrain rotator must react against the telescope tube, the rotator drive will have an effect on other telescope drives and is being considered in the overall servo system design.

4.8.4 Description of Computer Modeling

The Cassegrain area is modeled using Matlab 4.0 (a numerical computation software package). The model of the Cassegrain area was originally developed by Mike Burns of the Gemini Controls Group as part of the overall model of the telescope control system. The overall telescope model is shown in Figure 10 on page 112. Since the model is modular, it allows the Cassegrain area to be independently developed.

The simulations are used to determine the stability of the control loops and to predict the performance. They also allow tradeoffs of components (i.e., encoder resolution, gear ratios, motor performance, etc.) to be conducted. Stability is determined primarily through analyzing bode plots and step responses, see Figure 7 on page 109. Performance is estimated by "observing" image motion at the focal plane in the x and y directions. By enabling one or more subsystems at a time, errors are attributable to specific areas in the model or specific combinations of parameters. This helps to verify the Systems Error Budget.

The model of the Cassegrain area is based on the mechanical model shown in Figure 6 on page 108. The concept is that the telescope is coupled by a stiff spring to ground (the pier) and that the rotator is coupled to the telescope by a less stiff spring. The main characteristics of this model is that the Cassegrain rotator must react against the telescope tube and thus, affects and is effected by the rest of the telescope dynamics. It is also important to note that the rotator has no independent frame of reference (e.g. an inertial gyro) and so it can only "know" where it is with respect to the telescope.

Within the rotator, the interactions between the motors, drive train, and rotator moment of inertia are modeled. A simplified block diagram is shown in Figure 9 on page 111. This model is only concerned with rotation in the z-direction (telescope at zenith). The complete telescope control system model incorporates six degrees of freedom. The simplified model was used to determine the parameters of the PID controller and the lead-lag filter which conditions the input to the analog motor model.

In this model, position of the rotator relative to the telescope tube is compared to the demanded position. The demanded position in the model is user-supplied. In reality, this will come from the telescope control system. The error position is fed to the servo controller, where it is converted into a current which is supplied to the model of the motor. The parameters for the motor were supplied by the manufacturer, based on the compumotor DM 1015B. The motor produces a torque which will act on the motor's inertia. Before this torque can "act" on the motor inertia, it is reduced by a back torque which is due to the compliance between the motor and the drive train. The net torque acting on the motor inertia produces an acceleration. This acceleration is integrated twice to obtain the position of the motor "shaft". The net position between the actual position of the rotator, scaled by the gear ratio, and the motor shaft move a spring which represents the stiffness between the gears and the motor. This creates a torque (again, scaled by the gear ratio) which acts on the rotator moment of inertia, giving the actual rotator acceleration. The acceleration is then integrated twice to give the actual rotator position.

Friction of the bearing is also included in the model. The derivative of the net position of the rotator and telescope is taken to determine the actual velocity of the rotator. The friction model is velocity dependent, and is based on parameters supplied by Kaman Aerospace. Viscous friction is 1.4×10^4 Nm/(rad/sec). Above 5×10^{-6} rad/sec kinetic coulomb friction or running friction is added to the viscous friction. At velocities less than this, the bearing's friction characteristics are modeled by a fourth order polynomial which approximates the friction characteristics in the transition region from stiction to sliding friction. Static friction is not yet incorporated into the model.

This model has an approximate bandwidth of 13 Hz, with a phase margin of 35º and a gain margin of 20 dB. The Bode plots are shown in Figure 7 on page 109.

When the Cassegrain model is incorporated into the overall telescope model, its actual performance with respect to image motion in x and y can be determined. The error in the x and y direction independent of the other telescope drives is shown below. The rms error is 5.503×10^{-9} and 5.367×10^{-9} for x and y, respectively. These errors are the result of supplying the Cassegrain rotator with a ramp input.

The performance of the rotator as it follows a ramp input is shown in Figure 8 on page 110.

4.9 Description of Rotator Control Electronics

The rotator control electronics will contain the motor drive units, necessary PID control boards, and telescope control system interface electronics. These electronics will be located within two thermally conditioned enclosures located on the telescope center section as shown in fig xxx.

4.10 Requirements Placed on Mirror Cell

The rotator is bolted to the mirror cell and transmits the loading from the instrument cluster into the cell. It is sandwiched between the cell and the instrument support structure. The rotator drive motors protrude into the mirror cell through clearance holes where interfaces to the cabling and coolant system are required. Access by personnel is required in this area to service the motors. Self sealing or valved coolant lines are required to allow isolation of a drive motor for servicing. Access is also required for servicing the bearing including lubrication and torqueing of the mounting bolts.

4.10.1 Rigidity

The mirror cell must be locally stiffened in order to receive the loads that the rotator will transmit. The bearing manufacturer recommends a stiffening tube depth of 0.6 x bearing diameter if the full capacity of the bearing is to be realized. In our case, the bearing is only taking a fraction of its static load but the accuracy and stiffness specified still require a substantial backing structure. The mirror cell structure is almost ideal with its deep circumferential and radial webs.

4.10.2 Mirror Cell Mechanical Interface

The mechanical interface to the cell is a flat, annular machined area with an outside locating diameter of 1744.0 mm which registers on an accurately machined diameter on the mirror cell. 36 equispaced 19mm bolts on a 1674 mm PCD are used to fasten the rotator onto the mirror cell, through clearance holes. See Figure 20 on page 122.

4.10.2.1 Locating Features

The preferred radial locating technique for the bearing assembly (rotator) is an accurate pilot diameter, which facilitates location and maintains the circularity of the bearing. This is also insurance against potential creep of the assembly caused by cyclical shear loading (telescope tube moving in altitude). An annular flat surface perpendicular to the rotation axis will locate the assembly axially and in tilt.

4.10.2.2 Surface Flatness

The bearing imposes constraints on the initial out of flatness for the interface and the allowable out of flatness deformation.

INITIAL FLATNESS. This puts a requirement on the flatness of the upper and lower surfaces of the rotator upper ring and the mirror cell interface. The allowable tolerance for initial flatness is shared between these surfaces and the mirror cell interface. The mirror cell interface surface is given 75% of the tolerance, the balance is apportioned to the rotator upper ring (interspaced between the bearing and the cell). The bearing requirements are 0.127 mm per 25 mm for radial flatness (dishing) and 0.038 mm per 90º segment for circumferential flatness (waviness). Thus, the radial flatness must be 0.095 mm per 25 mm or better and the circumferential flatness of these surfaces must be 0.028 mm per 90º segment or better.

OUT OF FLATNESS DEFORMATION. The allowable out of flatness deformation tolerance is given completely to the mirror cell. The bearing manufacturer suggests a radial tilt less than 0.076mm / mm and circumferential waviness less than 0.254 mm /90º segment. This assumes a smoothly varying deformation with no discontinuities. An FEA model was constructed to investigate this effect. It is discussed in the next section.

LOCATING DIAMETER TOLERANCES. The locating diameter tolerance must be as precise as practical taking into consideration the ease of disassembly of the ISS from the rotator. From the ANSI standard tolerances B4.1 - 1967, R 1979, a locational clearance fit is chosen as H7h6. This gives a locating tolerance between -102 µm and +152 µm. This tolerance band will allow free assembly of the components. The h6 hole tolerance may be reduced as this is a feature of the rotator upper ring, a component which may be ground. The final tolerancing will be decided after discussion with the manufacturers when cost will be a consideration. The standard tolerances quoted can be achieved by normal turning.

4.10.3 Mirror Cell Interface Finite Element Analysis

A model of the mirror cell / rotator interface was constructed in IDEAS in order to investigate the local stiffness of the mirror cell, see Figure 21 on page 123. It is desirable to minimize the plate thicknesses used in this area of the mirror cell, while the rotator bearing has a requirement for out of flatness deformation which must be met. The model consists of a portion of the mirror cell and a deep cylinder which represents the instrument support structure. The bearing is modeled by spring and gap elements between these two.

The results show that the overall tilt of the Cassegrain assembly (27.8 µRad) is dominated by bearing flexures, see Figure 22 on page 124. The out of flatness deformation of the bearing interface (2.5 µm) is acceptable for a plate thickness of 63.5 mm.

The model shows that for thinner plates, there is increasing `print through' of the cell stiffening webs on the compression side during moment loading which will cause high local loading of the bearing. This can effect the smooth running of the bearing and reduce bearing life.

4.11 Requirements Placed on the Instrument Support Structure

The ISS must be stiff in order to transmit loads properly into the rotator. A raised flange is also required to allow outside access to the mounting bolts for disassembly. Similar out of flatness constraints apply to the ISS interface as those for the mirror cell interface.

Provision must be made to run cabling and services from the break out panels on the cable wrap inner to the A&G electronics enclosures and to support the A&G units.

4.11.1 Rigidity

As previously stated, the ISS must be locally stiffened in order to receive the loads that the rotator will transmit. The bearing manufacturer recommends a stiffening tube of depth 0.6 x bearing diameter if the full capacity of the bearing is to be realized. In this case the bearing is taking a fraction of its static load but the accuracy and stiffness specified still requires a substantial backing structure. The ISS structure is almost ideal with its deep internal cylinder and extensive webbing.

4.11.2 Instrument Support Structure Mechanical Interface

The Instrument Support Structure mechanical interface is a flat, annular machined area with a locating spigot (ϕ1392 mm) which registers into a locating diameter on the Cassegrain rotator. 36 equispaced 19mm bolts on a 1496 PCD are used to fasten the ISS onto the rotator, through clearance holes.

4.11.2.1 Surface Flatness

The bearing sets constraints on the initial out of flatness for the interface and the allowable out of flatness deformation.

INITIAL FLATNESS. This puts a requirement on the flatness of the upper and lower surfaces of the rotator lower ring and the ISS interface. The allowable tolerance for initial flatness is shared between these surfaces and the mirror cell interface. The mirror cell interface surface is given 75% of the tolerance, the balance is apportioned to the rotator upper ring (interspaced between the bearing and the ISS). The bearing requirements are 0.127 mm per 25 mm for radial flatness (dishing) and 0.038 mm per 90º segment for circumferential flatness (waviness). Thus, the radial flatness must be 0.095 mm per 25 mm or better and the circumferential flatness of these surfaces must be 0.028 mm per 90º segment or better.

OUT OF FLATNESS DEFORMATION. The allowable out of flatness deformation tolerance is given completely to the ISS. The bearing manufacturer suggests a radial tilt less than 0.076mm / mm and circumferential waviness less than 0.254 mm /90^{o} segment. This assumes a smoothly varying deformation with no discontinuities. An FEA model was constructed to investigate this effect, it shows that the deformations of the ISS (modeled crudely as a simple cylinder) are acceptable. The model is discussed in the chapter dealing with the ISS.

4.11.2.2 Locating Diameter Tolerances

The locating diameter tolerance must be as precise as practical taking into consideration the ease of disassembly of the ISS from the rotator. From the ANSI standard tolerances B4.1 - 1967, R 1979, a locational clearance fit is chosen as H7h6. This gives a locating tolerance between -102 mm and +152 mm. This tolerance band will allow free assembly of the components. The H7 hole tolerance may be reduced as this is a feature of the rotator lower ring, a component which may be ground. The final tolerancing will be decided after discussion with the manufacturers when cost will be a consideration. The standard tolerances quoted can be achieved by normal turning.

4.12 Endstops

The rolling cable loop arrangement has a limited travel and must be protected from overrun. There are three levels of protection. The telescope control system should always keep the rotator within a normal working range of ± 270º. Secondly, micro switches will provide an error signal to the motor controllers at ± 272º which will depower motors, regardless of telescope control signals. Finally, a mechanical endstop is provided beyond the micro switches at ± 272º, nominally. The operation of the buffers will signal the application of the rotator brake. The deceleration distance is 3º and so the total range of rotation is -5º to 545º.

4.12.1 Endstop Design

There are two endstops, one for clockwise and one for anti-clockwise rotation. They are linear hydraulic dampers with a progressive action and are attached to the stationary rotator ring. They are engaged by separate toggling pins which only operate in one direction. A trigger mechanism is employed to disable the endstop every other pass to enable the rotation to exceed 360º. See Figure 24 on page 126 and Figure 23 on page 125.

MECHANICAL BRAKE. The rotator brake serves the purpose of helping the mechanical endstops stop the rotator in an error condition. The brake may also be used to stop the rotator from moving in conditions where the motors are de-powered. The brake is failsafe on, having to be powered to release. The brake is attached to a pinion gear in contact with the rotator drive gear. In normal operation the pinion is free running. The gear ratio is 10:1.

POSITIVE LOCK. It will be possible to immobilize the rotator by manually inserting a locking pin. This will be required during servicing and commissioning.

5. *CASSEGRAIN CABLE / SERVICES WRAP*

This chapter describes the preliminary design for the Cassegrain Cable / Services Wrap and how the design meets the design requirements. The practical considerations of implementing the design are also discussed.

5.1 Description of Preliminary Design

The Cassegrain cable / service wrap has to maintain copper cables, data fiber cables, helium lines, coolant lines and vacuum lines to the instruments and Cassegrain mounted facilities through a working rotation angle of 540º. A rolling loop arrangement is used to achieve this. The cables are wound around a circular drum and then loop back onto an outer circular former. As the inner drum is rotated, the cables are paid out and deposited on the outer former. As this occurs, the intervening loop advances in the same direction as the rotation, and in effect, the inner can rotate more than twice the angle covered by cable. See Figure 25 on page 127, Figure 26 on page 128, Figure 27 on page 129 and Figure 28 on page 131.

The services are supported within flexible cable trunking which runs in two circular, concentric guide troughs. One is static, attached to the mirror cell and faces in towards the rotator. The other is attached to the Cassegrain rotator and faces outward. Each guide trough has two tracks, an upper and a lower in which the cable trunking runs. Two lengths of trunking will be used in each track giving four in all. The upper and lower cable loops will be wound in opposite directions. Regardless of rotator position, the shape of the upper loop will be the mirror image of the lower loop. This arrangement maintains balance of the cables wrt the rotation axis. The cable loops are guided by a semicircular shuttle which carries guide rollers.

The inner guide trough is attached to the Cassegrain rotator by means of eight support brackets. Eight break panels are provided on the lower surface, above the side looking instruments. Each panel will have a standard set of services which instruments can utilize. In between the break panels, panels are provided to allow access to a distribution channel for cables and services.

The outer former is fastened to the mirror cell at eight positions. Panels allow access to a distribution channel where the services run to one of two breakout panels that are reentrant into the mirror cell.

5.2 Meeting the Design Requirements for the Cable Wrap Assembly

The following sections describe how the overall design of the cable wrap assembly meets the design requirements indicated in the design requirements document and the performance requirements indicated in the systems error budget plan.

5.2.1 Mechanical Range

The cable wrap employs a circular rolling loop arrangement which allows a range of 560º. This satisfies the design requirements.

5.2.2 Capacity Requirements

The channel trunking has approximately 4600 mm^2 of usable cross section area in 4 channels 80 mm x 145 mm. Figure 26 on page 128 shows a full complement of cables and services within this available space including the necessary cable separators.

5.2.3 Mass

Table 5 -1 shows the mass and c of g positions of the cable wrap components.

TABLE 5 -1: Mass and c of g Positions of Cable Wrap Components

Item	Mass (kg)	C of G position in z, TTCS (m)	Mass moment wrt elevation axis (kg m)
Static cable guide	300	2.0	600
Rotating cable guide	200	2.0	400
Cable chain	140	2.0	280
Cables and services	326	2.0	652
Guide shuttle	160	2.0	320
Support brackets	74	2.1	157
Total	1200		2409

5.2.4 Size

Figure 4 on page 106 shows the Cassegrain cable wrap within the space envelope defined by the primary mirror cell and mirror cell support structure. The restriction in height available for the cable wrap leads to the requirement for two cable chains to be nested together in order to achieve the required capacity.

5.2.5 Cable Wrap Drive

The design for the cable wrap does not incorporate a separate drive, instead the inner rotating part is supported and driven by the instrument support structure and Cassegrain rotator. This is done for simplicity. The performance penalty due to the increase in friction and out of balance torques will be investigated in the servo system model. If there is a significant effect on the servo system, a separate drive can be incorporated.

5.2.6 Compressed Helium, Coolant, and Vacuum Lines

These services require multiple hoses of diameters up to 35 mm. The cable wrap has been sized accordingly.

Figure 26 on page 128 shows these services within the cable wrap. The minimum working bend radius in the cable wrap meets the manufacturer's recommendation for the minimum working bend radius of the Helium lines.

5.2.7 Balance

The cable wrap assembly is a substantial mass therefore balance must be considered as it effects the loads on the rotator drives, puts varying moment loads into the mirror cell, varying moment loads on the telescope tube drives and contributes to the rotator brake capacity. Contributions to out of balance are due to fabrication tolerances and the mass redistribution effects of the rolling loop arrangement.

ROLLING LOOP ARRANGEMENT. The cable chain loops change shape during operation see Figure 29 on page 132. From fully wound on the inner, to mid travel, to full travel the chain changes from circular to crescent to semi-circular in appearance and the c of g changes accordingly. The shift is approximately 1.2 m. This effect is compensated for by winding the upper and lower cable loops in opposite directions and keeping the mass of each loop the same. The residual out of balance due to the cable loops can be estimated by assuming that the masses will be maintained to 20%. The mass estimate for the rolling loops is 178 kg each, giving 35.6 kg. An rss of the residual for both loops gives $1.2x\sqrt{35.6^2+35.6^2}$ or 60kgm. which is within the allocation for the cable wrap for dynamic out of balance for the telescope tube.

FABRICATION ERRORS. Another source of imbalance for the cable wrap is eccentricity of the rotating cable former w.r.t. the rotation axis. When the inner loop is fully wound with cable, this will also contribute. Assuming an eccentricity of 10 mm, the out of balance will given by

$$\text{Out of Balance} = g \times e(MCL + MCD + MT) \qquad \text{(EQ 5 - 1)}$$

where: g is the gravitational constant, MCL is the mass of the cable loops on the inner former, MCD is the mass of the cables in the distribution channel and MT is the inner guide trough mass.

For e = 0.01 m, MCL = 178 kg, MCD = 44 kg and MT = 200 kg, the out of balance is 42 Nm.

MIRROR CELL AND TELESCOPE TUBE LOADS. The estimated out of balance of 640 Nm for the cable wrap is included in the Cassegrain assembly dynamic out of balance table. This figure assumes the telescope is near zenith. For horizon pointing the change in c of g does not effect moment loading of the cell or the altitude drives.

EFFECT ON ROTATOR. The out of balance torque is added to the load torques in determining the motor capacities. For this purpose the telescope tube is assumed to be pointing at horizon. For pointing near zenith, the change in c of g position will not effect the rotator. This will be included in the servo system model.

5.2.8 Cable Access

The inner and outer cable chain guides provide access from beneath by removing inspection panels. The flexible channel trunking can be opened from either side to extract cables or lay new cables / hoses in place.

Redundancy is inherent in the cable wrap design in that instruments generally will use a subset of the available services on each breakout panel. In addition, panels are identical and so instruments can be connected to an adjacent unused panel in the event of a failure. This also facilitates the easy interchange of instruments between ports.

5.2.9 Operational Performance

MOMENT OF INERTIA. The moment of inertia is estimated by

$$J = M \, x \, r^2 \qquad \text{(EQ 5 - 2)}$$

where M is the mass in kg and r is the radius of gyration in m.

For M = 496 kg and r = 1.39 m, inertia = 959 kg m^2, within the 2000 kgm^2 allocation.

DRIVE FRICTION. There are four main contributors to drive friction as follows:

1. Load induced friction of the rotator bearing. This is already accounted for in the bearing load friction detailed in the chapter headed 'Cassegrain Rotator'.

2. Sliding friction of the rolling loop against the cable guides. During rotation the only parts of the cable loop in relative motion to the channel guides are the ends of the rolling loop. If coulomb friction is assumed to dominate, the friction torque can be estimated by

   $$F_r = M \text{ x } g \text{ x } \mu \text{ x } r_a \qquad \text{(EQ 5 - 3)}$$

   where F_r is the friction force in N, M is the mass supported by the area subject to sliding action in kg, m is the friction coefficient, and r_a is the average radius from the rotator axis in m.

   M is assumed as equal to twice the mass of the loops. For M = 73 kg, m = 0.1, and r_a = 1.86 m, F_r = 133 Nm.

3. Sliding friction of the cables within the cable carrier. If cables are offset from the bending radius, they will move relative to the cable carrier during motion and cause friction. If similar assumptions are made to the previous sliding friction, a very rough estimate can be made by repeating the calculations using only the mass of the cables. For M = 44 kg, the friction torque estimate is 81 Nm.

4. Hysteresis and flexing of the cables and pipes and friction due to relative motion. These effects are difficult to estimate but the designs of the cable wrap will minimize the effect by implementing the following measures.

   a. The cable chains are relatively narrow in the bending direction. This keeps cables and hoses closer to the bending axis of the cable chain, reducing the amount of relative motion possible.

   b. As per the manufacturers recommendations, the cables and hoses will be separated by dividers, allowing them free movement.

c. As per the manufacturers recommendations, adequate free space (40%) will be left to allow the cables and hoses space to move to prevent binding on rotation.

d. Cables and hoses will be chosen with properties suited to this type of flexing. Helium lines will have PVC outer sheathing, copper cables will be selected with coverings which are designed specifically for use in this type of application.

SPEED OF ROTATION. The accelerations and speeds are relatively standard and are well within the specified capabilities of the flexible channel trunking.

5.3 Static Cable Chain Support

The static cable chain support is circular, with a cross-section providing two stacked 'U' channels facing in towards the center. These act as the guides for the cable chain. An inverted 'U' channel is provided with removable inspection covers on the outside, allowing services to be distributed from two breakout panels positioned within the mirror cell to a single slot where they enter into the inward facing u channel. The services are strain relieved at this point by clamping. The services enter the flexible trunking which carries the cables around the inward facing channel, doubling back in a loop, and onto the guide channel of the rotating cable chain support. The structure of the cable chain support is a sheet metal fabrication from stainless steel.

5.3.1 Mirror Cell Mechanical Interface

The mirror cell breakout boxes are reentrant into the mirror cell and therefore, clearance holes must exist in the mirror cell structure. Figure 30 on page 133 shows the cable wrap interface to the mirror cell. The mirror cell services distribution system will interface in these locations. The cable chain outer support is attached to the mirror cell on eight equispaced pads. The pads will be machined at the same time as the rotator interface to provide a flat surface for the outer cable wrap, independent of the mirror cell fabrication errors. 16 M8 tapped holes are provided on two PCR's of 2066.0 and 2420.0 mm.

5.3.2 Mirror Cell Breakout Panels

Two breakout panels are used to interface with the mirror cell services distribution system. They are 800 x 300 mm mounted on breakout boxes attached to the static cable guide. These boxes are reentrant into the mirror cell; all cables / hoses terminate with through bulkhead connectors. Helium lines, vacuum lines, and coolant lines will have self-sealing connectors.

5.3.3 Strain Relief of Cables/Hoses

Along the distribution channel and at the point where the cables / services go from the outer distribution channel into the inward facing channel, provision is made to secure the cables. Clamps are provided in the cable chain support channels which act on the flexible channel trunking. Within the distribution channel a cable tray is mounted and retainers are attached.

5.3.4 Mass

The mass is estimated to be 300 kg . It has a c of g position 172 mm from the mirror cell interface, 2000mm from the telescope tube elevation axis.

5.4 Rotating Cable Chain Support

The rotating cable chain support is similar in construction to the static support with the exception that the ‘U’ channels face outward, away from the rotation axis. The cable chain loops around from the static chain support and winds around the rotating support where it reaches a slot. The cables are strain relieved at this point by clamps and they pass through the slot and into the distribution channel. The distribution channel is a downward facing ‘U’ channel with removable inspection covers and breakout panels. The services are distributed to eight breakout panels which are the services interface to the Cassegrain facilities and instrumentation. There is one panel for each of the 5 ports, one for the science field fold mirror assembly, one for the guidance / wavefront sensor assembly, and one auxiliary. The inner cable chain support is attached to the instrument rotator by means of eight brackets.

Both chain supports must be installed in the zero position, fully wound on the inner guide. This is because the loops travel at different speeds (dependent on the ratio of the inner and outer diameters) and will collide if assembled any other way.

5.4.1 Mechanical Interface to Rotator

Eight support brackets are used to join the inner cable guide to the Cassegrain rotator. These have four M12 tapped holes on 1116.39 and 1085.9 PCR’s, offset in either direction from the bracket center line by 30mm.

5.4.2 Services Interface Panel

There are eight semicircular panels nominally 420 x 170 mm located on the underside of the rotating cable wrap near the corners of the ISS. These subtend an arc of 20 degrees on the distribution channel. They are positioned towards the corners of the instrument support structure for accessibility and to maximize available headroom above the instrument ports. These panels each supply identical services which instruments or facilities can use.

5.4.3 Mass

The mass is estimated to be 200 kg with a c of g position 172 mm beneath the mirror cell interface, 2000 mm from the altitude axis. The mass moment of inertia about the rotator axis is 386 kg m^2.

5.5 Flexible Cable Chain

The flexible cable chain is a form of articulated trunking formed by hinging rigid sections together. It is capable of supporting a lateral load while bending freely in-plane. There are a number of proprietary designs, and they are manufactured in a variety of sizes. For our application, four chains, each of cross section 80 x 145 mm, will be required to carry the expected services.

5.5.1 Rolling Loop Arrangement of the Flexible Cable Chain

The rolling loop arrangement is useful in that it minimizes friction. It is commonly used in large industrial machinery for linear applications, in conjunction with the flexible trunking. The range of 540º could pose problems for the cable wrap, but the rolling loop arrangement demonstrates an advantage in this respect. As the inner wrap is rotated, cable is peeled off the outer in a loop and laid down on the inner. The loop itself travels in the same direction as the rotation, but half as fast (for inner and outer of similar diameter). This gives a factor of two on the travel, see Figure 31 on page 135. In addition, because the inner loop is smaller than the outer, it travels even slower. This means more travel, estimated as follows:

$$\Theta = \beta \left(1 + \frac{R_2}{R_1}\right) \qquad \text{(EQ 5 - 4)}$$

Where Θ = the rotation of the inner cable wrap, β = the angle through which the rolling loop travels, R_1 is the inner loop radius and R_2 is the outer radius.

For the inner loops, R_1 = 1403 mm and R_2 = 2290 mm, β = 205º for 540º rotation (Θ = 540º). For the outer loops, R_1 = 1529 mm and R_2 = 2264 mm, β = 218º for 540º rotation. This difference shows the importance of proper installation of the cable chains.

5.6 Cable Guide Shuttle.

An annular shuttle is used to guide the cable chains and keep them in the guide troughs. This is especially important in the case of the Cassegrain cable wrap where the whole assembly will be rotated through 90º relative to the gravity vector allowing lateral loading of the cable chains (the cable chains may tend to fall out of the guides). The shuttle consists of an annular circular framework with 6 free running guide rollers. The shuttle is driven by the cable wrap loops.

6. *INSTRUMENT SUPPORT STRUCTURE*

This chapter describes the preliminary design for the instrument support structure and how it satisfies the design requirements. The practical considerations of implementing the design are also discussed.

6.1 Description of Preliminary Design

The instrument support structure interfaces the instruments and facilities to the Cassegrain rotator. An upper flange locates on the Cassegrain rotator and the assemblies are bolted together. Beneath the flange, the structure is roughly cubic in shape. In effect, it forms a type of three dimensional "optical bench". There are five available faces which form mechanical interfaces to instruments and facilities, one upward looking and the rest side looking. The faces will have the same mounting detail, which will allow instruments to be swapped between ports. Science instruments, facility instruments, calibration units or Adaptive Optics units can be attached in a variety of configurations. There is a science beam port in the center of each face, and the side looking port has an additional port, higher up, to feed the Adaptive Optics unit. See Figure 32 on page 136 and Figure 33 on page 137.

The bottom of the box is detachable to allow access to the acquisition and guidance assemblies inside. These include the high resolution wavefront sensor module, the science field fold mirror module, and the peripheral guider / low resolution wavefront sensor module. The modules are stacked, one on top of another, and the whole assembly attached to the ISS base.

6.2 Meeting the Design Requirements for the Overall Assembly

This section will describe how the overall design of the instrument support structure meets the design requirements.

6.2.1 Overall Dimensions

The overall dimensions are 1600 x 1600 x 1650 mm across the flats (l x w x h), telescope at zenith. The expected requirements of instruments and facilities call for large mounting areas and available volume. This drives the size of the ISS upwards. The size, however, is limited by considerations of the back focal length of the telescope in addition to the consideration that the telescope focal plane will lie at least 300 mm beyond the structure and that the available space for instrumentation will not be reentrant into the mirror cell.

6.2.2 Mass

The mass of the instrument support structure is 3800 kg. The optimized stiffness achieved by this structure for this mass gives 50 µm decenter of the upward looking instrument port, relative to the rotator when the telescope tube is moved from horizon to zenith. The material is steel. The flexure is used as a criteria in the FEA optimization to achieve a given mass. This mass is compared to that apportioned from the total Cassegrain mass balance budget. The flexure values obtained are input into the bottom-up pointing and tracking error budgets. See section 6.8.1 on structural FEA analysis.

6.2.3 Focal Stations

The science focal stations are geometrically central to the port faces. The science field ports have a diameter of 400 mm. A seven arcminute science beam at f/16 is 288 mm diameter where it intersects the port face.

The adaptive optics focal station is located 517 mm directly above (positive z direction, telescope tube coordinate system) the science port on the side looking face (duplicated on each side looking face). The port diameter is 200 mm. A 3 arcminute adaptive optics beam at f/16 is 170 mm diameter where it passes through the port.

6.2.4 Dimensional Accuracy

All of the locating and reference surfaces on the ISS will be machined. Readily achievable tolerances for NC machining have been assumed and the resulting expected errors have been included in the bottom-up pointing error table. It will be possible to achieve better precision levels and this will be a cost/benefit design trade off issue addressed in the critical design phase.

In addition to pointing considerations, instruments must be accurately aligned to the telescope optics. This places a requirement on the dimensional accuracy of the instrument port relative to the rotator axis, because the rotation axis of the Cassegrain rotator defines the telescope optical axis. A common requirement for IR instruments is alignment of a cold stop to the secondary. The stated interface port tilt tolerance of 0.0055º will correspond to a shift at the secondary of 1.3 mm which represents 0.1% of the secondary diameter. This is an acceptable fraction as instrument field stops are generally 5-10% larger than the secondary mirror.

The position of the focal plane between instrument ports due to the ISS is 50 µm which is acceptable. Greater accuracy can be achieved but at an increased cost.

6.2.5 Dimensional Stability

The dimensional stability of the ISS effects the pointing and tracking of the telescope. The major effects are thermal contractions and gravity induced deformations.

6.2.5.1 Thermally Induced Deformations

Differential thermal contractions between the ISS and the instrument rotator are avoided by matching the material (both are steel). At this time the alloy has not been chosen, but the goal will be to match the CTE with the Cassegrain rotator and primary mirror structure. (ASTM A36 CTE 8.3 x 10^{-6} / ºC). The overall dimensions will scale with temperature through the coefficient of thermal expansion and this can be significant on such a large structure. However, these effects can be calibrated out. Once calibrated, differences during a nights' observation will be negligible since the expected enclosure temperature drift (as predicted by the telescope enclosure group) is small (0.1 degree/hour).

Another potential source of thermally induced deformation is due to external heat sources which may cause long term or transient changes in the ISS and the rotator. There are no variable heat sources of significant magnitude in contact with the ISS (this requirement from the telescope enclosure group thermal management plan). The enclosure ambient air is coupled through convection but the change in enclosure temperature is sufficiently slow and the thermal mass of the ISS and rotator is sufficiently high that structures will remain isothermal to a high degree.

6.2.5.2 Flexural Stability

The most significant effect on the dimensional stability of the ISS is gravity induced flexure from the loads attached to the structure and from self weight. As the telescope tube changes in altitude and as the rotator rotates, the structure is reoriented relative to the gravity vector. The resulting changes in loads will cause deformations of the structure which will in turn effect the pointing and tracking. These deformations have been estimated for the preliminary design using FEA and the results are included in the Cassegrain assembly bottom up pointing and tracking error budgets.

Another source of deformations are induced deformations from the various mechanical interfaces. If a rigid structure is bolted to any of these interfaces and is not sufficiently co-planer, the ISS will deform significantly. This could effect the pointing model. The Interface Control Documents for the various assemblies attached to the ISS will ensure that the specifications for mating surfaces are adequate.

6.2.6 Flexure Compensating Models.

Flexure compensating models are commonly used to improve pointing and tracking performance of precision systems. These predict flexure errors from analytical sources or previous calibrations and rely on the repeatability of the errors. Two major sources of non-repeatability in flexure terms for the ISS are configuration changes of the systems attached to it and hysteresis.

6.2.6.1 Effects of Attaching Subsystems to the ISS.

When subsystems are attached to the ISS they will apply loads according to their particular configuration. Although the overall loads on the structure will be the same, the local loading may be different, thus, effecting the pointing terms associated with the ISS. To reduce this effect the local mounting points on the interfaces are designed to spread the loads into the structure.

In addition to acting as loads, structures attached to the ISS will interact with it, making it stiffer. This will change the pointing and tracking terms associated with the ISS. These effects are not considered to be significant.

6.2.6.2 Hysteresis.

Hysteresis is an inherent physical property of all materials, and is very small for steel, particularly for small strains. In the ISS, because of the requirements for low flexure and rigidity, strains are small and, therefore, the inherent hysteresis is small. The hysteresis in most structures is dominated by ‘working’ of fastened joints. The mechanical interfaces of the ISS are designed to be accurately co-planar and use positive location when shear loads are significant. This, in conjunction with adequately preloaded fasteners, will minimize the effects of hysteresis. A figure for hysteresis of 5% of the flexure magnitude has been assumed for estimating the non-repeatability of flexure. This is assumed to be a limit to the level of correction achievable with a look up table.

6.2.7 Light Tightness.

It is desirable to protect the area around the instrument windows from sources other than the telescope beam. The receiver detail bosses on the ISS will therefore form a light tight seal. In addition, the science and AO ports have standard interface detail for mounting baffle assemblies which will be supplied by the instrument builder. See Figure 34 on page 138.

6.3 Cassegrain Rotator Mechanical Interface to the ISS

The Cassegrain rotator interface performs the functions of locating the ISS on the rotator and of transmitting the structural loads from the ISS to the rotator. The requirements on the support of the rotator bearing play a major role in the specification of this interface. The interface is designed to distribute loads evenly into the rotator, and to deform in a smoothly varying manner with a limited amplitude. The initial flatness of the interface is also important to the smooth operation and operating life of the bearing. The design incorporates a circular flange attached to the internal cylinder of the ISS. The upper surface of the flange will be machined to provide a locating pilot diameter and a flat interface surface. The flange has a PCD of clearance holes for fasteners. The flange is deep enough to allow access to the fasteners and to facilitate their extraction from outside the ISS.

6.3.1 Initial Flatness

Flatness on this interface is determined from the requirements of the rotator bearing. This tolerance was apportioned between the top and bottom surfaces of the lower rotator ring, and the ISS interface. The ISS interface is apportioned 75% of the tolerance as it is a much larger component and, therefore, more difficult to machine. The tolerance required is 0.127 mm per 25 mm for radial flatness (dishing) and 0.038 mm per 90º segment for circumferential flatness (waviness). Thus, the radial flatness must be 0.095 mm per 25 mm or better and the circumferential flatness of these surfaces must be 0.029 mm per 90º segment or better. These tolerances are achievable for a component of this size.

6.3.2 Allowable Out-of-Flatness Deformation

Bearing manufacturers specify out-of-flatness deformation as radial and circumferential slopes over a given spatial scale. The assumption is that the slopes are smoothly varying and have no steps.

From the bearing manufacturers' requirements: Radial (dishing) deformation must be within 0.076 mm / 25 mm; Circumferential (waviness) deformation must be within 0.254 mm / 90º segment.

A finite element analysis model was constructed of the ISS and bearing interface. This model was loaded in the least favorable condition (horizon pointing) and the results showed that the deformations are well within the above requirements.

6.3.3 Fastener Detail

The fasteners attaching the ISS to the rotator are clearance bolts which clamp the circular flange of the ISS to the rotator. The flange underside has cleaned surfaces for each hole to allow proper seating of the bolts. Clearance between the underside of the flange and the ISS body allows bolts to be inserted or extracted from outside the ISS.

The bolt lengths exceed 5 times the bolt diameter. This facilitates proper preloading of the bolts which will be tightened to 70% of yield.

6.3.4 Locating Diameter

The ISS interface has a locating spigot which engages with the rotator interface. This provides a positive location for the ISS, a reference diameter for the overall dimensions of the ISS, and helps to keep the rotator interface circular. The diameter is xxxxx mm and the fit is H7h6.

The locating diameter tolerance is a trade-off between the desire to locate the ISS on the rotator accurately and ease of assembly. A locating clearance fit is used for this interface to ease assembly and disassembly.

6.4 Instrument Interfaces

The side looking ports are parallel to the xz- and yz-planes of the telescope tube coordinate system when the rotator is at the zero angle of rotation. Each side looking interface has two possible ports through which the telescope beam can be directed: the main science port, located central to the interface; or a higher port (in positive z direction) used by the Adaptive Optics system. The mechanical interface is formed by an array of raised bosses into which receivers are inserted. The receivers define a mounting plane. Instruments will use a subset of these receivers for mounting and support.

The upward looking port is parallel to the xy plane of the telescope tube coordinate system. The term ‘upward looking’ refers to the telescope tube at zenith. The telescope beam will pass directly through the main science port, located central to the ISS interface. The mechanical interface is identical to the side looking instrument interface with the exception that there is no AO feed port allowing two additional fastener receivers.

In order to simplify reconfiguration of the Cassegrain instruments, the overall interface loads will be constant. This is achieved by mounting a ballast weight with each instrument which maintains the loading and center of gravity position. In this way, the telescope tube and rotator balance are maintained as well as the validity of the telescope pointing model.

6.4.1 Telescope Foci

The telescope focus is located central to the mechanical fastening detail and is 300 mm out from the interface plane. At the upper adaptive optics port, the central axis is located 517 mm above the science port (positive z direction, telescope tube coordinate system) and is, therefore, 817 mm out from the interface plane.

6.4.2 Mounting Face Size

Each raised boss has a circular locating area 100 mm in diameter. These are arranged on an orthogonal grid, centered on the science port. The pattern is interrupted by the science and AO ports. These locations are shared by the instrument, associated electronics, and its ballast weight. The extreme bosses will form a square 1200 mm x 1200 mm, the largest interface foot print available to instruments.

6.4.3 Mounting Face Loads

The four side looking ports are divided into two opposite ports which carry 2000 kg, each and two opposite ports which carry 800 kg. These are designated ports 2 and 4, 3 and 5, respectively. The upward looking port (designated port 1) will carry 2000 kg. The loads have their centers of gravity along the port axis and 1 meter from the mechanical interface. The load includes the instrument, associated electronics, and a ballast weight. These loads and c of g positions are consistent with the telescope tube balance budget.

All the ports are identical in detail (the upward looking port has no AO feed) and load bearing capability, The loads are apportioned to each face in accordance with the Cassegrain assembly mass moment table and are consistent with the requirements for large instruments and the need to balance the rotator.

6.4.3.1 Relation of Port Load c of g to Available Mass

Science instrument ports, 1, 2 and 4, are capable of supporting 2000 kg with a c of g 1 meter out from the port mechanical interface. This includes the instrument, instrument electronics, and ballast weight. If the instrument and electronics package c of g is not located at the design position, ballast must be used on the port face to correct the c of g position for the combined port loading. The allowable instrument mass is, therefore, 2000 kg - ballast mass.

Facility ports 3 and 5 are capable of supporting 800 kg with a c of g 1 meter out from the port mechanical interface. This includes the instrument, instrument electronics, and ballast weight. If the instrument and electronics package c of g is not located at the design position, ballast must be used on the port face to correct the c of g position for the combined port loading. The allowable instrument mass is, therefore, 800 kg - ballast mass.

6.4.3.2 Ballast Weight

Each port payload includes a ballast weight that when combined with the instrument places a load on the port of 2000 or 800 kg with a c of g central to the port face and 1000 mm from the port face. Given the range of sizes and masses of instruments it is impractical to design a universal ballast weight and support system which satisfies all requirements. As a rule of thumb, for smaller instruments the Gemini project office will design the ballast system, while builders of larger instruments will design the ballast weight for their instrument. Ballast weights equivalent to the total port payload will be required for commissioning the telescope (maintenance of tube balance).

6.4.4 Receiver Details

The receivers are shouldered inserts which are screwed into the bosses on the ISS faces providing replaceable location features for instrument fasteners. In order to facilitate rapid instrument changes they are capable of accepting dowels that can safely support at least 1000 kg in shear loading. They also accept fasteners which are intended to provide pure clamping (clearance bolts). Instrument builders are able to use a combination of both features depending on the instrument configuration. A suggested arrangement for this is shown in Figure 39 on page 143 and Figure 38 on page 142.

6.4.4.1 Accuracy

The location diameter of the receiver is a location clearance fit in the ISS boss. The internal diameter which receives the instrument locating dowel is also a locating clearance fit. These fits are used for applications where accuracy of location is important, and ease of assembly. Table 6 - 1 shows the combination of tolerance build up on the locating position for an instrument.

TABLE 6-1: Fastener Location Tolerance

Item	Diameter (mm)	Value (mm)
Boss Location w.r.t. Rotator Interfaces	--	±0.025
Boss Hole Tolerance	72	+ 0.03 - 0.0
Receiver Diameter	72	+ 0.0 - 0.019[a]
Receiver Eccentricity (inner w.r.t. outer)	--	±0.005
Fastener Hole	50	+ 0.025 - 0.0[a]
Fastener	50	+ 0.0 - 0.016[a]
Total		± 0.041

a. Diametral tolerance, magnitude halved for rss

6.4.5 Instrument Mechanical Changeover Time

From the Gemini Science Requirements, the goal for instrument changeover is 20 minutes. The design of the fastener detail supports this goal by providing a standard interface that is compatible with the instrument handling equipment. The time required for the mechanical deattachment and attachment of instruments should not dominate instrumentation changeover times.

6.5 Instrument Support Structure Base

The instrument support structure base forms the upward looking instrument mechanical interface and also the mechanical interface to the assemblies contained within the ISS. The base of the instruments support structure is removable, to allow access to the assemblies housed inside.

The base is rigid, but efficient in terms of mass. It has a fraction of the mass apportioned to the ISS in the Cassegrain system mass / mass moment budget. Optimization of the ISS for flexure vs. mass includes the base.

The design consists of a top and bottom plate sandwiching orthogonal shear webs in an ‘eggcrate’ pattern. The bosses for the instrument fastener receivers are located at the shear web intersections and run between the top and bottom plate. The resulting structure is efficient and allows high ‘point’ loading at the bosses.

6.5.1 Mechanical Interface to the ISS

The interface is rigid, repeatable and easily engaged / disengaged.

A locating diameter is used with an H7h6 fit. The ISS is bolted to the rotator with clearance fasteners. The hole tolerance is -0.0, +0.127, and the shaft tolerance is +0, -0.076.

6.5.2 Mechanical Interface to the Guidance / Wavefront Sensing Modules

The design consists of a guiding pilot diameter which is a clearance fit on the guiding / wavefront sensing module. Accurate location is obtained by engaging self-jacking or expanding dowels, and the process will be completed by bolting the assemblies together with clearance fasteners.

Locating the guider interface on the base of the ISS compensates, to some extent, the lateral gravity induced flexure of the upward looking instrument interface, improving facility tracking performance.

6.6 Guidance / Wavefront Sensing / Science Fold Mirror Assembly Interfaces

The design of the ISS supports interfaces to the above assembly. At this time, the implementation of these functions is the subject of a design study by the UK Royal Observatories. The interfaces to the ISS are, therefore, only in a preliminary stage. The Acquisition & Guidance assemblies are comprised of three separate cylindrical modules located within the ISS. The ISS modules are stacked together forming a subassembly which is attached to the ISS base.

6.6.1 Space Requirements

The space available within the ISS is a cylindrical cavity 700 mm on radius and 1400 mm high. The design for the internal modules meets is functional requirements within this space envelope.

6.6.2 Mechanical Interface

The mechanical interface for the modules is on the ISS base. The ISS / ISS base interface is designed to facilitate disassembly to aid in access to the internal modules. The A&G modules are located radially by a spigot diameter and axially by a land. Fasteners are provided to bolt the assembles together. A dowel will be used to located the assembly in rotation about the rotation axis.

6.6.3 Electronics Interface

The electronics interface allows efficient disassembly and re-assembly of the A & G module to the ISS. Provision is made for supporting and routing of a cabling / services harness. This harness connects the module to its electronics enclosure. Sufficient space is available for locating the module's electronics enclosure outside the ISS. A mechanical interface for mounting the electronics enclosure is also provided.

The electronics enclosure interfaces to a standard instrument interface panel on the Cassegrain cable wrap.

6.6.4 Optical Interface

The ISS provides AO feed ports on each side looking instrument interface to allow the telescope beam to be directed into the AO unit (a function of the peripheral guider / LRWFS unit). The science ports are provided to allow the telescope beam to be directed toward the side looking instruments (a function of the science field fold mirror unit).

6.6.5 Mass Balance

From the Cassegrain mass/balance budget, the A&G internal modules have been apportioned a combined mass of 650 kg, with a c of g on axis (on the z-axis of the telescope tube coordinate system) and 2.84 m from the elevation axis (negative z direction, TTCS).

An allowable out of balance during operation of 50 Nm is given to allow for unbalanced moving elements within the A&G units.

6.7 Adaptive Optics System Interface

The design of the ISS supports interfaces to the Adaptive Optics (AO) System. At this time, the implementation of an Adaptive Optics system is the subject of a design study by the Dominion Astrophysical Observatory, Canada. The interfaces to the ISS are, therefore, only in a preliminary stage. The current concept has the AO module mounted on a side looking port. It accepts the telescope beam through the upper (AO) feed port, and returns the corrected beam, back through the science field port to be directed to an instrument via the science fold mirror.

6.7.1 Optical Interface

An AO feed port is provided on each of the side looking interfaces of the ISS. The telescope beam will be redirected by the AO feed mirror (a function of the A&G module) through this port, and into the AO module.

The feed port is of sufficient diameter to pass a 3 arcminute field (at f/16) and has provision for fitting light tight baffles. It is positioned above the science field port (positive z in the telescope tube coordinate system).

The corrected science beam is returned into the ISS through the science field port on the same face as the AO feed port. It is directed to the other instrument ports by means of the science field fold flat. The science port is 1100 mm up from focus (positive z in the telescope coordinate system) and is located at the midpoint of the instrument interface. Provision is made for fitting light tight baffles.

6.7.2 Mechanical Interface

The mechanical interface for the AO unit is the same as the standard science instrument interface. It is subject to the same restrictions as any instrument mounted on a facility port (ports 3 or 5, see previous section ‘Instrument Support Structure’ regarding Instrument Interfaces).

6.7.3 Electrical and Services

The AO module is treated the same as a science instrument. It has access to the standard set of instrument services. These are provided on an instrument services panel located above the unit on the cable wrap inner.

6.8 Structure

The overall size and shape of the structure is determined by the telescope focus positions and interface requirements of the various modular units which it supports. It is basically a cube with an internal cylindrical cavity. The cylinder is extended upward forming a flanged interface to the rotator. Stiffening webs run between the cylinder and the box. The base of the box is removable.

The instrument mounting detail has a major effect on the construction. With the current model raised bosses are supplied which accept threaded inserts. These inserts can receive fasteners each capable of supporting instruments weighing 2000 kg. This kind of detail lends itself to casting as a manufacturing technique. In addition, the raised bosses allow thinner sections to be used and facilitate accurate machining of the structure. The material is steel. The goal will be to match the CTE with the Cassegrain rotator and primary mirror structure. (ASTM A36 CTE 8.3 x 10^{-6} / ºC). The choice of alloy may be limited if casting is used as the manufacturing technique.

6.8.1 Structural Finite Element Analysis

An IDEAS Finite Element Model was constructed of the instrument support structure, see Figure 35 on page 139 and Figure 36 on page 140. The model was attached rigidly to ground at the rotator interface. Each port face was loaded by a lumped mass representing the port face payloads. The position of each lumped mass was along the port optical axis, one meter from the ISS / Instrument Interface. This model was used to determine the expected flexure of the ISS, fully loaded, when the telescope tube is moved from horizon to zenith.

The IDEAS optimization routine was used to minimize the mass of the structure for a flexure criteria of 50 μm shift of the instrument port face relative to the rotator. The resulting mass was 3800 kg. Figure 37 on page 141, shows the optimization mass history for a flexure criterion of 50μm.

7. ACQUISITION & GUIDANCE

At this time, the acquisition and guidance functions are the subject of a design study by the UK Royal Observatories. This section is based on the preliminary design concept as it exists at this time. It should be noted that this material is provided for information only with the interfaces and space allocations being the most important aspects at this time. The A&G system will be subject to an independent review process.

The design consists of three cylindrical modules, housed within the instrument support structure. See Figure 41 on page 143. These modules form a column which when bolted together house the engineering assemblies. Access and mounting will be gained by removing the base plate of the ISS. The first module houses the Calibration / High Resolution Wavefront Sensor; the second houses the Science Field Fold Mirror; and the third houses the Peripheral Guider / Low Resolution Wavefront Sensor and AO Fold Mirror. These will be discussed briefly in the following sections.

7.1 Calibration / High Resolution Wavefront Sensing

See Figure 42 on page 144 and Figure 45 on page 148.

7.1.1 Functional Requirements

The detailed functional specifications are outlined in "Acquisition and Guidance Functional Specification". The main functions are described below.

This unit will provide a deployable wavefront sensor into the science field center, for the purpose of calibrating the telescope optical system.

The structure also forms the rigid interface between the science fold mirror module and the instrument support structure.

7.1.2 Probe Deployment Mechanism

The details of this mechanism have not been developed at this time. It will be a relatively simple design as the probe is only required at the field center and is not required to track independent of field rotation.

7.1.3 Wavefront Sensor

The wavefront sensor has not been designed at this time, but is baselined as a 20 x 20 subaperture Shack-Hartmann sensor.

7.2 Fold Mirror Assembly

The parallel and orthogonal axes of rotation provide positional deployment of the 500 mm diameter lightweight folding mirror. Fine adjustments to the instrument ports are also provided from these motions. The mirror will be positioned and tilted to accuracies of approximately 0.005

measured at the deployed positions relative to a fixed reference point on the ISS. Movements will be made through DC servo motors, precision gear and pinion drives and will be monitored by absolute shaft encoders. A linear mechanical bearing will drive the mirror out of the telescope axis to a parked position clear of the science on-axis beam. Cleaning or changing this mirror, for one with an optimized coating will be possible during the day by day crew personnel. See Figure 40 on page 142.

7.2.1 Functional Requirements

The functional specifications are outlined in "Acquisition and Guidance Functional Specification”. The main functions are described below.

To enable the deployment and articulation of a science field fold mirror, capable of directing up to a 7 arcmin field at f/16 to any science port. This mirror will also direct facility calibration sources to instruments (if implemented) and the corrected science beam from the Adaptive Optics Unit.

The fold mirror and deploying mechanism will allow an unvignetted 12 arcmin field when retracted.

7.2.2 Mirror Deployment Mechanisms

The mirror is supported on a gimbal which allows it to rotate about a horizontal axis from vertical to plus or minus 45^{o}. This gimbal is mounted on a linear slide which is used to retract the mirror. This assembly in turn, is mounted on an annular rotating table used to index the mirror about the rotator axis.

The mirror deployment mechanisms will be designed to ensure the structural stability and repeatability consistent with the Gemini pointing error budget, and the structural stability consistent with the tracking error budget.

Mirror positioning is essentially indexing in nature, but small offsets are required for initial alignment. The mechanism’s motors will power down when in position.

7.2.3 Optical Design

The folding flat is capable of folding a 7 arcmin field at f/16. The details of the mirror and its support have not been fully developed at this time.

7.2.4 Interfaces

The fold mirror assembly will be located within the Instrument Support Structure and mounted off the structure of the high resolution wavefront sensing unit.

The mass of the assembly must be consistent with the upper mass limit of 600 kg for the entire A&G assembly.

7.2.5 Electronics

The drive electronics are located outside the ISS in one of two thermally conditioned electronics enclosures reserved for the Acquisition and Guidance assemblies.

7.3 Peripheral Guider / Low Resolution Wavefront Sensor (PWFS) Probe Assembly

In this module the PWFS systems and AO deployable mirror are housed. The PWFS fields of view are 10 arcseconds in diameter. The guide probes can, on demand, reach the center of the field and when the science instruments are in use leave a 3.5 arcminute diameter unvignetted science field. They are designed to work out to a maximum 12 arcminute diameter field. Guiding is achieved using the same pick off mirrors to rapidly track image motion and focus using the secondary tip - tilt / focus system. See Figure 43 on page 145.

7.3.1 Functional Requirements

The detailed functional specifications are outline in "Acquisition and Guidance Functional Specification". The main functions are described below.

This unit will be capable of deploying two independent guide probes / LRWFS anywhere in the telescope beam, from on-axis to the guide field periphery 6 arcminutes from center.

The probes will have tracking capability.

The probes will provide fast tip / tilt signals up to 200 Hz, and low order wavefront information every 30 - 60 seconds from natural guide stars with > 90% field coverage (at the North Galactic Pole).

This unit will also supply the feed to the Adaptive Optics Unit via an articulated folding flat mirror.

7.3.2 Probe Deployment Mechanisms

The probes consist of a pick off mirror (10 arcsec field) supported on a rotating arm. This arm can pivot out into the science beam, reaching the center if required, rather like a record player stylus. The pick off mirror directs the telescope beam into the guider / wavefront sensor optical system which rotates with it. The rotation will be provided by a DC servo actuator, the probe assembly is mounted directly on the output. The actuator rotation axis is tilted in towards the rotator axis, allowing the probe to follow the field curvature. This entire assembly is mounted, in turn, on a gear driven rotating table. This enables the probes to access all of the available guide field. There are two such assemblies, allowing two independent probes. The guide probe assemblies are located above the science field fold mirror, within the Instrument Support Structure. See Figure 44 on page 147.

These mechanisms will be capable of powering down once in position, but when necessary, will also be capable of controlled tracking movement.

7.3.3 Adaptive Optics Feed

A fold mirror capable of folding a 3 arcminuted field at f/16 into the Adaptive Optics Module can be deployed from one of the LRWFS rotating tables. The deployment mechanism is similar to that which positions the guide probes, but it is either deployed into the field center or parked.

7.3.4 Wavefront Sensors

The type of wavefront sensor used has not been decided at this time, but it must provide low order wavefront information over timescales of 30 - 60 seconds using natural guide stars with a field coverage of > 90% (at the North Galactic Pole).

7.3.5 Interfaces

The guider / LRWFS assembly is mounted off the fold mirror assembly structure within the instrument support structure.

7.3.6 Electronics

The electronics are located outside the ISS in one of the two thermally conditioned electronics enclosures reserved for the Acquisition and Guidance assemblies. One enclosure will house the drive electronics, etc and the other the CCD control electronics.

8. *ADAPTIVE OPTICS SYSTEM*

8.1 Functional Requirements

The functional requirements for this system are, at present, being developed by the Dominion Astrophysical Observatory. It should be noted that this material is provided for information only. The AO system will be subject to an independent design review process.

8.2 AO System Layout

A potential layout for a Gemini AO system is shown in Figure 46 on page 149. This area is, at present, in the early stages of the design process.

8.3 Interfaces

8.3.1 Mechanical

The Adaptive Optics system is mounted on an instrument port which is described in section "Instrument Support Structure".

8.3.2 Services

The AO unit will have access to a services panel, identical to the instrument services panel described in the section "Cables and Services".

8.3.3 Optical

A feed port is provided for the AO unit on all the side looking ports. The LRWFS module can deploy a mirror which can feed a 3 arcmin field at f/16 through this port into the AO unit.

The return beam from the AO unit is directed to the instrument by means of the science folding flat

9. SCIENCE INSTRUMENTS

The specifications for the science instruments are under development at this time. Configuration, size and mass are driven by the scientific requirements and detector technology, which will change with time. The current design provides a versatile instrument support facility catering for instruments of up to 2000 kg with dimensional envelope of approximately 2.5 meters, (linear dimension).

9.1 Available Space Envelope

In general, instruments can extend beyond the telescope focus by 2.5 meters, and laterally away from the port center by about the same amount (with the exception of headroom for side looking instruments, limited to 650 mm from the port center). See Figure 47 on page 150.

9.2 Instrumentation Mass Requirements

The instrument port faces, one upward looking and two opposite side looking ports, can accept 2000 kg loads with the center of gravity 1 meter from the port mechanical interface. This mass includes electronics cabinets and any ballast weights required to maintain the c of g position.

9.3 Instrumentation Facilities

9.3.1 Services

Instrument services will be available from a horizontal services panel located on the cable wrap inner, above the instrument interface. A description of the services provided can be found in the Chapter 11 "Cabling and Services".

9.3.2 Mechanical Interfaces

Each port face has 35 raised circular bosses, of which, the outer surfaces form the mechanical interface plane for instruments. Instruments can use any subset of these. The mounting detail at each of these locations is a locating diameter and a tapped hole. A more detailed description is provided in the section "Instrument Support Structure". The instrument builder can use these features in a variety of ways to locate and secure the instrument.

9.3.3 Optical Interface

Each port can supply up to a 7 arcmin science field with a focus 300 mm beyond the mechanical interface of the ISS. All ports are identical.

9.4 Operational Versatility

The preliminary design allows for up to three instruments to be mounted simultaneously in addition to two facilities (imaged calibration, or Adaptive Optics unit). The instruments are addressable in a matter of seconds by means of the folding flat mechanism. This provides a versatile system allowing efficient scheduling of instruments during changing conditions at night.

In addition to supporting backup observations in the event of deteriorating observing conditions and instrument failure, these changes can be carried out remotely by the telescope operator.

9.4.1 Reconfiguration

Physically changing an instrument or instruments at between ports will be a daytime operation. The telescope will have to be immobilized during the change. The design of the mechanical interface allows a straight forward detachment / attachment of the instruments. The services interface are similarly simplified. The rotator and telescope tube must be re-balanced and the drives enabled. This process is outlined in the section "Instrument Handling".

10. INSTRUMENT HANDLING

Instrument handling refers to many aspects relating to the operation of instrument systems. Storage of instruments, transport of instruments, servicing, and instrument changeover on the telescope are included.

10.1 Site Operational Facilities

The on-site facilities include an instrument disassembly / assembly area with adjoining Opto-mechanical and Electronics labs. A service lift is supplied to transport personnel and small instruments up to the observing floor. Large instruments will use the mirror lifting platform. See Figure 48 on page 152.

10.1.1 Storage of Instruments

Storage space is required for Instruments and associated hardware. These will include the instrument handling rig, alignment fixtures, special equipment and spares. This will be in either the instrument area or the enclosure basement. It is not planned to store instruments on the observing floor level nor to operate instruments off the telescope on the observing floor level.

10.1.2 Instrument Preparation and Reconfiguration

A relatively clean area is required for disassembly of the instrument. This must be large enough to accommodate the instrument and its handling rig in addition to the disassembled components. Adjacent electronics and mechanical clean rooms are required with adequate bench space for the disassembly of precision mechanisms, optics and electronics, etc.

10.2 Instrument Handling Rigs

All instrument work packages shall include the provision for a handling rig, of which the main purpose will be to provide for the safe movement of the instrument within a normal lab environment. Any special requirements for instrument handling during servicing such as orienting the instrument or hoists for disassembly will be built into this rig. The instrument handling rig must be able to deposit the instrument on the Cassegrain handling rig, or receive an instrument from it. The instrument handling rig will protect the instrument from shock while moving within the preparation area and enclosure.

Handling rigs which include lifting facilities will be certified for a safe working load exceeding the instrument mass. This safe working load will be clearly labeled.

10.3 Cassegrain Handling Rig

The Cassegrain handling rig is used to mount and demount instruments on the Instrument Support Structure and the ISS on the Cassegrain rotator. This function will include moving on the observing floor. It will have a lifting platform 1.2 m^2, capable of lifting a 4000 kg load vertically by 3 meters. Fine lateral adjustment will be provided to align instrument mechanical interfaces to the instrument support structure.

10.4 Instrument Changeover Procedure

The following events illustrate the changeover procedure between an instrument mounted at Cassegrain and one which has been off line.

10.4.1 Assembly

Assuming that the instrument has been partially disassembled for maintenance or a configuration change, the instrument will be assembled in the assembly area. Depending on the size of the instrument this procedure will take place with the instrument on its handling rig, perhaps utilizing features of the handling rig (hoists or handling fixtures).

10.4.2 Instrument Preparation Area

Once assembled and prepared for operation (e.g., pumped, cooled, etc.), the instrument will have services hooked up and will be tested. (Much of this testing will be automated either from a local workstation or from the telescope control room.) If the instrument is a cryogenic instrument the pump down can begin after a successful warm test. If all is acceptable, the instrument can remain in a state of readiness.

10.4.3 The Observing Floor

During an instrument changeover the following procedure will occur. The telescope will be brought to Zenith and the telescope drives locked, including the Cassegrain rotator. The lifting platform will be lowered. The waiting instrument in the preparation area will be moved, by means of the handling rig onto the lifting platform. The handling rig, of the instrument to be replaced will also be moved from its storage position in the preparation area onto the platform. The platform will be raised to the observing floor.

Meanwhile --

The Cassegrain handling rig will be positioned beneath the instrument to be removed and the platform raised to within a few mm of the instrument base. The non-locating fasteners of the instrument will be released (side looking instrument). The platform will be raised to take the weight of the instrument, and the handling rig moved away from the Instrument Support Structure. Upward looking instruments are simpler. With the platform raised to within a few millimeters of the instrument base, the fasteners are undone except three, straddling the center of gravity. These three are then removed in stages until the weight is taken by the platform and then removed. The instrument is lowered.

The instrument handling rig is brought forward from the lifting platform and the instrument is transferred to it. The instrument may now be withdrawn to the platform lift.

The replacement instrument will now be positioned on the Cassegrain handling rig and offered up to the Instrument Support Structure. Attachment is similar to detachment.

The instrument services can now be coupled.

The empty instrument handling rig can now join the other instrument and rig on the platform lift and both can be taken to a storage area within the basement.

10.5 Instrument Mounting Detail

10.5.1 Instrument Support Structure

The instrument fastening has been designed to accommodate a range of instrument sizes and weights. Instrument builders can choose a subset of many possible fixing points. There is an array of these fixtures 1200 mm square at 200 mm centers on each port. The detail pattern is only interrupted for the science field port, and on the side looking faces for the Adaptive Optics feed port. The fixing detail consist of a circular flanged collet, screwed into a raised boss on the instrument support structure. The flanged receivers form a flat surface to which instruments can be attached. The receivers have an accurate locating bore, 50 mm diameter and 50 mm deep, terminating in an M19 tapped portion. The collet can therefore act as a receiver for a self jacking dowel, or a plain 19 mm bolt. The large diameter dowel is particularly important for the side looking instrument interfaces. It allows a method of safe load transfer from the Instrument Support Structure to the Cassegrain handling rig and back again. It can also act as a location feature prior to engaging secondary locating fixtures or plain clearance fasteners.

10.5.2 Instrument

The instrument builder must consider both cases of instrument orientation, upward looking or side looking. In addition, the limitation of the Cassegrain handling rig must be taken into consideration, it has a straight lift capability, with limited lateral and rotational adjustments. The mounting detail on the Instrument Support Structure can be used in a variety of ways, but safe load transfer from the handling rig to the ISS is a necessity. After transfer the platform will be lowered slightly, clear of the instrument.

10.5.3 Instrument Location

There are no adjustments provided for on the ISS. For side looking instruments, adjustment of the locating features (i.e., translation of locating flat and V) may be provided on the instrument to align the remaining instrument fasteners to the ISS mounting detail (a one-time adjustment).

10.5.4 Instrument Securely Fastened

Once aligned, by the locating features or secondary dowels, the clearance fasteners can be engaged.

10.6 Maintenance of Telescope Tube Balance

The balance of the telescope tube must be re-established after instrument reconfigurations. The telescope has a balance system for minor balance adjustments but this is not designed to compensate for large mass moment changes. The instrument / electronics assembly will also contain a ballast weight, which will bring the total weight on an instrument port to a set target, to within a few kg. This way, the Cassegrain instruments can be reconfigured without need for a large capacity balance trimming system on the telescope.

10.6.1 Off-line Trimming

A facility which emulates the instrument port face will be provided at the telescopes. This facility will allow instruments to be mounted on a dummy interface to check compatibility and simulate operation. It will also have the capability of measuring the mass and center of gravity position of the instrument / electronics / ballast weight system. Any residual out of balance of the reconfigured Cassegrain can be reduced by the telescope balance trim system. Also, any residual must be within the allowance given to the dynamic out of balance for the Cassegrain area.

10.6.2 Dynamic Out of Balance

The static telescope tube balance can be achieved with the telescope trim system, but there are components that move during observations and between sky positions. These are mainly the Cassegrain cable wrap and the science field mirror, AO fold mirrors, and components within the instruments which cause a shift in the c of g during operation. The maximum allowable dynamic out of balance figure for the Cassegrain assembly is 1000 Nm.

10.6.3 Telescope Simulator (flexure rig)

A telescope simulator will be supplied at the base facility in Hilo and at the site facility in Cerro Pachon. It is proposed to use a modified welding manipulator that will have a standard interface identical to that of the ISS. (Copies of the ISS base may be used for this purpose). Instruments can be attached to this simulator and oriented to different positions as they would be on the telescope during operation.

Potentially this set up could be used to determine the ballast weight requirements to maintain mass and mass moments of the Instrument payloads as previously mentioned.

11. CABLING AND SERVICES

11.1 Cable Wrap

The Cassegrain cable wrap is required to carry services to the Cassegrain facility instruments and science instrument cluster. These services include power, data lines, control and status lines, cooling system hoses, and high pressure helium lines. The working rotation range is 540º.

11.1.1 Capacity Requirements

To determine the required capacity of the cable wrap it is necessary to determine how many breakout panels the instrument support structure will support and to list the services which are required at each port. Our estimated capacity is believed to be more than adequate for future needs of instruments. We have selected eight breakout panels to provide services and cables to the instruments at Cassegrain. Eight panels will provide redundancy and will allow up to 4 instruments, Adaptive Optics Units, Acquisition and Guiding Units, and the flip-in mirror to be connected at the same time. The outer diameter of the cables and services which will go through the cable wrap are estimated below.

11.2 Description of Cables Provided

The following cables will be supplied through the cable wrap: Telescope Control Reflective Memory, Time Bus, Status and Instrument Control, Science Data, and Cables for Visitor Instruments.

11.2.1 Telescope Control Reflective Memory

The representative fiber optic cable that has been assumed contains 4 breakout fibers. This enables one cable to be taken through the cable wrap; which can then be split off to form a daisy chain among the ports of 2 supply fibers and 2 return fibers. The fibers meet FDDI optical specifications and have a 62.5 µm core. The minimum required bend radius for long term application is 72 mm.

11.2.2 Time Bus

The time bus is made up of 4 coaxial cables. These cables will also be daisy chained about the instrument support structure breakout panels. The following signals will be supplied by the coax cables: IRIG B time code; 1 kHz signal; 100 kHz signal; and a 1 Hz signal.

11.2.3 Status and Instrument Control

The status and instrument control cable is also assumed to contain two breakout fiber optic cables which meet FDDI optical specifications. These cables will supply command controls from the control room to the instruments (or facilities) and will return status signals. The minimum required bend radius for long term applications is approximately 60 mm.

11.2.4 Science Data

Based on the expected future requirements for Gemini Instruments, 4 dedicated science data fibers per breakout panel have been assumed. The cable that will go through the cable wrap will consist of 1 cable with 24 fibers (minimum required bend radius of 172 mm) or 2 cables of 18 fibers (minimum required bend radius of 148 mm).

11.2.5 Visitor Instruments

To meet the potential demands of instruments developed for other telescopes and loaned to Gemini or visitor instruments, each breakout panel will contain 25 shielded twisted pairs and 4 coaxial cables. It is expected that only one instrument station would use these cables at any one time and therefore the cables will be daisy chained among the breakout panels, with the unused terminations blanked off to prevent inadvertent use.

11.2.6 Power

A general purpose Power cable will be provided in the wrap. A representative cable may have an outer diameter of 23 mm and could contain 8 triads (24 conductors) of 7 x 16 AWG wire. These cables will carry 8 independent power feeds (120V, 50/60 Hz) and will be locally distributed to the breakout panels terminating in 6 captive, 3 wire connectors (per panel) rated at 125 V.

11.3 Services

The following services will be supplied through the cable wrap: High pressure Helium lines for closed cycle cooling systems, plumbing lines for the water/glycol feed to the instrument cabinet heat exchangers, and a vacuum hose.

11.3.1 High Pressure Helium Hoses

The high pressure helium hoses are required to operate closed cycle coolers and/or Joule-Thomson coolers on infrared instruments. These will be manifolded connections. Three sets of hoses will be provided. One set will supply the closed cycle coolers, one will supply the Joule-Thomson coolers and one set will be used as a spare. The hoses have an outer diameter of 27.94 mm and a minimum flexing bend radius of 190.5 mm. The possibility of using the same supply lines for the JT coolers and closed cycle coolers is being investigated. This would cut down the number of lines required.

11.3.2 Water-Glycol Coolant Hoses

The water-glycol hoses will service the heat exchangers which will be incorporated into all electronic enclosures at Cassegrain. These hoses will be similar to hydraulic hoses found in industrial applications with a PVC or PUV jacket. The outer diameter will be 27.94 mm.

11.3.3 Vacuum Lines

Vacuum lines are required to supercool liquid Helium. The vacuum required is approximately 10^{-2} torr. The vacuum line will be daisy chained among breakout panels and will also have an outer diameter of approximately 28 mm. Appropriate flow control valves and back filling apparatus will also be provided. The vacuum pump will be housed in the plant room.

11.4 Overall Lengths of Cables

The cables which have to be routed from the Cassegrain wrap to the telescope control room include data cables, status and control cables, the time bus, and visitor instrument cables. Based on the latest drawing which show a simplified routing of cables through the telescope, the estimated length of cables is approximately 60 m. The services (high pressure Helium, vacuum, and plumbing for the heat exchangers) are estimated to be 61.2 m.

12. THERMAL CONDITIONING

12.1 General

The stringent image quality specifications for the Gemini Telescopes along with the requirements for excellent IR performance puts emphasis on thermal conditioning of the telescope systems.

If sufficiently large, uncontrolled heat generation at Cassegrain would be detrimental to the telescope performance. This can occur through three mechanisms;

The first is the relatively large temperature difference between the gas exhausted from electronics racks and the enclosure ambient air. This will cause plumes within the enclosure which may enter the telescope beam. A related effect is the local heating of the telescope structure which is released into the telescope beam by convection.

The second effect is the proximity of heat generated to the mirror, telescope beam, and instrument windows. Hot sources will emit a thermal signature which can be a significant source of background noise.

The third effect is thermally induced distortions of structures and optics caused by transient heat generation.

The main step taken to reduce these effects is to actively remove the heat from the Cassegrain area by employing air to liquid heat exchangers for the electronics and liquid cooling of the rotator drive motor subplates.

12.2 Power Generated

The instruments and facilities will generate heat which will be released into the enclosure unless controlled in some way. The heat generated is summarized in Table 12 -1.

12.3 Electronics Enclosure Heat Exchanger System

The instrument electronics boxes will be sealed and insulated and have an integral air to liquid heat exchanger. The liquid coolant will be transferred through the cable wraps, and plumbed to remote chillers situated in the plant room. The chillers will exhaust the heat into the telescope heat exhaust duct.

TABLE 12-1: Cassegrain Area Heat Generation

Source	Heat Generated (kW)	Heat Removal Method	Residual (kW)	Comments
Rotator Drive Electronic	2 (2 cabinets)	Air / Liquid Cooled Enclosure	0.1	Cabinets on center section
Rotator motors	0.124 (4 motors, sidereal output)	Liquid cooled motor subplate	0.01	Residual dissipates into rotator structure / mirror cell
Bearing and Drive Friction	0.26 (sidereal rate)	Passive Dissipation	n/a	Dissipate into rotator structure
Guidance / WFS / Fold Mirror Electronics	1	Air / Liquid Cooled Enclosure	0.05	Cabinets mounted outside ISS
Instrument / Calibration / AO / Electronics	5	Air / Liquid Cooled Enclosure	0.250	Cabinets mounted with units
ISSΔT	0.03	Passive Dissipation into ISS/Cell Cavity	0.03	DT Assumed to be 1ºC
Heat Leakage from coolant return lines	0.04	n/a	0.04	Well insulated lines impractical for cable wrap
Total			0.53	

12.4 Air to Water Heat Exchangers

We have assumed that the electronics boxes are sealed units, generating 1 kW each and that their internal temperature is stabilized at 20 ºC. Further, we have assumed that the liquid coolant is supplied at ambient temperature (0 ºC) to avoid thermal insulation problems. In order to select an appropriate heat exchanger, we must determine the thermal resistance required for proper performance. This is given by the equation below:

$$\Theta = (T_{air(in)} - T_{W(avg)}) \,/\, Q \qquad 12 - 1)$$

where: Θ = thermal resistance, ºC/kW; $T_{air(in)}$ = inlet air temperature, ºC; $T_{W(avg)}$ = average water temperature, ºC; Q = required heat dissipation rate in kilowatts.

For each kilowatt of heat removed from water flowing at 1 gal/min, the temperature will increase approximately 4 ºC. If we assume a flow rate of 1 gal/min then the average temperature of the water in the heat exchanger is 2 ºC. Thus Q = 18 ºC/kW. Several commercially available heat exchangers can meet these requirements.

12.5 Remote Chiller System

The purpose of the remote chiller system is to remove heat from the liquid coolant which supplies the heat exchangers on the electronics racks. The liquid coolant will return to the chiller at approximately 4 ºC and will be cooled to approximately 0 ºC before returning to the electronics heat exchangers. The electronics enclosure heat exchangers and the rotator motor heat exchangers are plumbed into the telescope liquid coolant system. The chillers will be located in the plant room of the telescope enclosure and will exhaust the heat into the telescope heat exhaust duct.

12.6 Recirculating Coolant Pumping Requirements

In order to determine the pumping requirements for the system, an estimate of the pressure drops must be made for the required flow rate. In order that each of the air to liquid heat exchangers located on the electronics racks can remove 1 kW of heat, they must be supplied with at least 1 gal/min of coolant (assumes water). If the coolant lines are manifolded into one 3/4 inch bore before the Cassegrain rotator, the total flow rate for 6 kW of generated heat is 6 gal/min (instrument drive motors are assumed to dissipate heat into the instrument support structure). Pressure drop for 3/4 in. pipe is 4 psi per 100 ft. plus 1.5 psi per 90º short radius bend. If we assume that the heat exchangers are connected in parallel, the worst case pressure drop is for the case where 6 gal/min are going through 1 heat exchanger, which has an associated drop in pressure of approximately 5 psi. Total for a 200 foot system with approximately 10 bends including the heat exchanger is about 30 psi. These requirements are met by the telescope water cooling system.

The remote chiller system must be capable of removing 6 kW for a ΔT of approximately 4 ºC. These requirements are met by the telescope water cooling system.

12.7 Heat Loss to Enclosure

The heat loss to the enclosure includes the following sources: Electronics Cabinets; Coolant Return Lines; and Heat Generation within the Instrument Support Structure. Heat loss due to these sources is calculated, assuming that conduction is negligible.

12.7.1 Electronics Cabinets

The electronics cabinets will require thermal isolation. We assume there are 6 identical square cabinets, with each side 500 mm. Each cabinet has an internal operating temperature of 20 ºC. We further assume that the heat transfer is dominated by the thermal insulation surrounding the cabinets. We assume the insulation is 25.4 mm thick with a thermal conductivity of 0.045 W/(m ºC). Heat transfer is calculated from the following relationship:

$$q = \frac{1}{\frac{x}{k} + \frac{1}{h}} A \frac{(T_c - T_{air(in)})}{x} \qquad \text{(EQ 12 - 2)}$$

where: q = heat transferred, W; k = thermal conductivity of the insulation, W/(m ºC); A = total area, m^2; (T_c - $T_{air(in)}$) = temperature drop from inside cabinet to ambient, m; and x = insulation thickness, h is the passive heat convection coefficient.

For the assumptions above, q = 37 W.

12.7.2 Coolant Return Lines

Heat loss due to the supply lines is neglected as they should be approximately 0 ºC (close to ambient). If we assume that the return pipe is not insulated, heat loss to the enclosure is estimated with the following relationship:

$$q = \frac{1}{\frac{x}{k} + \frac{1}{h}} A \frac{(T_w - T_{air(in)})}{x} \qquad \text{(EQ 12 - 3)}$$

where: q = heat loss, W; U = overall heat transfer coefficient, W/(m^2 ºC); A = surface area, m^2; and (T_w - T_{air}) = mean temperature difference, ºC.

For 27mm line diameter, 30.5m lines, wall thickness of 3.1mm and return temperature of 4 degrees C, q = 41 W.

12.8 Electronics Enclosure Air Circulation

The enclosures will be sealed and air will circulate through the air-to-liquid heat exchanger. The enclosure temperature is therefore controllable, by controlling the coolant flow rate, in the same way as domestic central heating radiators. The thermal stability and ability to have "room temperatures" should enhance the reliability of the electronics. However, the air must be recirculated and the cabinets insulated.

12.8.1 Temperature Monitoring

Because the electronics enclosures will be closed systems they are dependent on the cooling system. The electronics may cease to function or be damaged when operated with the coolant system shut down. Some form of temperature monitoring with error reporting to the telescope control system will be incorporated.

12.9 Heat Generation Within the Instrument Support Structure

12.9.1 Intermittent Heat Sources - IR mode, aO and AO active, Guider Active

Guide probes and mirrors will have drives which move components into position prior to observation. This will generate heat within the instrument support structure. This is an intermittent source of heat which will convect into the chamber and conduct into the connecting structures. Individual components which tend to get hot will radiate thermally (even if the heat involved is very small, i.e., motor windings). All of these effects will decay with various time constants when the activity ceases, they are considered negligible effects to the overall thermal integrity.

12.9.2 Continuous Heat Sources

Items such as guiding, wavefront sensing, and AO will continuously produce heat when used. In addition, there will be friction heat load from the bearing and residual heat conduction from the rotator motors, through the telescope structure. This heat is released into the cavity within the ISS and mirror cell bore, exits the mirror bore, mixes with the air flushing the telescope and traverses the primary mirror. The table shows estimates for these heat loads.

TABLE 12 -2: Estimated Heat Loads

Item	Heat convected into cavity (w)	Comment
Rotator Bearing (tracking speeds)	0	
Rotator Motors (rated load)	1.2	Local heating of cell
A&G Assembly	50	Design goal for A&G
Mirror Cell Structure ($\Delta T = 1^oC$)	34	Unconditioned cell
ISS Structure ($\Delta T = 1^oC$)	33	Unconditioned structure
Total	118	

AIR VOLUME. The air volume enclosed by the ISS and mirror cell is given by

$$V = \frac{\pi D_c^2}{4} H_c + \frac{\pi D_i^2}{4} H_i \qquad \text{(EQ 12 - 4)}$$

where: D_c and H_c are the diameter and height of the cylindrical cavity in the mirror cell in m. D_i and H_i are the diameter and height of the cylindrical ISS cavity in m.

For $D_c = 1.5$, $H_c = 1.8$, $D_i = 1.4$, $H_i = 1.6$, $V = 5.6\ m^3$.

PASSIVE FLUSHING RATE. The exchange rate assumed for this volume is 1 volume every 10 minutes. The mass exchange rate is given by

$$\dot{M}b = \rho \ x \frac{\dot{V}}{60} \qquad \text{(EQ 12 - 5)}$$

where r is the air density in kg/m^3 and is the volume exchange rate in m^3 /min.

For $\dot{V} = 5.6$ and $\rho = 0.8\ kg/m^3$, $\dot{M}b = 0.075$ kg/sec.

Assuming perfect mixing of the air, the temperature rise of the convected gas exiting the volume due to the heat input can be estimated by $\Delta Tb = \frac{Q}{C_p \ x \ \dot{M}b}$ where Q is the heat input (w), Cp is the specific heat capacity of the gas and $\dot{M}b$ is the mass flow rate from the tube. For Q = 118w, Cp = 1 x 103 w/^{o}C, and $\dot{M}b$ = 0.075 Kg/sec, $\Delta Tb = 1.57\ ^oC$.

HEATING OF AIR ABOVE PRIMARY MIRROR. If we assume that the passively convected air mixes with the air moving across the primary mirror bore, the mixed air temperature can be estimated by

$$T = \frac{\dot{M}a \ x \ Ta + \dot{M}b \ x \ Tb}{\dot{M}a + \dot{M}b} \qquad \text{(EQ 12 - 6)}$$

where $\dot{M}a$ and Ta are the mass flowrate of flushing air (kg./sec) and flushing air temperature respectively (ºC). $\dot{M}b$ and Tb are the mass flow rates (kg/sec) and temperatures of the convected air (ºC) respectively.

The mass flow rate of flushing air is estimated by

$$\dot{M}a = A \ x \ Vf \ x \ \rho \qquad \text{(EQ 12 - 7)}$$

where: A is the cross sectional area of the flushing/mixing control volume (m^2), Vf is the flushing velocity (m/sec), and ρ is the flushing air density (kg/m^3). A is assumed to be equal to the primary mirror bore diameter x 0.3m.

For *Vf* = 1 m/sec, and ρ = 0.8 kg/m^3, $\dot{M}a$ = 0.29 kg/sec.

T is now estimated as 273.32 K, for Ta = 273 K.

EFFECT ON IMAGE QUALITY. The effect of this temperature increase on the 50% encircled energy diameter (arcsecs) is estimated by 0.156 x $dT^{6/5}$. This relationship is used by the Gemini optics group and Enclosure group to estimate the seeing effects due to thermal pluming from the telescope structure and secondary mirror assembly. For dT = 0.32^{o}C, seeing = 0.040 arcsec for a flushing air velocity of 1m/sec. This figure would be for a dT covering the entire mirror surface. The control volume represents only 10% of the mirror surface. Assuming the seeing effect scales with area, the estimated seeing will be of the order of 0.004 arcsec.

12.9.3 Systems Thermal Management

It is difficult to select one solution for all of the effects, especially at this time when all the details of the mechanisms and electronics are not known. However, the following will be used as guidelines in development of the Cassegrain area.

1. Reduce the heat generated - by using, where possible, efficient mechanisms which will require smaller motors.

2. Where possible using motors and mechanisms which can be depowered when stationary.

3. Match motor sizes to the drive load to minimize thermal loads.

4. Insulate against convection or conduction, where appropriate and practical.

5. Heat sink generating sources - heat intensity is a factor, efficient heat sinks will diffuse the heat.

6. Reduce radiative effects - parts which tend to get hot should be shielded, i.e., motor windings, individual electronic components.

7. Allow flushing of convective areas within the instrument support structure.

8. Actively cool components - the cooling system could be extended to locally water-cooling individual assemblies or components.

13. DESIGN TRADE-OFFS

This section will explain in some detail the reasoning behind the Cassegrain preliminary design. Some of the alternative concepts which were considered and rejected are described along with the rationale. This section presents some of the more detailed background work not covered in the main report.

13.1 General

The requirements for wide spectral coverage and operational versatility of instruments combined with stringent image quality goals for the Gemini telescopes has led to a novel concept for the Cassegrain Instrument Support Structure / Rotator. Central to the design is the simultaneous mounting of multiple instruments at the Cassegrain. The approach taken is to mount these instruments rigidly to an instrument support structure in an arrangement which allows one instrument to be fed by the direct telescope beam (throughput and emissivity optimized) and to redirect the telescope beam to the other instruments by means of a folding flat. The entire assembly is mounted on a rotator which physically derotates the entire Cassegrain cluster.

13.2 Fixed Instrument vs. Instrument Exchange Scheme

An instrument exchange scheme was considered which allowed any Cassegrain instrument to occupy the direct telescope beam, with advantages of throughput and emissivity. The requirements of instrument services, particularly the IR instruments meant that standby instruments would have to be stored on the bottom surface of the mirror cell. This restricted the available space for instruments. In addition, maintaining telescope tube balance during instrument changes would have been difficult. It was decided that it would be an expensive and risky undertaking to fully automate this type of instrument changeover scheme.

13.3 Effect of Removal of Nasmyth Foci

The removal of Nasmyth foci was driven by cost and performance considerations for the telescopes. However, it was a prerequisite that large instruments, expected to be up to a few meters in size, and weigh up to 2000 kg, could be supported at Cassegrain. This is difficult to do with an instrument exchange scheme and still retain the demanded instrument versatility and performance.

13.4 Instrument Rotator

The instrument rotator physically rotates the instrument cluster to orient and track the field rotation. This is the conventional approach, the only area of contention is the large loads that the Cassegrain cluster will impose on the rotator and mirror cell given the stringent image quality specification. It is shown in the design that this large instrument mass poses no special problems for the components concerned. The telescope mirror cell exhibits no problems that are associated with the relatively large moment load imposed by the Cassegrain cluster.

13.5 Rotator Bearing

The bearing type chosen for the Cassegrain rotator is a crossed-roller type bearing. Other bearing types that were considered are outlined below, but this was identified as a good choice weighing cost, risk and performance.

13.5.1 Mechanical Bearings

Static capacity was not a factor in bearing selection. Given the internal diameter of the bearing and driven by the requirement to clear the telescope beam, all mechanical bearings that were considered had more than adequate capacity. High friction, which is non-linear at slow speed is a property of all large diameter mechanical bearings. Different bearing configurations, however, have slightly different properties and requirements for the mounting structures.

13.5.2 Gothic Arch or Four Point Contact Bearing

These bearings have the advantage of being tolerant to mounting surface irregularities, either due to manufacturing errors or deformation. It is quite common to have large variations in the no-load running torque, depending on angle of rotation (~ 300%).

13.5.3 Three Row roller Bearing

These bearings are inherently stiffer than other types of mechanical bearings, have higher capacity and have the lowest friction. They do, however, have the most stringent requirements for the mounting surface and are 4 to 5 times more expensive than the equivalent crossed-roller bearing.

13.5.4 Wire Race Bearing

Wire race bearings have the most uniform friction characteristics. They were ruled out because of the difficulty in preloading them consistently and because of their low rigidity.

13.5.5 Hydrostatic Bearings

Hydrostatic bearings have the great advantage of nearly negligible friction and very high rigidity, very desirable attributes as far as the drive servo system is concerned. They were rejected over the mechanical bearings because of high risk and complexity in the supporting infrastructure. The rotator bearing has to cope with changing load types during operation. At Zenith, it supports thrust loads, at horizon, it supports radial and moment loads, with combinations of all three in intermediate positions. This changing load environment complicates the design of a hydrostatic bearing.

13.5.6 Hydraulic Bearings

Hydraulic bearings have an additional problem associated with oil contamination. Not a major problem in the other telescope drives, it would be difficult to protect the Cassegrain instruments and optical components from contamination given the position of the bearing and the changing orientation.

13.5.7 Air Bearings

Air bearings get over the contamination problem but would inject high frequency vibration into the structure, given the high capacity required.

13.6 Rotator Drives

The rotator drive consists of a large rotating ring gear (~ 1600 mm PLD) driven by two sets of opposing pinion pairs, four motors in all. This is a conventional approach, the only area of concern is the accuracy required of the drive given the image quality specifications. The report shows that the performance is acceptable. Other types of drives were considered as listed below.

13.6.1 Cable Traction Drives

This type of drive has advantages of smooth operation and higher accuracy than gear drives, but was seen as more risky than a conventional gear drive. The space restriction in the rotator area was also a consideration.

13.6.2 Direct Friction Drive

Accurate and smooth in operation, this type of drive has a very low torque capacity rendering it unsuitable for use with a heavily loaded mechanical bearing.

13.6.3 Direct Drive

A large diameter motor can be constructed using the structure of the rotator itself. A component of the rotating part of the rotator acts as the rotor, while the stator would be attached to the stationary part. There are therefore, no drive components as such. This is an elegant way to design out the drive components. This type of motor is capable of sufficient torque. It was rejected over conventional gear drives primarily for the reasons of cost. There were, however other concerns regarding thermal management.

13.7 Encoding

The encoding scheme used in the rotator design consists of rotary encoders driven by anti-backlash pinions. there is provision for four encoders, each 90º apart. This is a conventional approach. Eccentricities in the bearing and rotator housing in addition to gear indexing errors and geometric errors in the drive train will lead to encoder position errors in excess of the required precision. A calibration scheme is essential to linearize these errors. This is possible to a high degree since the errors are repeatable.

13.8 Inductance Tape Encoders

Provision is made for the possible addition of an inductance tape encoder. This would reduce but not eliminate the need for calibration. Bearing errors, registration errors and eccentricities of components would be significant.

13.9 Cable Wrap

The cable employs a rolling loop arrangement. Cables carried in a supporting flexible conduit are wrapped around an inner circular former and looped back onto a circular outer former. As the inner former is driven, the loop advances and cable is wound off the inner and deposited on the outer. Four loops are used for the required capacity. This type of arrangement is used in several existing telescope systems. One loop would be preferable, but this would increase the depth of the cable wrap, restricting instrument space. Other arrangements were considered and rejected as described below.

13.9.1 Spiral Wrap

This arrangement allows rotation by winding the cables in a spiral form, like a clock spring. This arrangement requires movement of the entire length of the cable wrap, increasing drag (undesirable for the rotator servo). In order to get the desired rotation range of 540º, the cable lengths would be excessively long. Supporting the cables under transverse gravity loading (telescope at horizon) is also difficult.

13.9.2 ZigZag Frame

This involves a hinged carriage made from sections in the form of a zigzag, wrapped around the rotating part. It has similar problems to the spiral option. It is useful if the orientation does not change.

13.10 Cable Wrap Drive

The cable wrap inner is supported from, and driven by, the rotator. This is unlike the other drives on the telescope which employ independently driven cable wraps to protect the drive servo systems from being dominated by cable wrap drag and stiction. This approach is taken at the Cassegrain because the mechanical bearing dominates the stiction and friction of the rotator and the accuracy required is an order of magnitude less than the other telescope drives. Advantages of this approach are simplicity, low cost and compactness of design.

13.11 Break Panels

There are eight break panels on the inner part of the cable wrap which form the instrument services interface. The outer part of the cable wrap carries two break out boxes which are reentrant into the mirror cell.

13.11.1 Instrument Services Breakout Panels

These panels are flush with the bottom of the cable wrap inner. In this way they present the cleanest profile when the Instrument Support Structure is removed. This arrangement also allows the instruments to potentially use the space laterally out from the port face.

An alternative arrangement is to house the breakout panel in boxes stood off from the cable wrap inner (hanging down, telescope at zenith). These would be located on the diagonals of the Instrument Support Structure box. This arrangement will restrict instruments from using space laterally out from the port face, but would provide maximum headroom.

13.11.2 Mirror Cell Breakout Boxes

The position of these boxes is largely determined by the telescope services distribution system which runs inside the mirror cell. There are two of these, 90º apart. In the cell the boxes can be larger than if they were outside, a desirable feature allowing for slack in the cables and hoses.

13.12 Instrument Support Structure

The instrument support structure is a monocoque design with a cubic outer shell and a cylindrical inner shell joined by stiffening shear webs. Circular bosses are located at the intersection of the shear webs and these house the inserts for the instrument mount fastening components. The bases are proud of the surface and machined to define the locating geometry of the structure. This type of structure is very efficient while allowing many possible mounting configurations. It is however, structurally complicated and almost implies casting as a manufacturing technique. Other possibilities were considered and are outlined below.

13.12.1 Fabricated Truss Structure

The frame structure is possible but it is difficult to have more than a very few hard points for mounting assemblies. The rotator bearing also requires a rigid mount which distributes the loads evenly.

13.12.2 Fabricated Space Frame Structure

This would involve construction from square tubular section, with shear webs in the panels. More attachment points for instruments are available than with the truss structure, but it was found to be much less rigid than the monocoque design. It has the advantage that it would be easier to fabricate by welding than the monocoque design.

13.13 Material

The material chosen is steel because of its weldability and low cost. Although the chosen method of manufacture is casting, it may be necessary to cast the structure in parts and weld it together. Aluminum could be used with appropriate attention to spreading fastener loads and the interface design. It is expected that using aluminum would give slightly better rigidity for a given mass, once optimized. Using Aluminum would make the performance of the rotator susceptible to temperatures changes due to the difference in CTE between it and the rotator however structural stability of the ISS may be compromised by bolting rigid aluminum instruments to a steel ISS.

13.14 Size and Position

The size of the ISS is determined by the back focal distance of the telescope and the distance that the focus is out from the mechanical interface. This distance is reserved for baffling and calibration of IR instruments. It is set at 300 mm. If it were reduced, the ISS could increase in size or be moved down, increasing the instrument headroom. The 300 mm distance is seen as a minimum, and the back focal distance is fixed.

13.15 Instrument Mounting Detail

The concept involves a number of raised bosses on each port face into which a receiver insert is fastened. The receivers are flanged with the outer face forming a circular pad. These pads form the instrument interfaces. The internal detail of the receivers has a locating diameter and a threaded portion. They are positioned at regular intervals, 200 mm apart. This allows up to 42 possible locating positions on each face. There are no adjustments, accuracy is determined by the geometric tolerances of the ISS and the locating diameter clearances.

The receivers are capable of accepting dowels which will support up to 1 tonne each. This is a requirement for safe load transfer when mounting large instruments. This places a stringent requirement on the local strength and rigidity on the ISS. Increasing the number of available attachment points greatly complicates the internal structural detail.

13.16 Access to Internal Assemblies

Internal access to the ISS is achieved by removing the ISS base. The base forms the interface to the fold mirror and guider / wavefront sensor assemblies. It may be possible to clean the internal optics without removing the base, but more involved maintenance will require base removal. Access panels or holes in the ISS body could be added but this will compromise the structural performance and take up space which could be used for instrument mounting.

13.17 External AO Unit Concept

The original concept for the AO system had the unit mounted inside the ISS with the A&G. Increasing demands on this space by the A&G and in an attempt not to compromise the AO system the unit was moved to one of the ISS side ports. The AO unit will interface to the ISS in the same way as an instrument. It is fed through a port provided, above the science field fold mirror. The AO feed mirror is part of the Guider / Wavefront sensor module. The corrected beam is fed back through the science field port and directed by means of the science field fold mirror. Having this external AO unit releases space within the ISS at the price of supplying the AO feed mirror.

13.18 Guider / Wavefront Sensing Module Layout

As the guider, and WFS requirements became better developed so did the functionality of the A&G Unit. The current design has the peripheral WFS(s) located above the Science field fold mirror. This allows the guider / WFS probes to access a guide field that is unrestricted by the fold mirror. Thus, one science fold mirror can be sized to accommodate the largest science field (7 arcmins) and can be used for all smaller science fields.

13.19 Number of Probes

Two independent probes are provided which allows simultaneous guiding on two guide objects, allows for a degree of redundancy, a check on the rotator servo rate and possibly a check on variation of the plate scale of the science field.

13.20 Thermal Management

The design of the Cassegrain thermal management system relies on the concept for locating the instrument and rotator drive electronics in air conditioned enclosures. This will remove the majority of heat generated at the Cassegrain, leaving some residual leakage from the insulation. The remaining heat sources are from motors and mechanisms in the rotator, instruments, and fold mirror / WFS assemblies. If detailed calculations show it is necessary, some motors may be mounted on water cooled mounts (particularly the rotator motors). The heat generated can reduced by proper selection of motors and the use of efficient mechanisms.

13.20.1 Electronics Enclosure Heat Exchangers

The system used is an air to liquid heat exchanger, with a recirculating fan unit. The enclosure environment is essentially sealed, reaching an operating temperature of 20 ºC and heat is removed due to the temperature difference between the enclosure air and the coolant.

A water cooled system was chosen as fairly large heat loads can be removed with moderate temperature differences and flow rates. Routing coolant hoses through the cable wrap is also much easier than ducting, required for an air system. The heat exchangers are commercially available, and are very compact.

13.21 Handling Rigs

The instruments will have their own handling rigs for support, protection, and transport and to assist in maintenance. A second handling rig will be used to mount all instruments on the telescope. This approach is taken because the Cassegrain handling rig must have some features which may be difficult and expensive to duplicate on each individual handling rig. These are namely: lift height; stability; and fine alignment control.

Figure 1. Inter-relationship of Gemini Subsystems Documentation

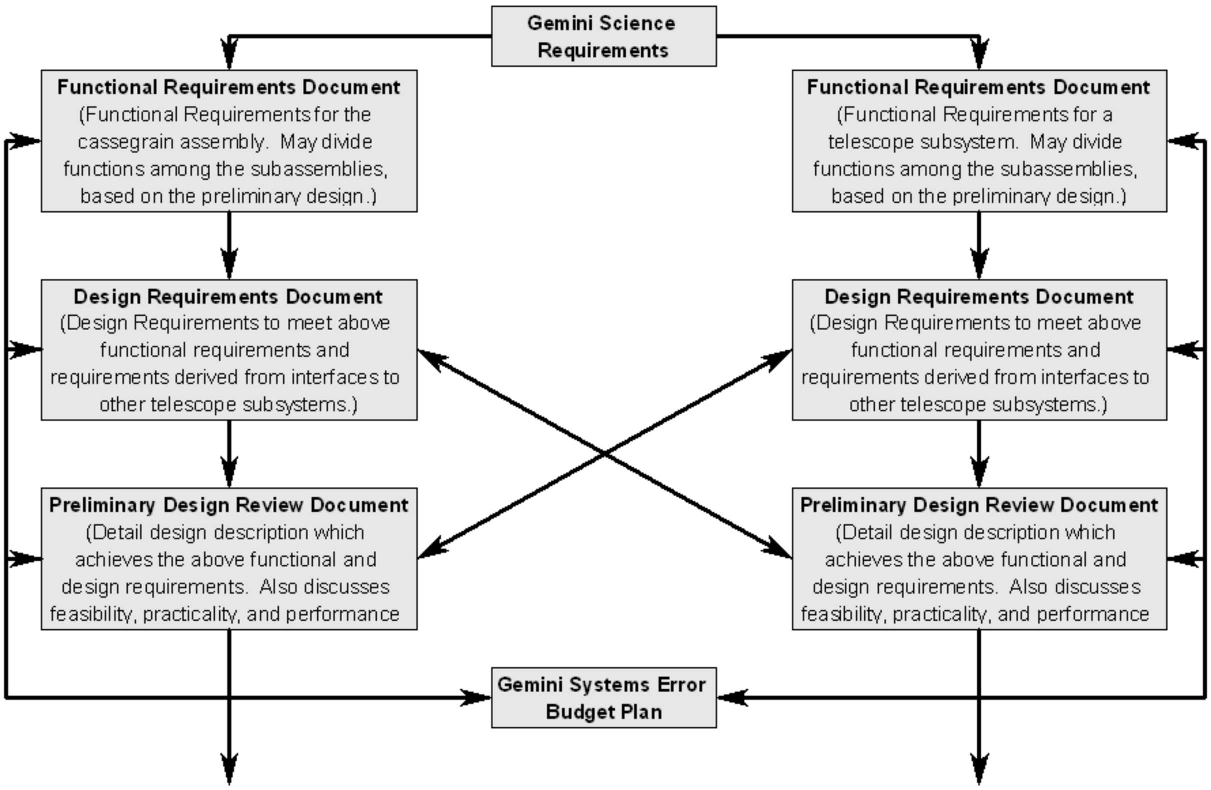

Figure 2. Exploded View of Cassegrain Assembly and Part Section of Mirror Cell

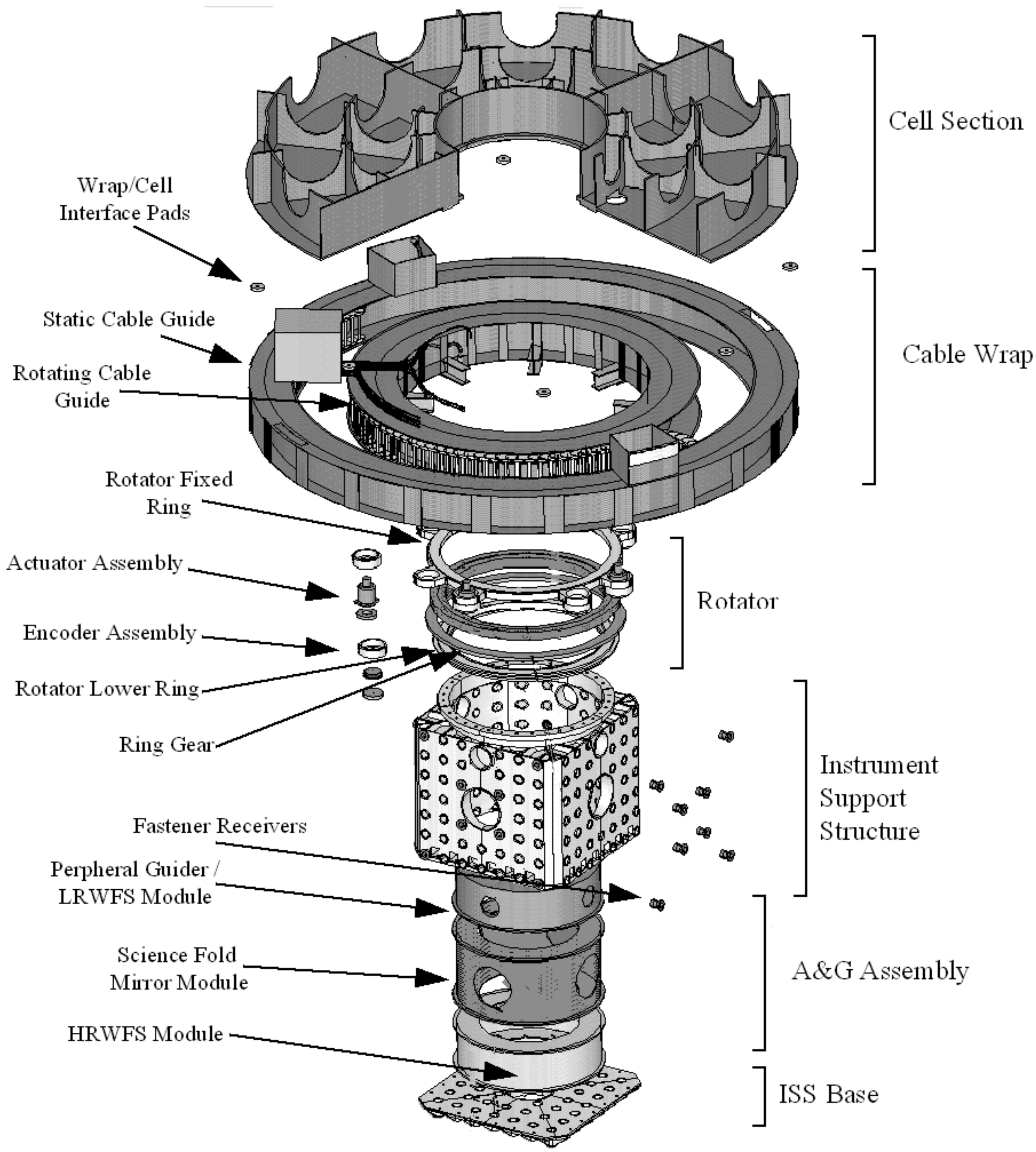

Figure 3. Solid Model of Cassegrain Assembly

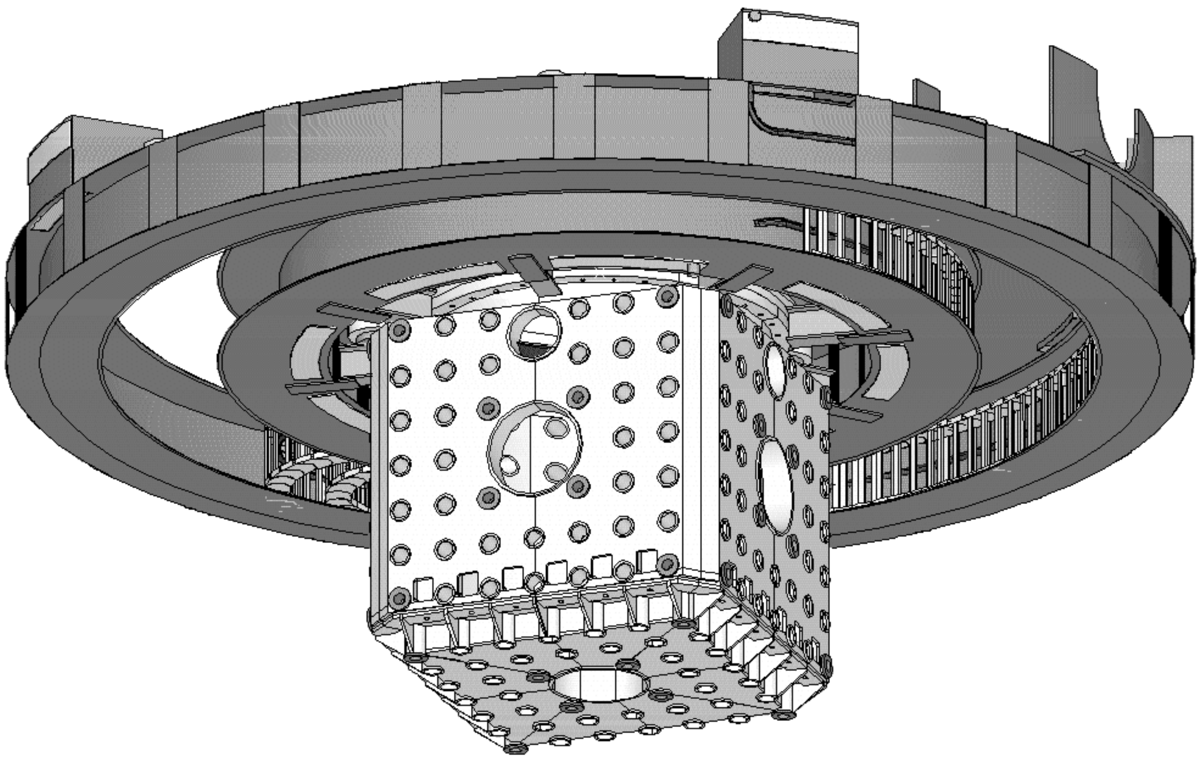

Figure 4. Cassegrain Assembly on Telescope

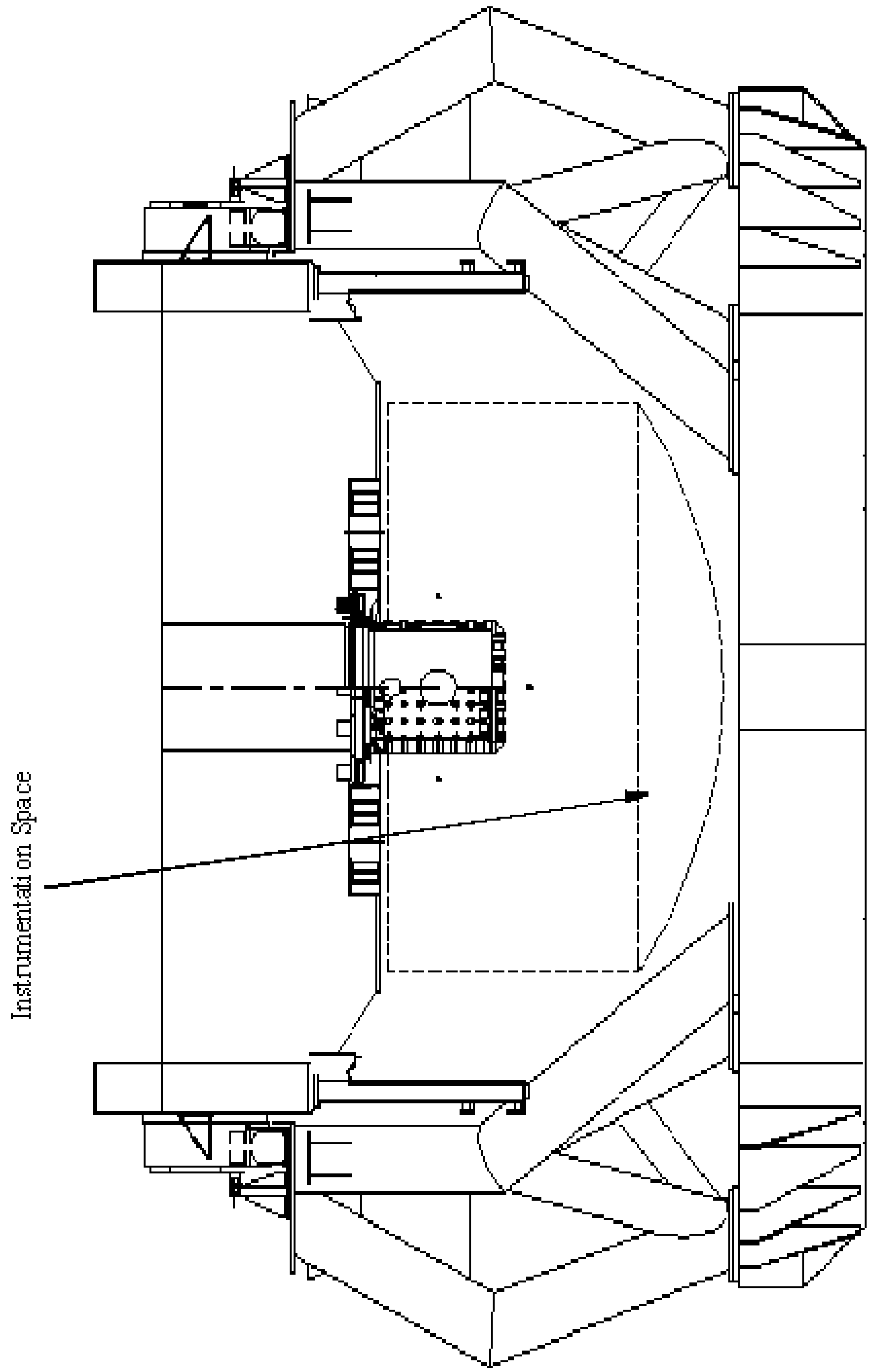

Figure 5. Cables/Services Routing Through Mirror Cell

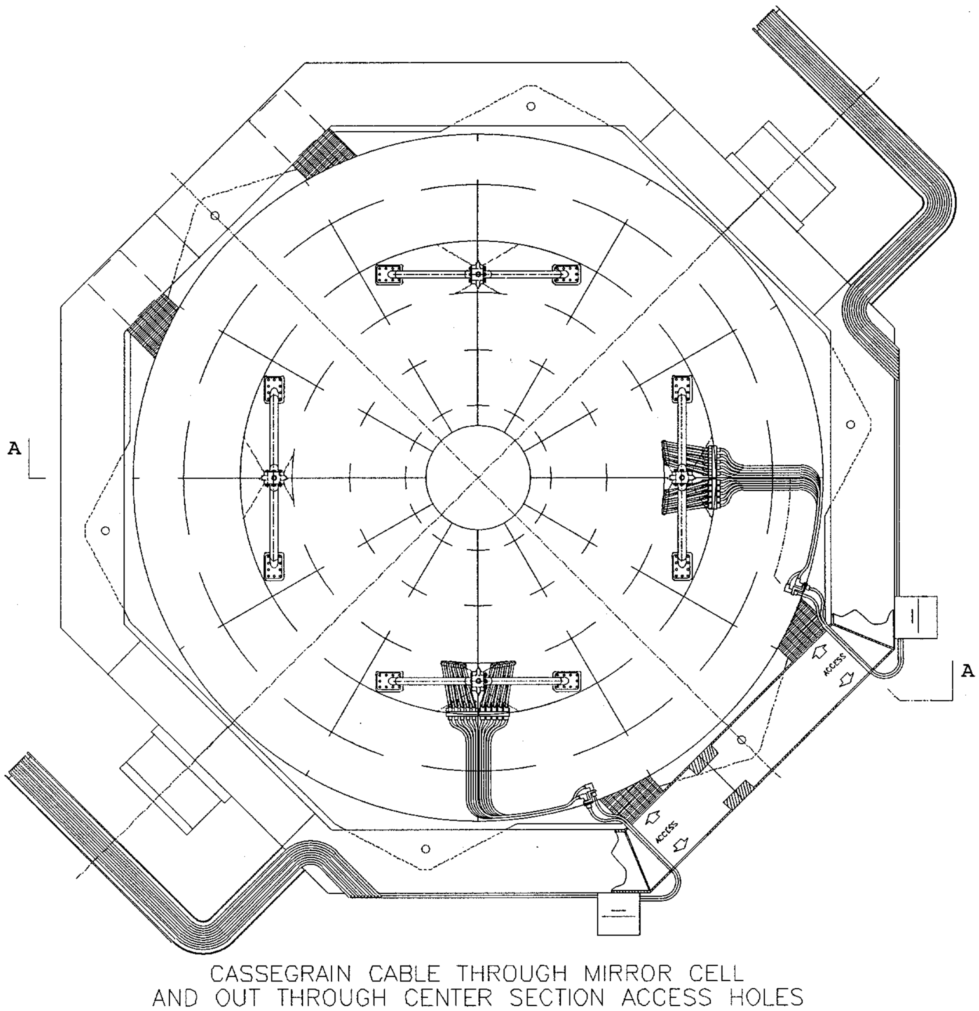

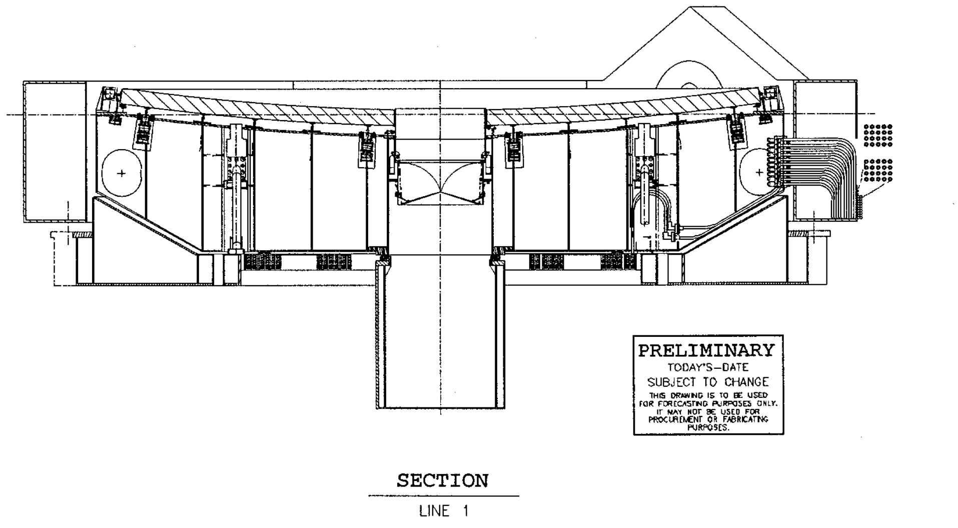

Figure 6. Mechanical Model of Telescope and Cassegrain Rotator

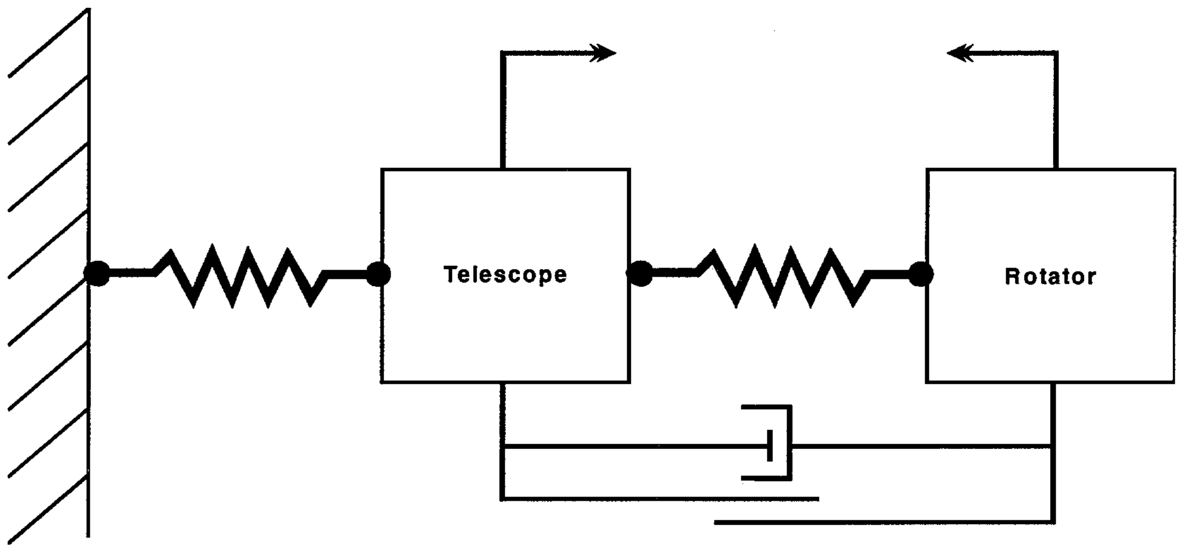

Figure 7. Bode Plot of Cassegrain-only Linearized Model

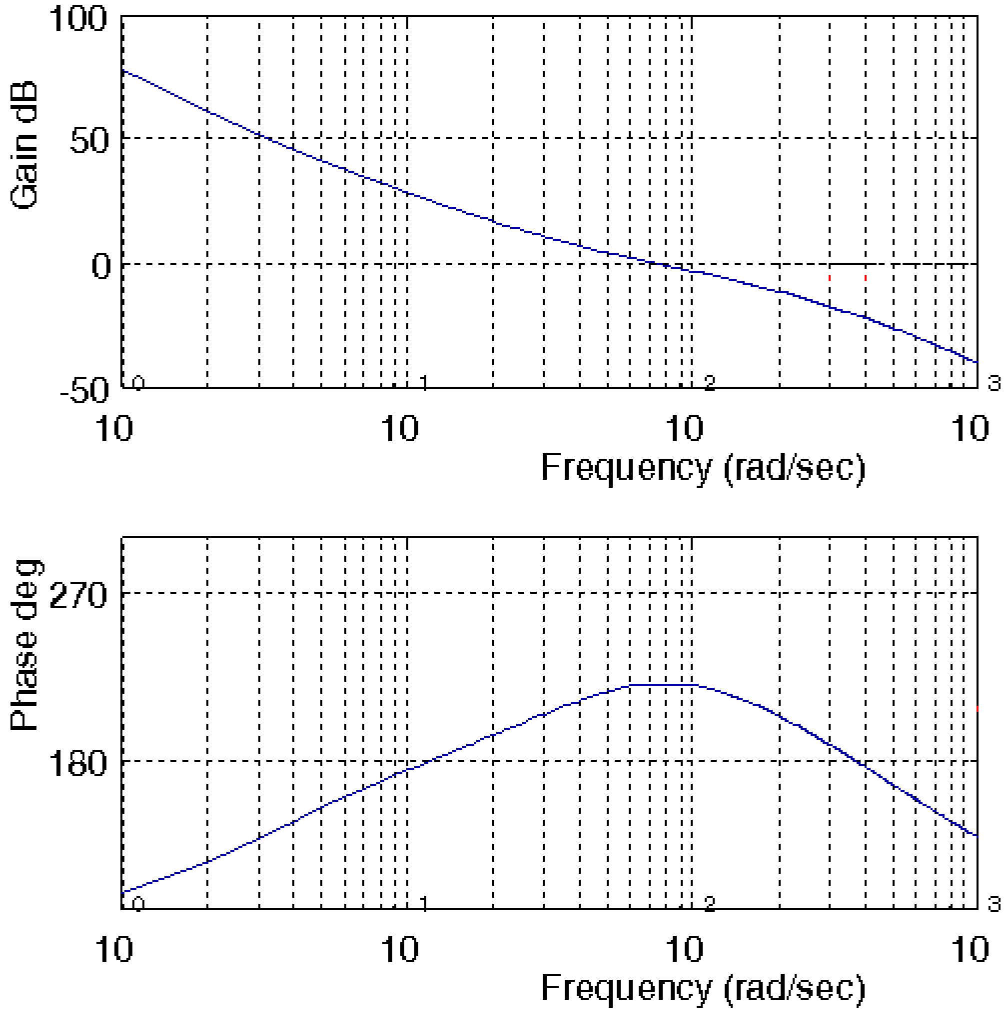

Figure 8. Response of Cassegrain to a Ramp Input

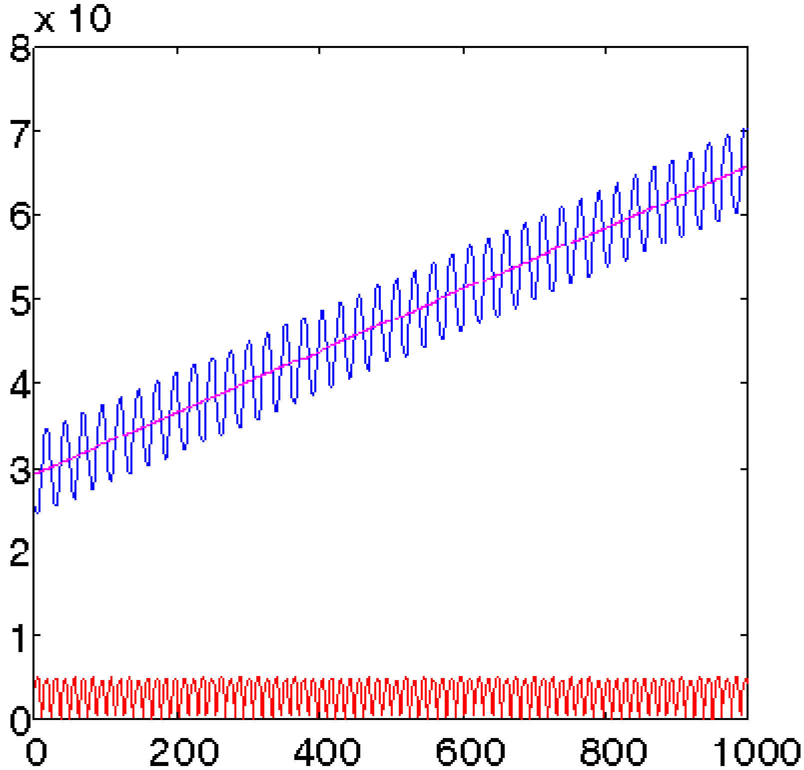

Figure 9. Simplified Cassegrain-only Model

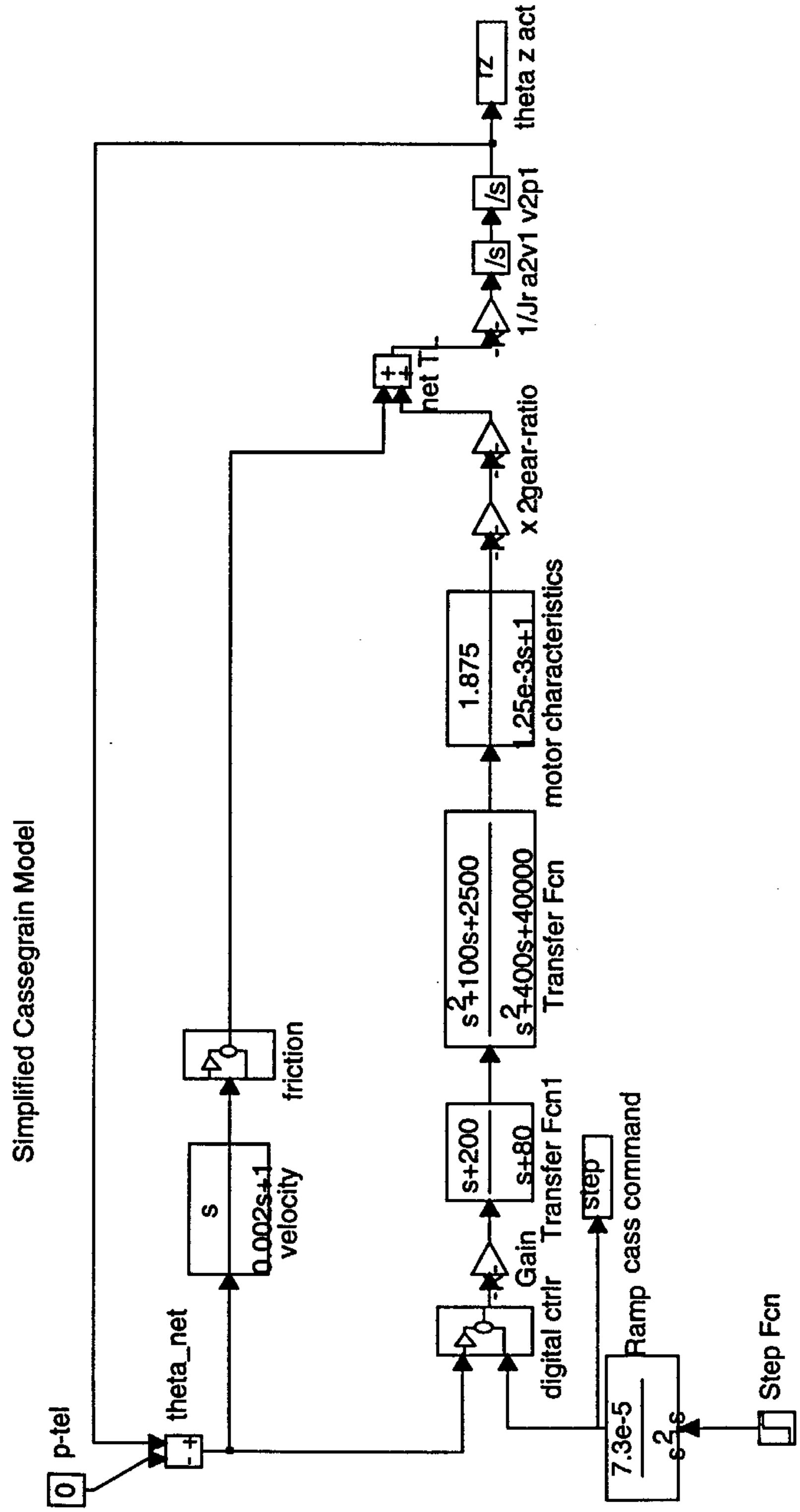

Figure 10. Telescope Control System Matlab Model

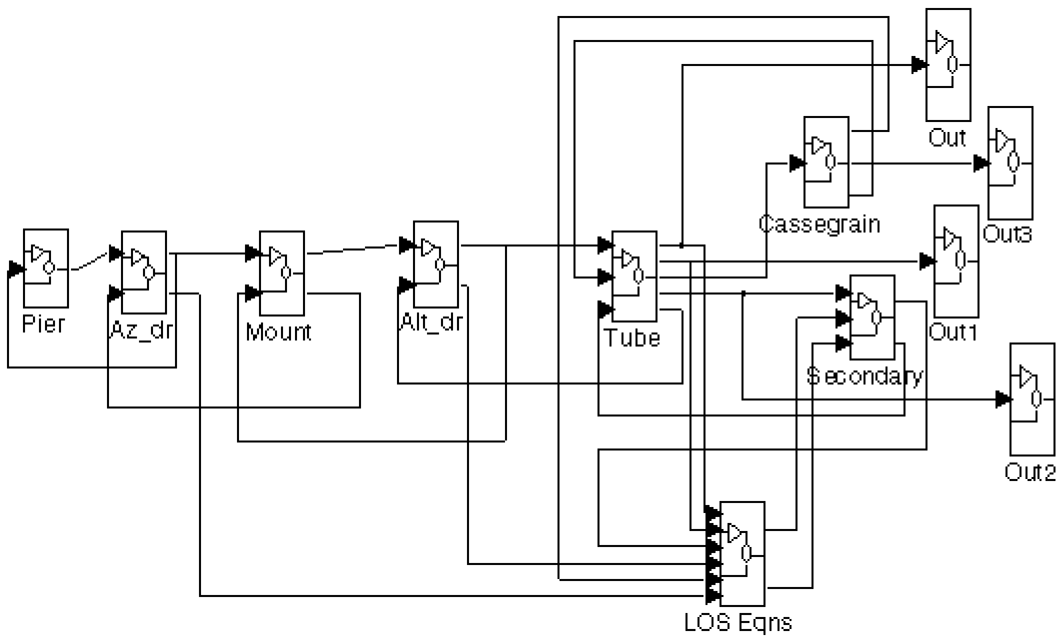

Figure 11. Solid Model of Cassegrain Assembly

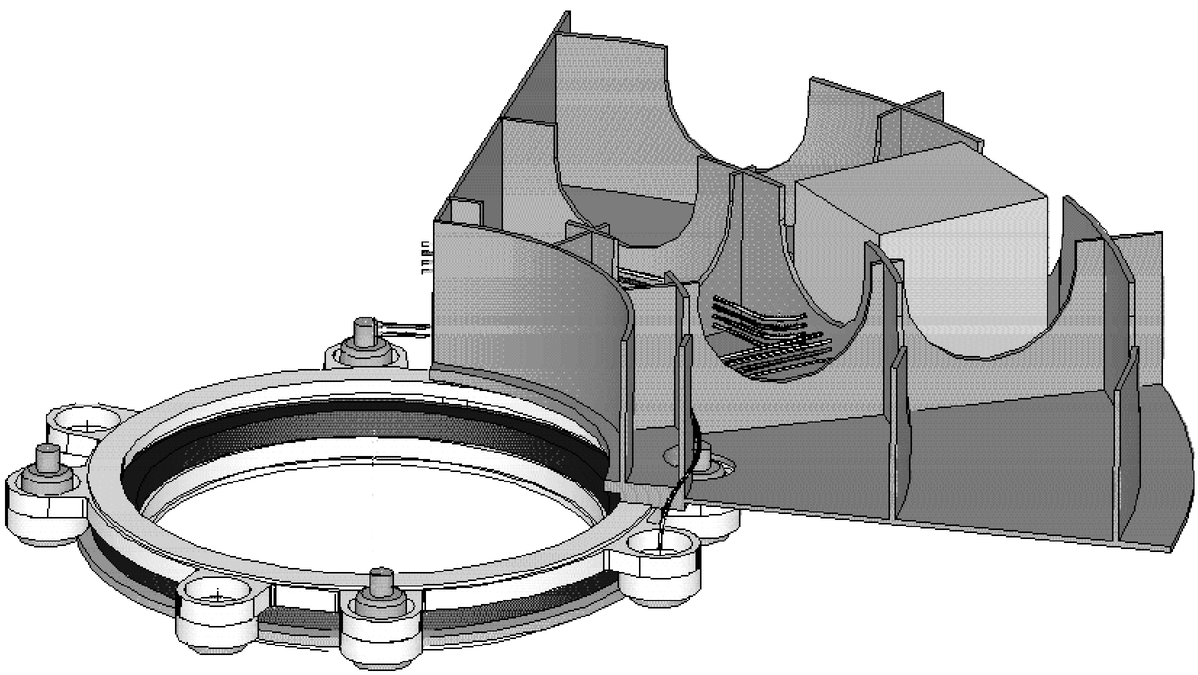

Figure 12. Telescope Tube Coordinate System

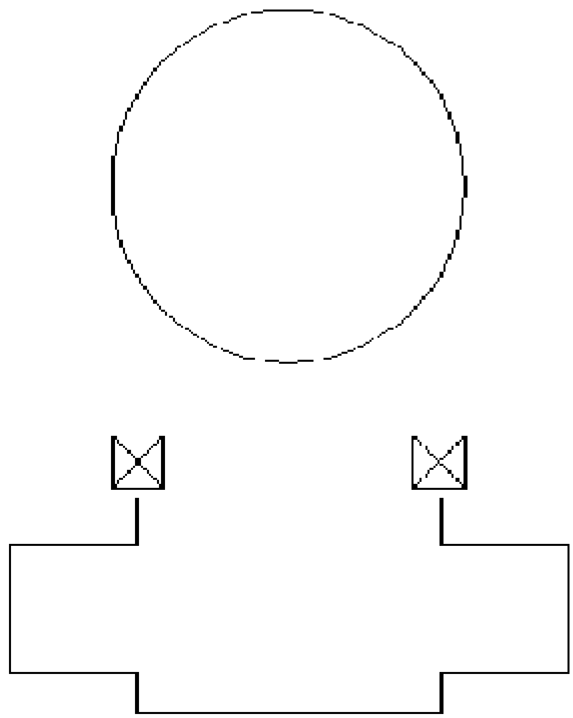

Figure 13. Rotator Assembly

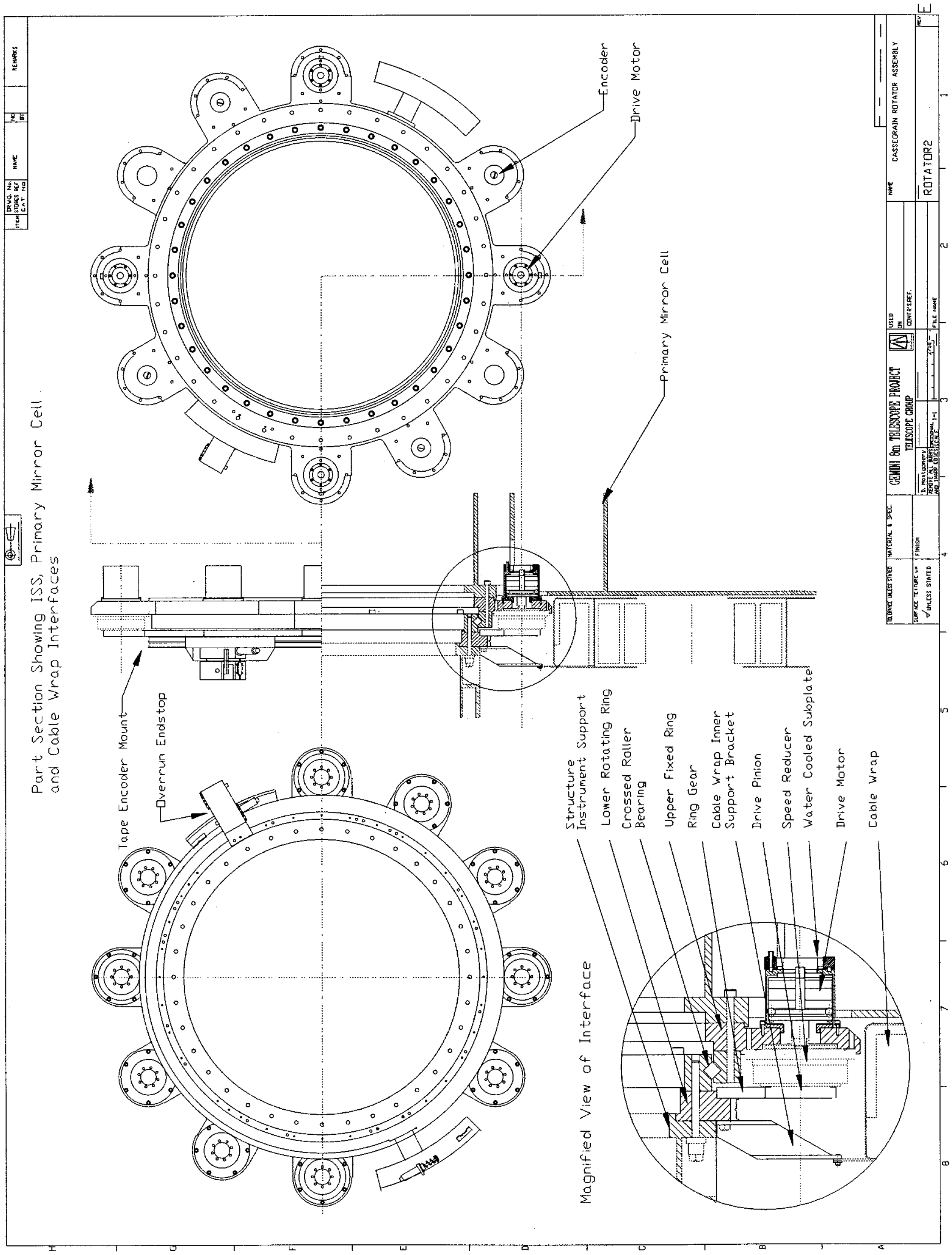

Figure 14. Rotator Sectional View

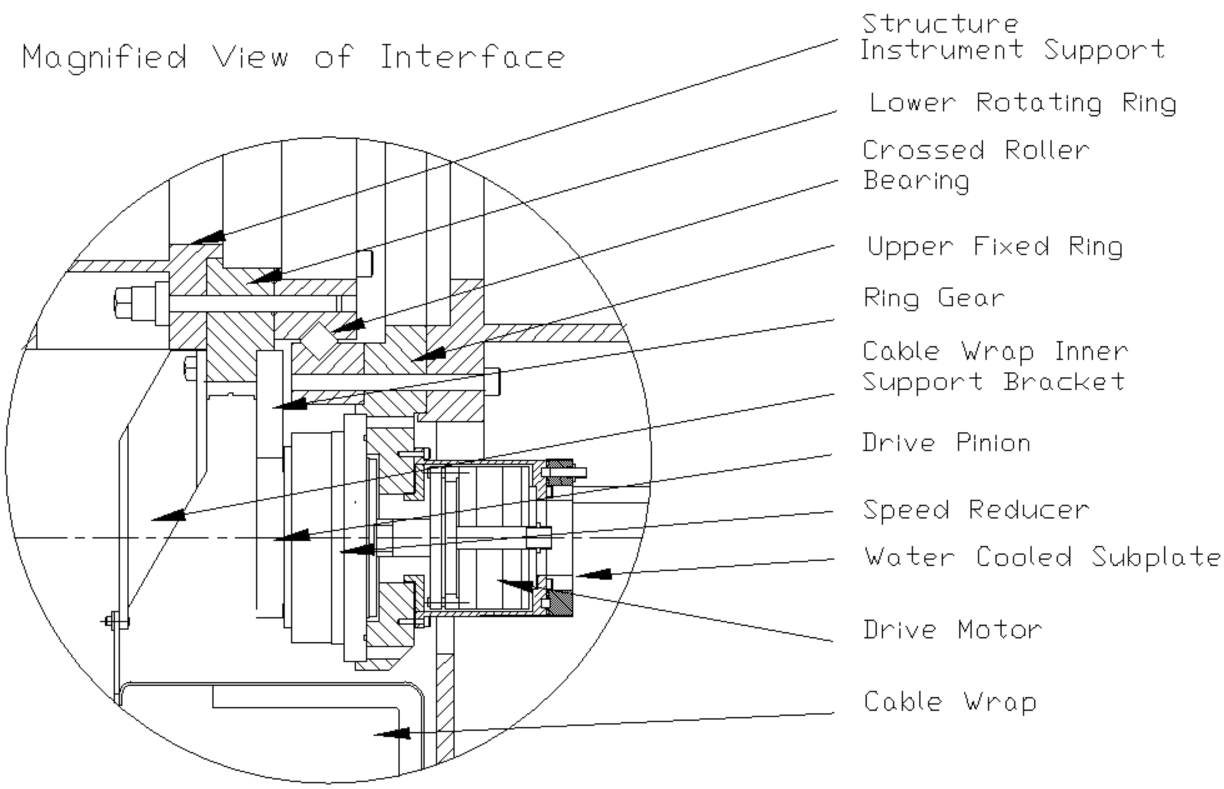

Figure 15. Assumptions for Flexure Calculations on Motor Mounts

Solid Model of Motor Mount

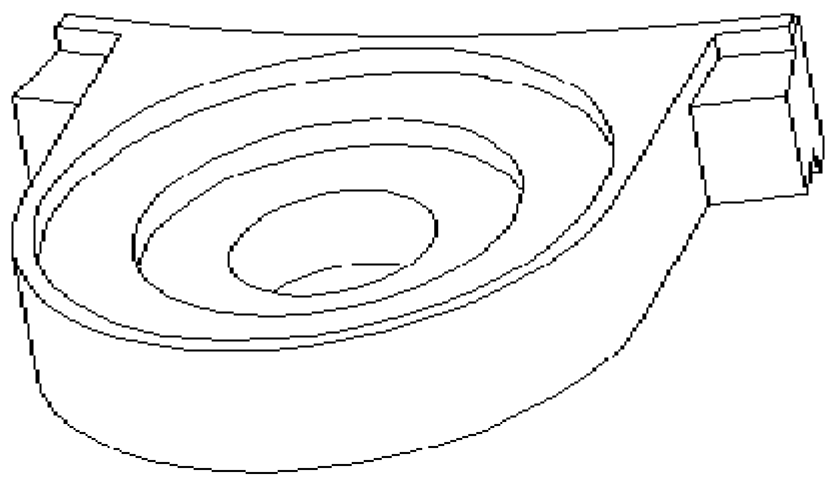

Simplified Flexure Model as Cantilevers

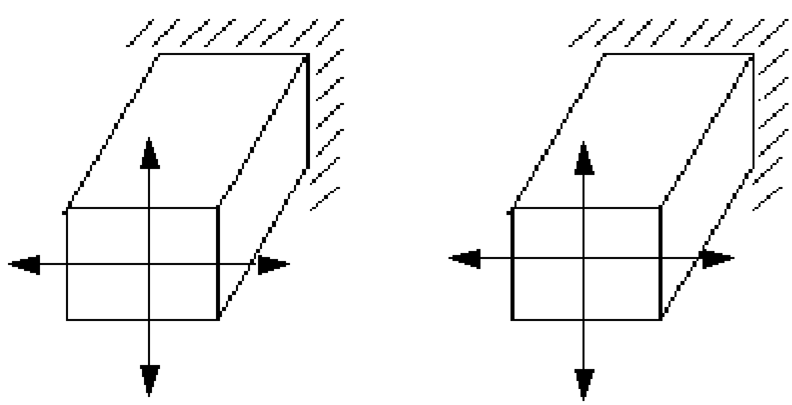

Figure 16. Offset Loading on Speed Reducer

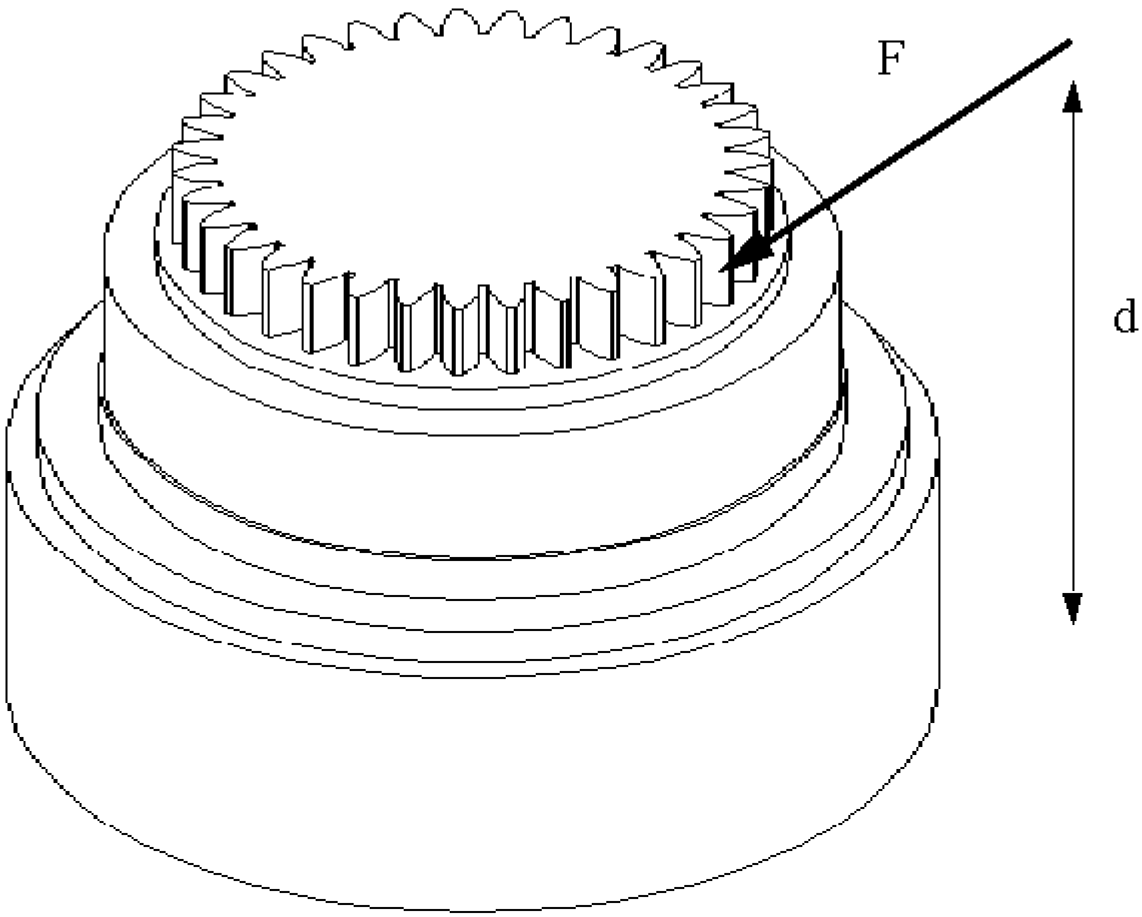

Figure 17. Motor Drive Unit Heat Paths

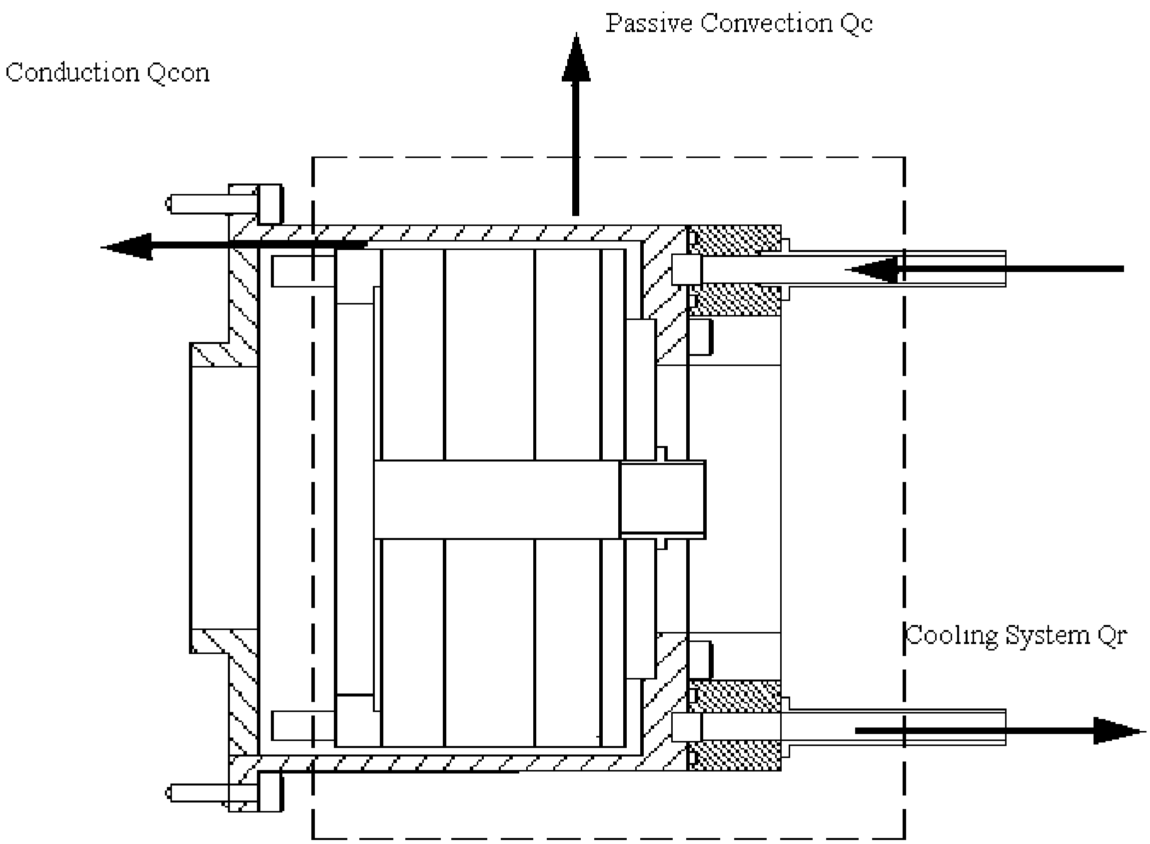

Figure 18. Finite Element Model of Actuator Mount and Adjacent Cell Structure

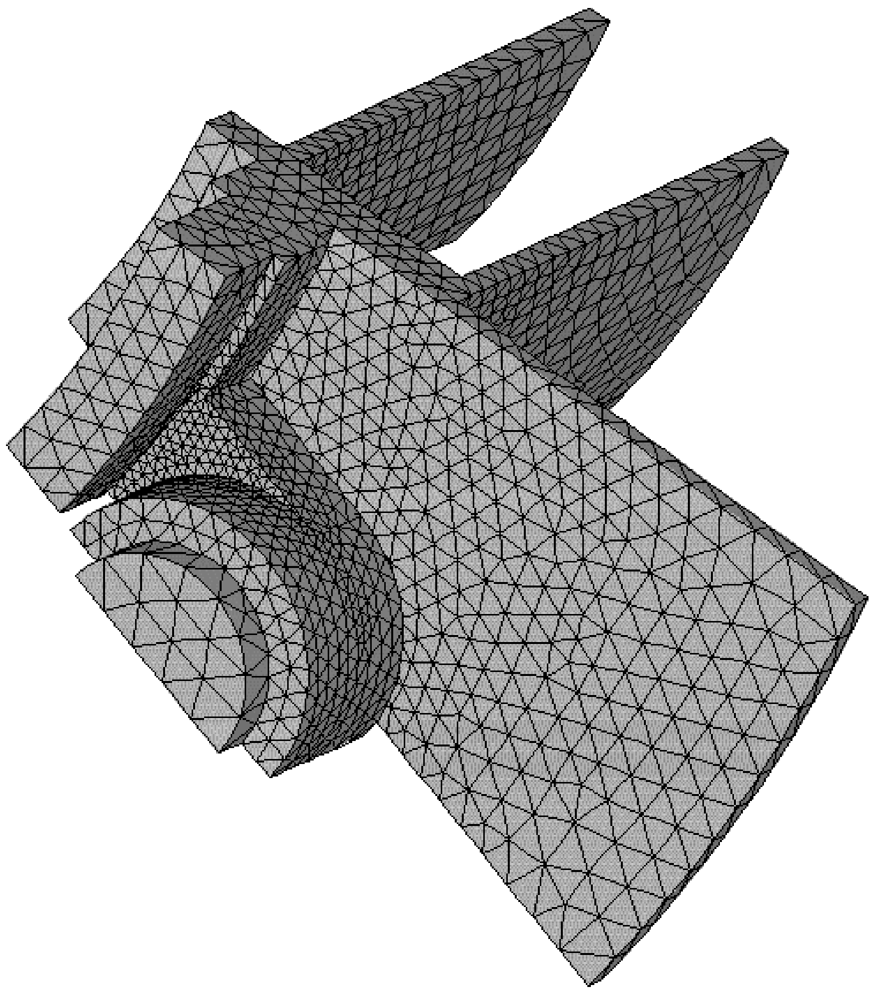

Figure 19. Steady State Analysis of Rotator Actuator Heat Loads

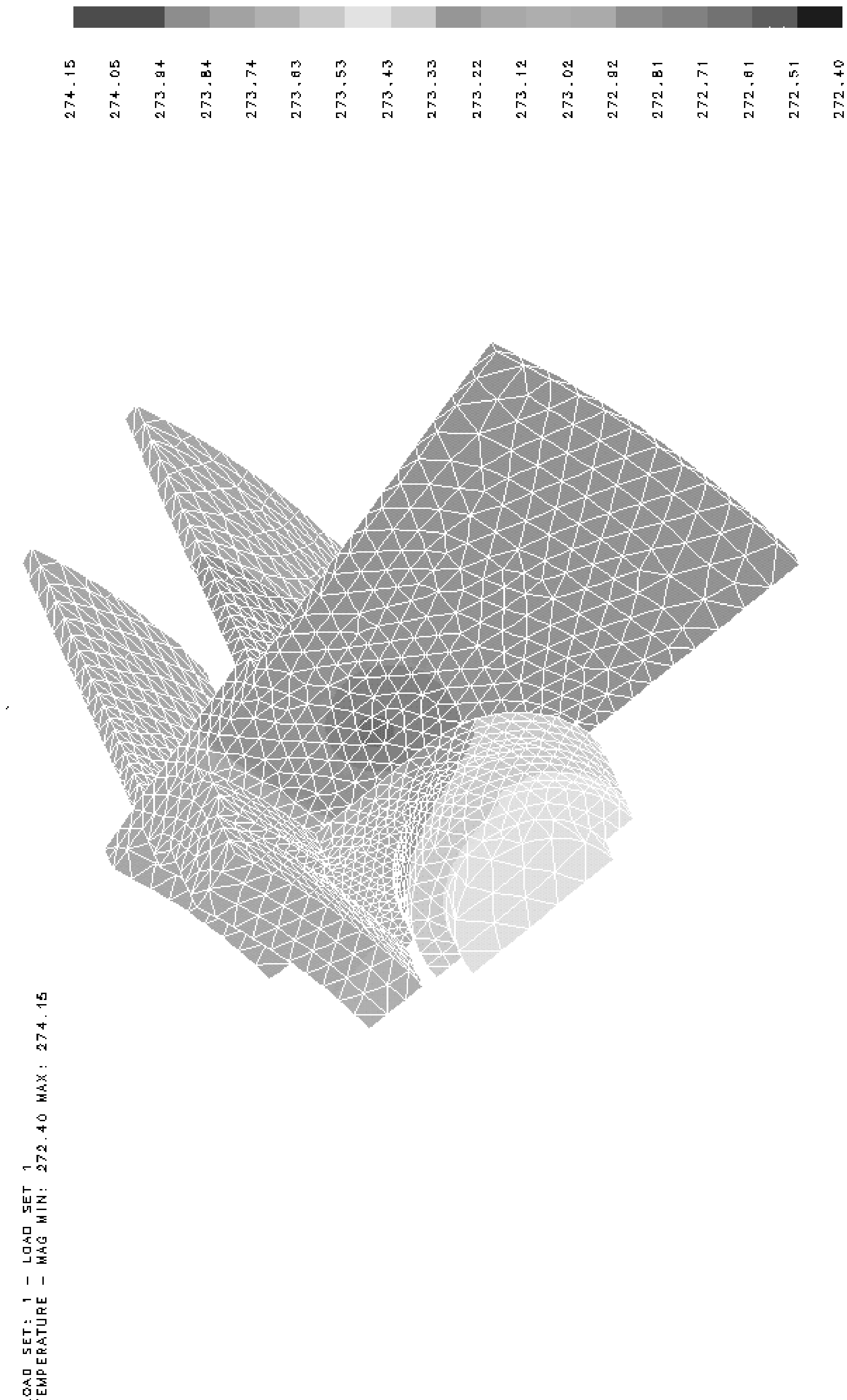

Figure 20. Mirror Cell Interface

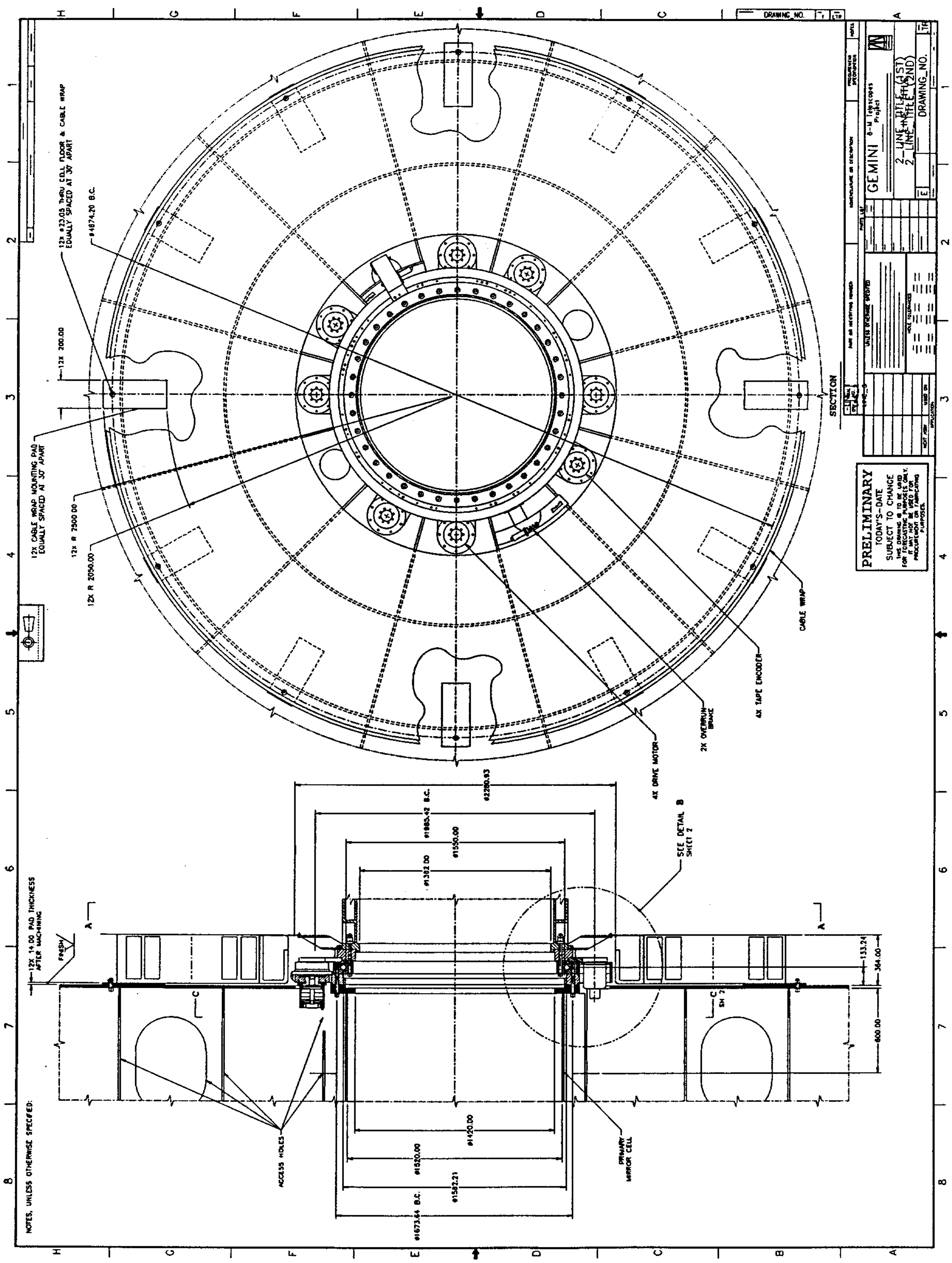

Figure 21. Finite Element Model of Rotator/Cell Interface

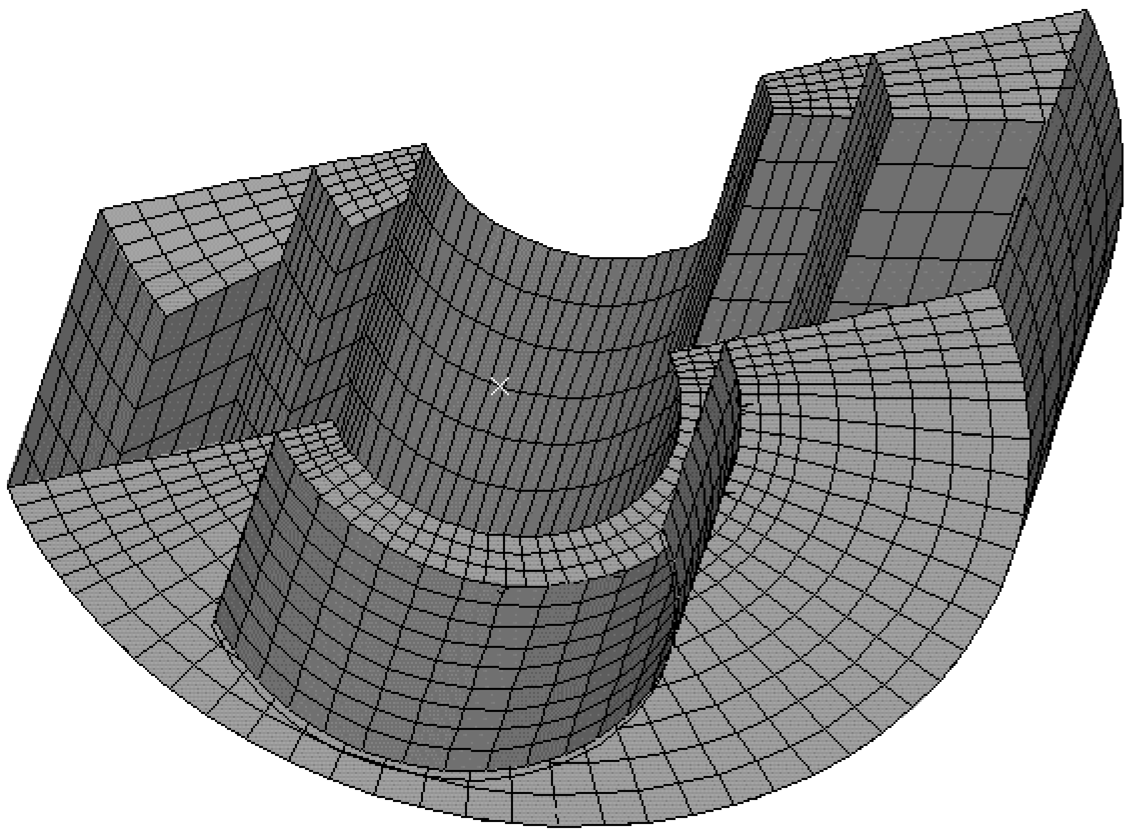

Figure 22. Rotator/Cell Interface Analysis Results

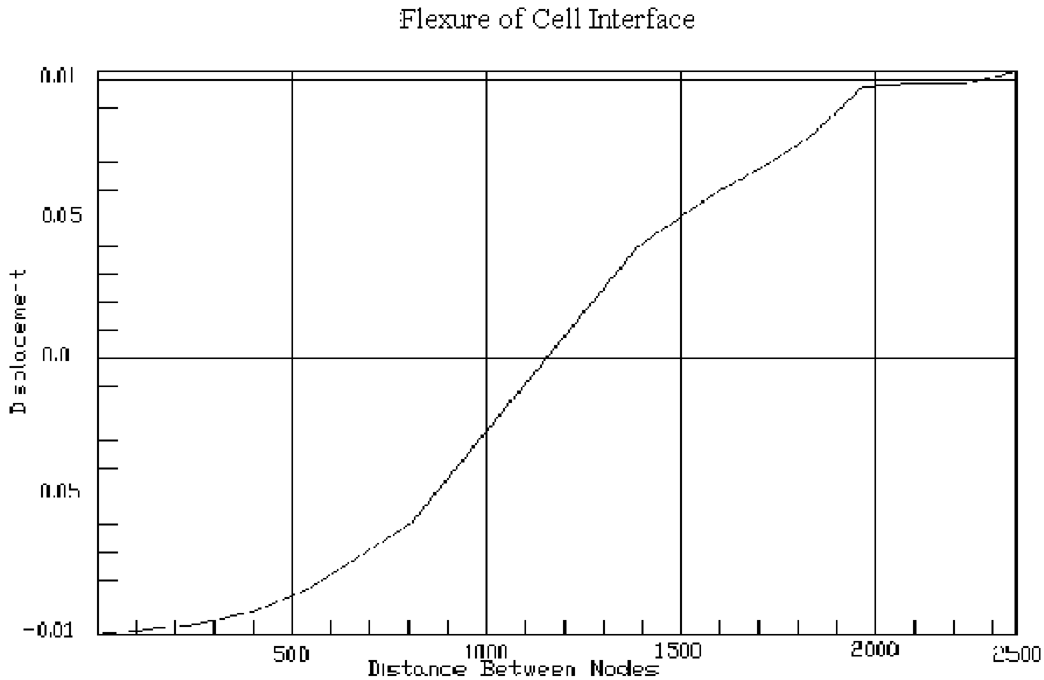

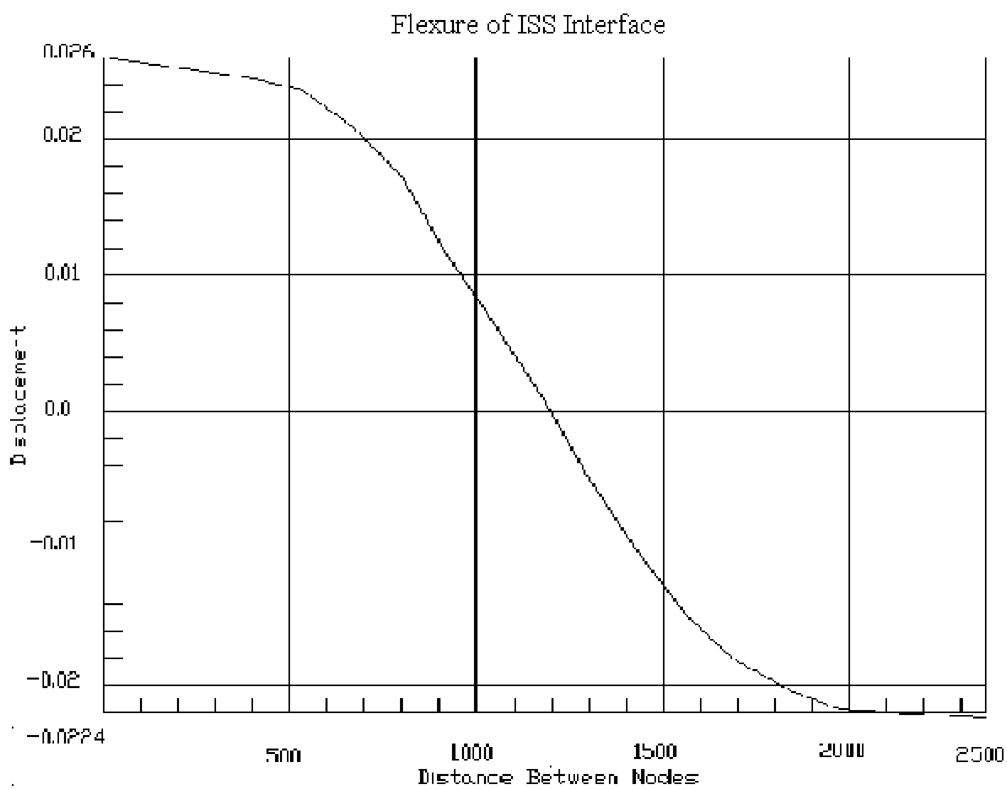

Figure 23. Endstop Actuator Sequence

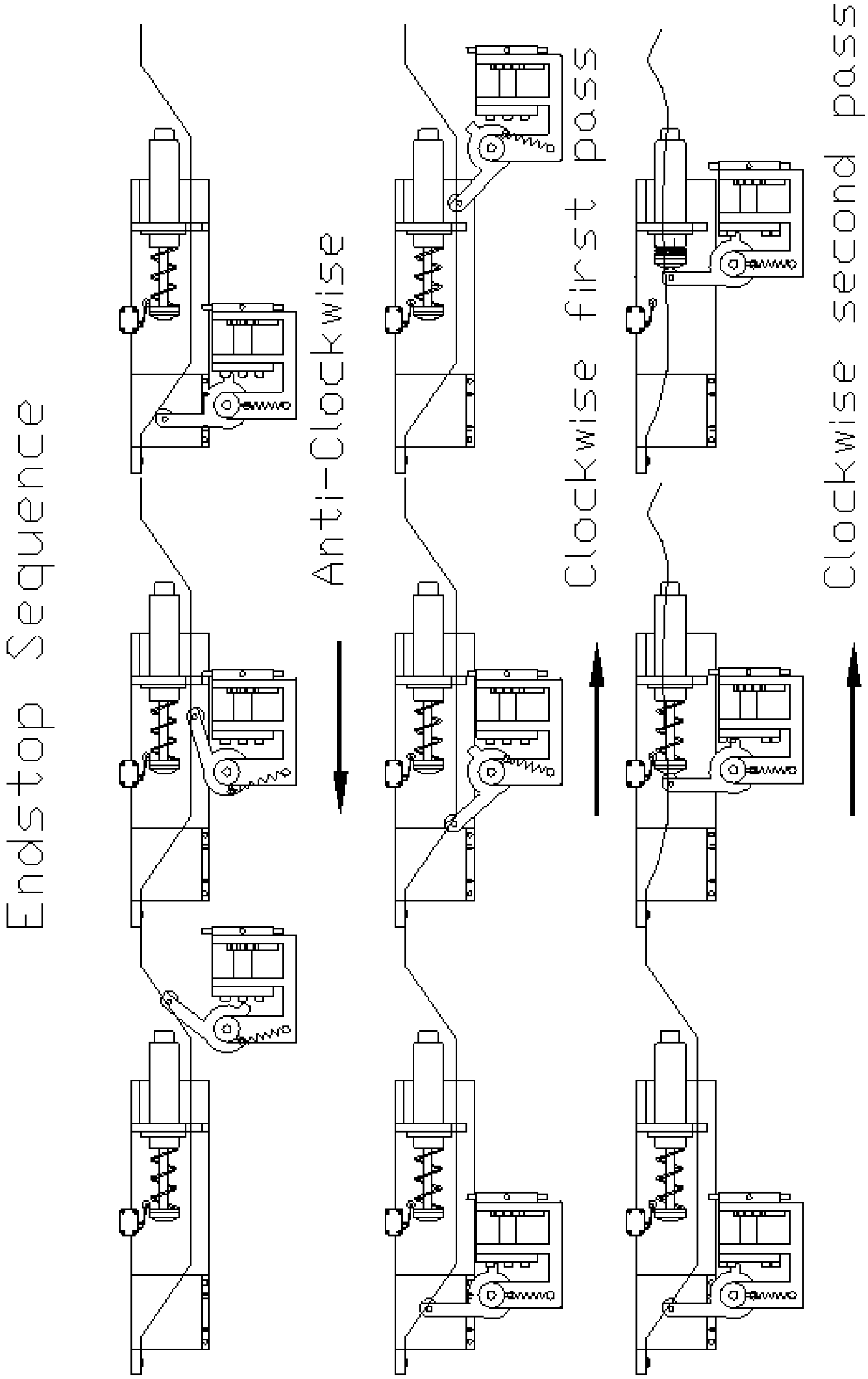

Figure 24. Endstop Layout

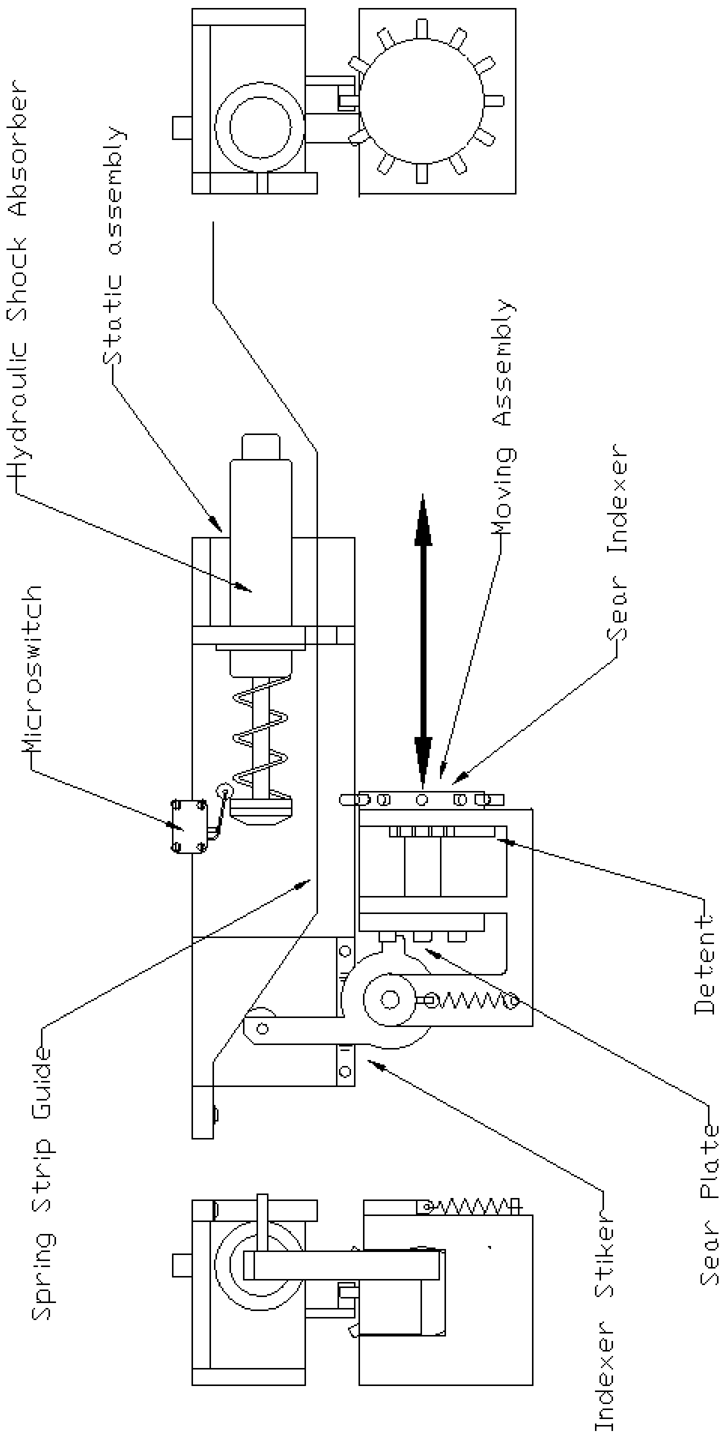

Figure 25. Cable Wrap Assembly*

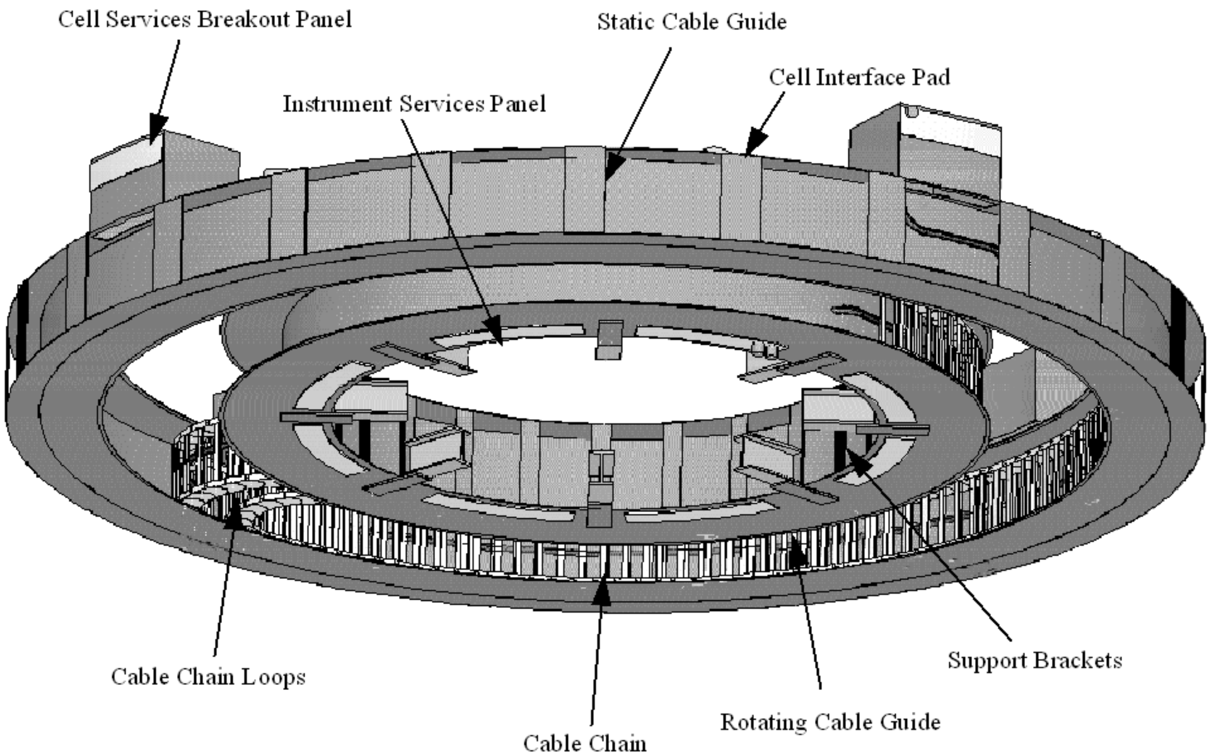

*Note: This solid model rendition shows an obsolete version of the cable wrap design with a single track and two cable chains. The new version has two tracks and four cable chains.

Figure 26. Cable Wrap Cross Section

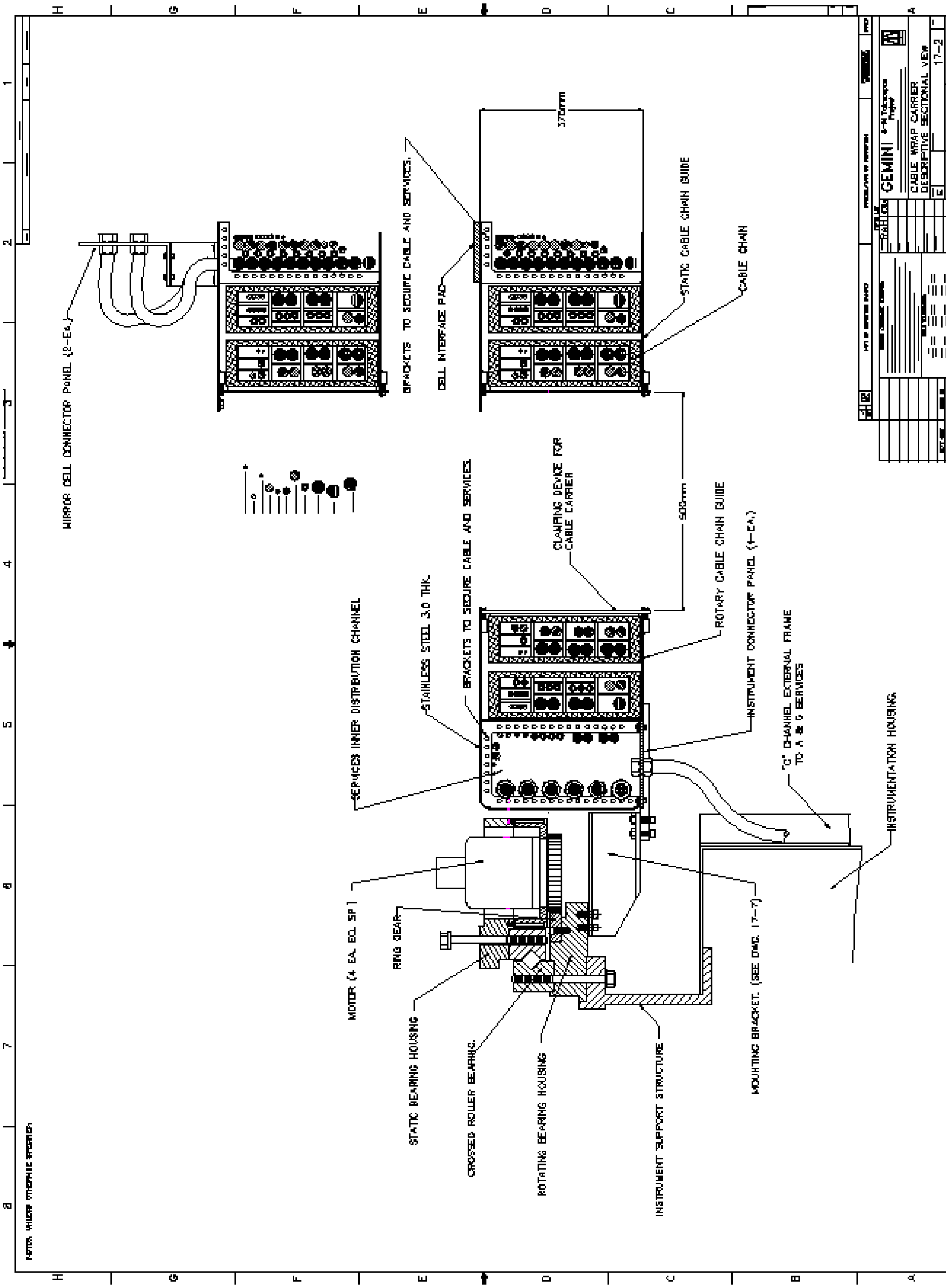

Figure 27. Cable Wrap Section

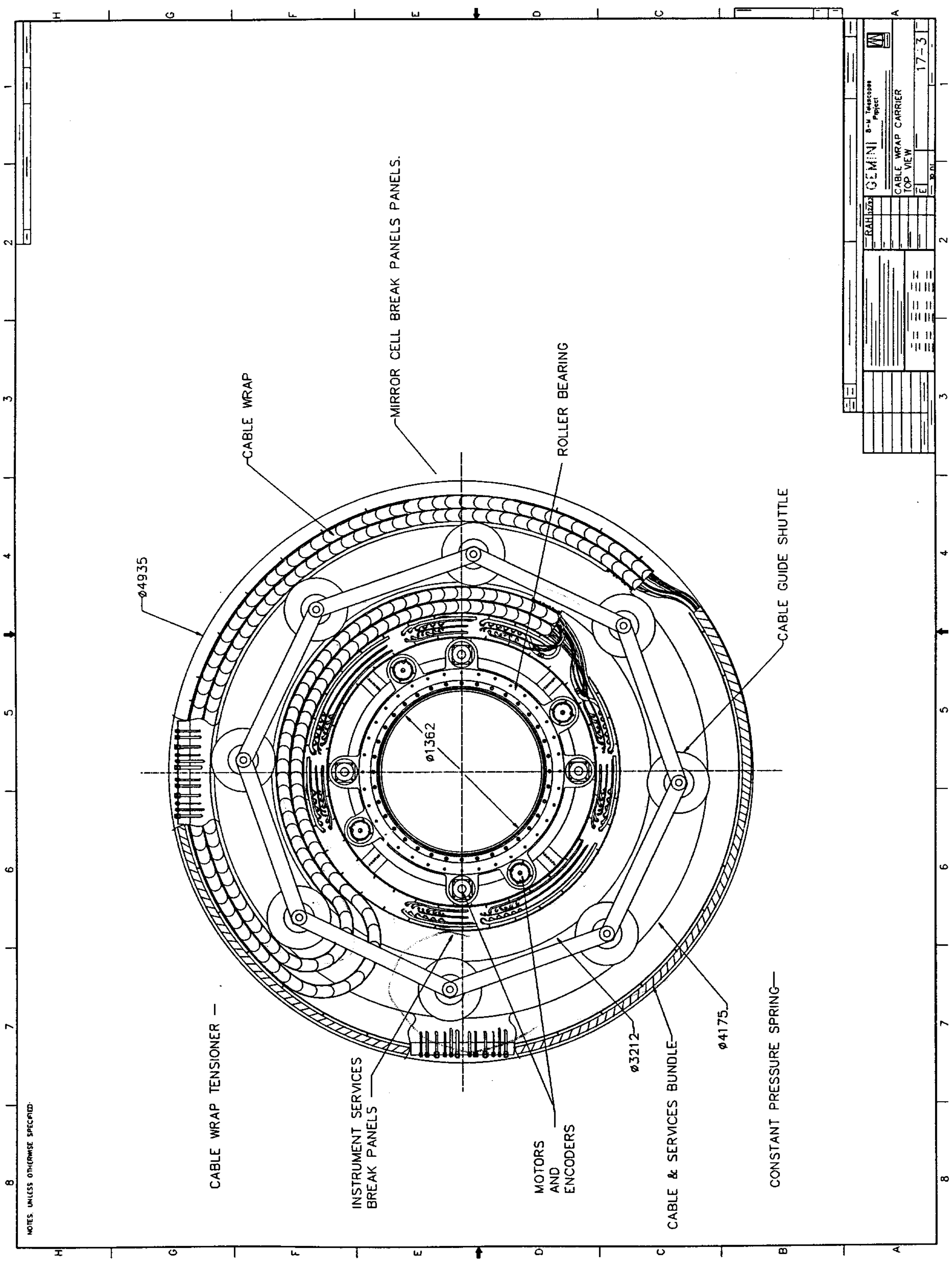

Figure 28. Cable Wrap and ISS

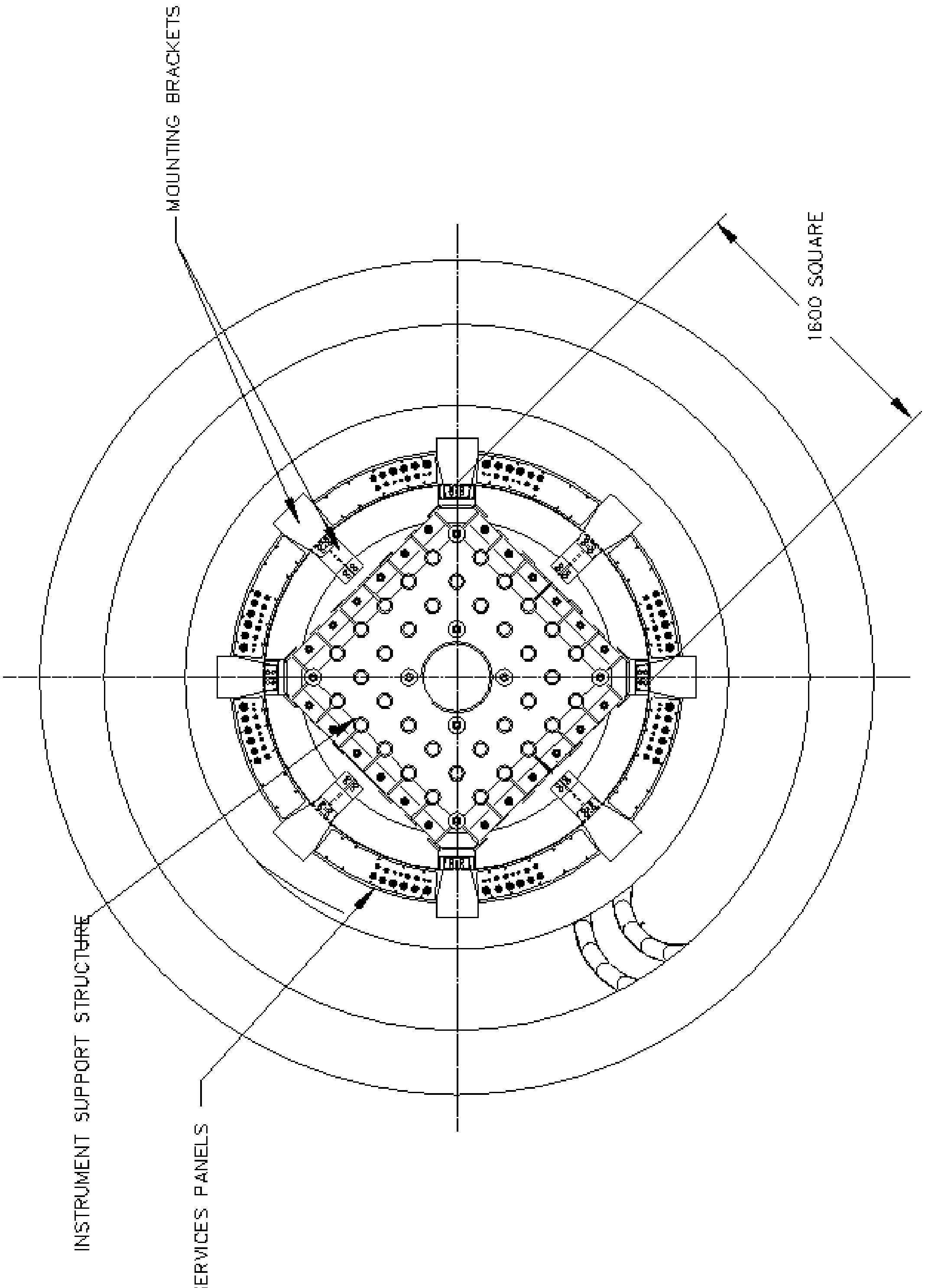

Figure 29. Change in c of g for Cable Loop During Rotation

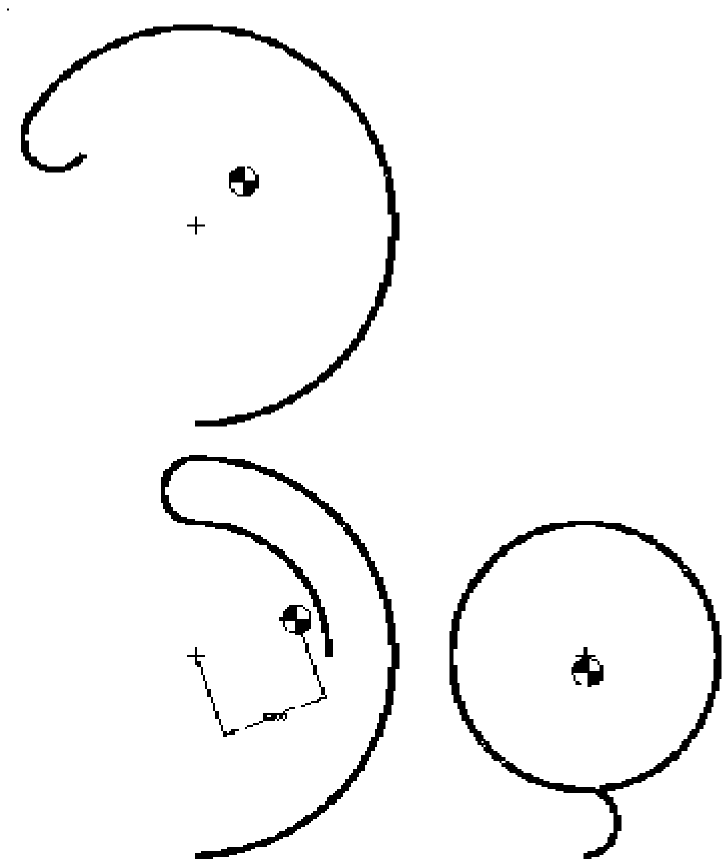

Figure 30. Mirror Cell Interface

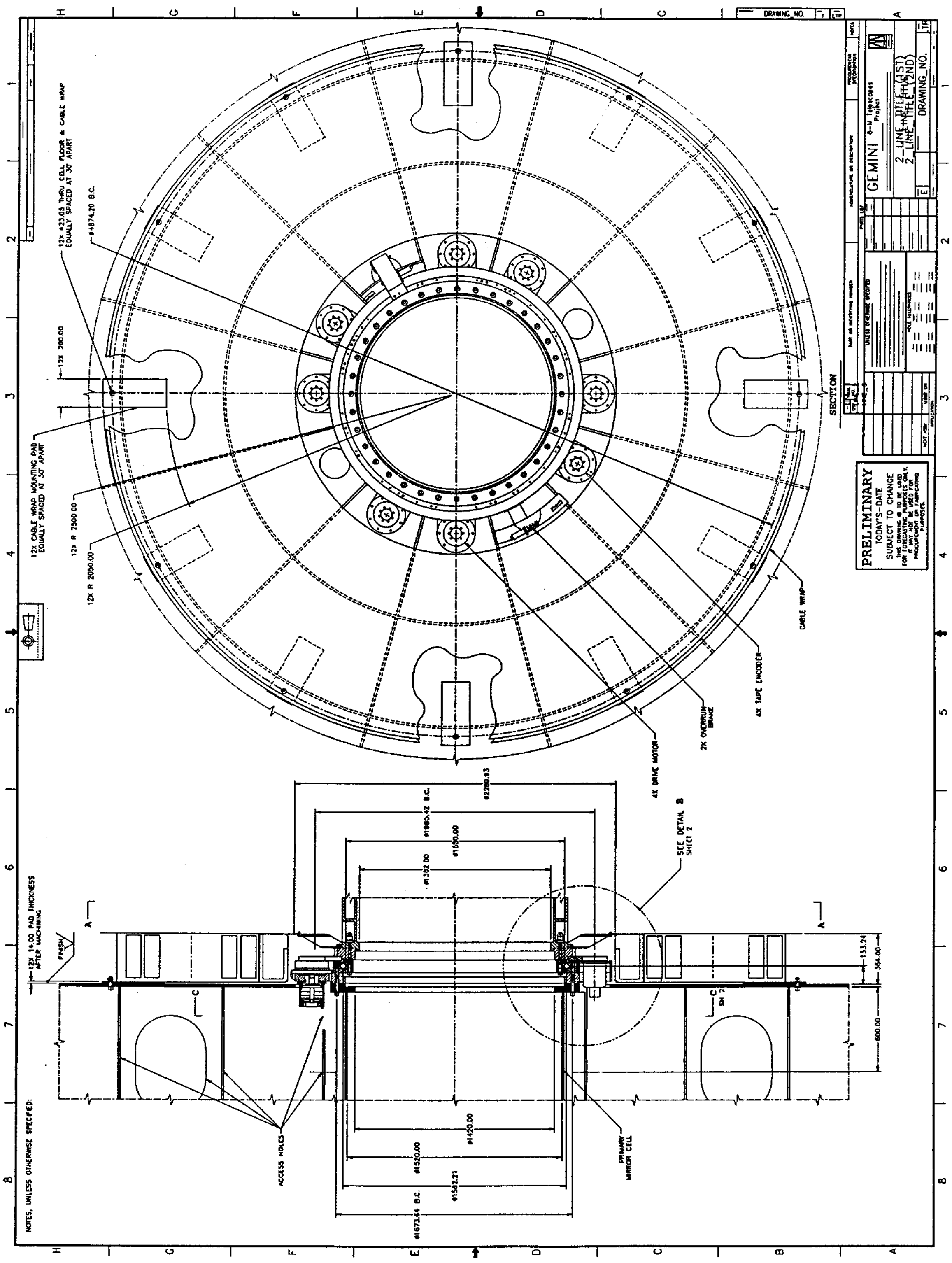

Figure 31. Diagram Illustrating Terms in Cable Loop Travel Calculation

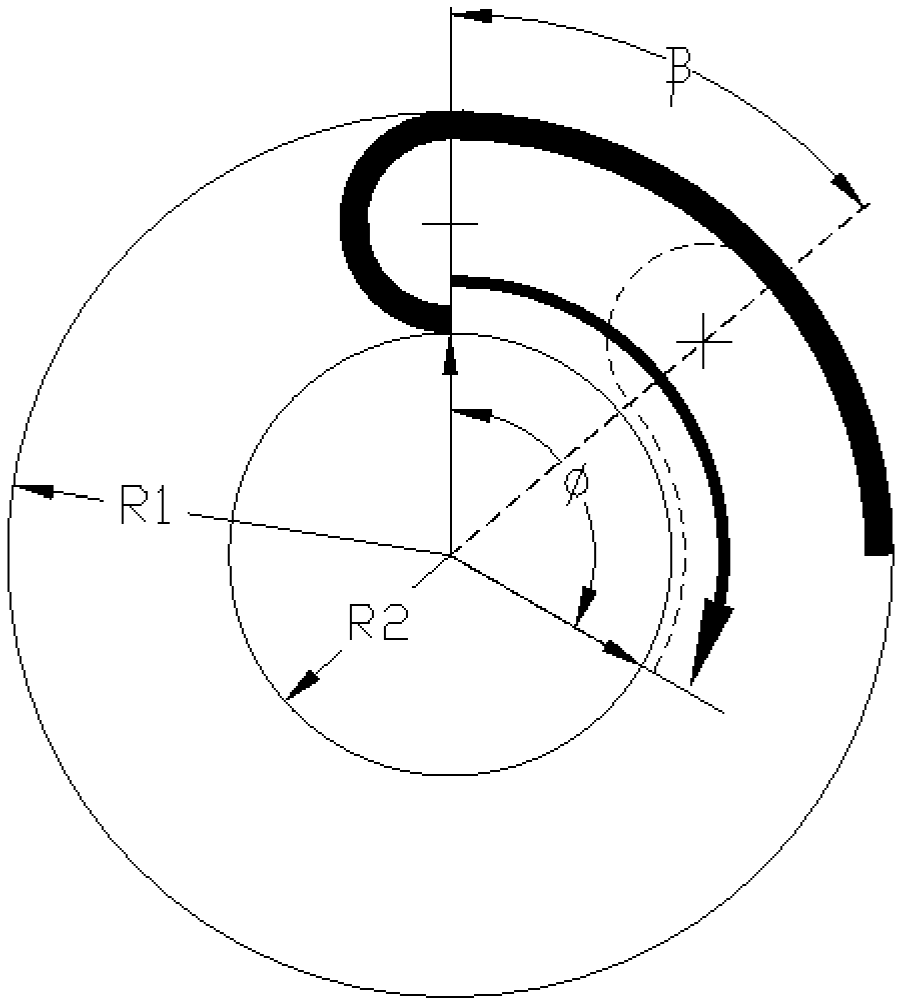

Figure 32. Instrument Support Structure

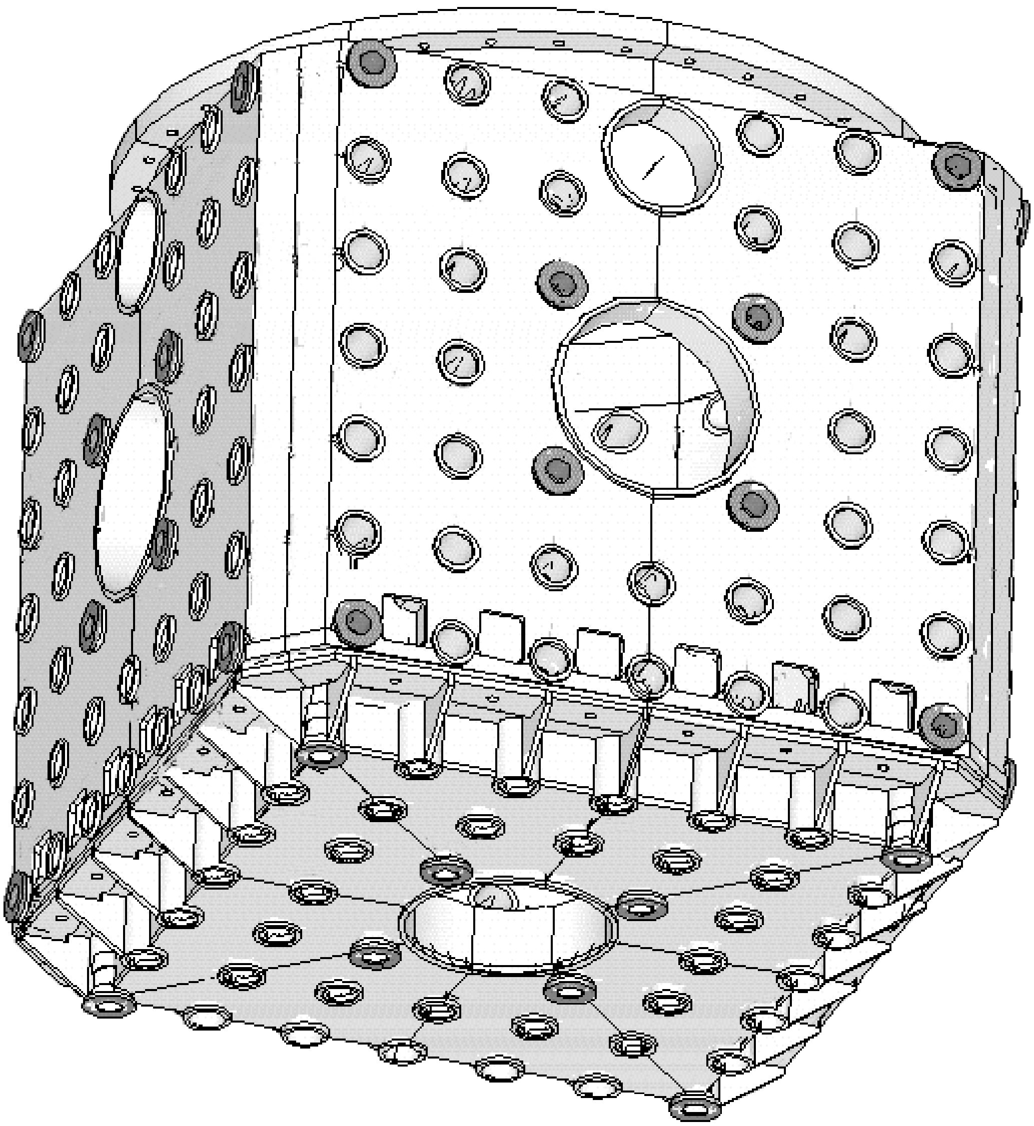

Figure 33. Instrument Support Structure Assembly Layout

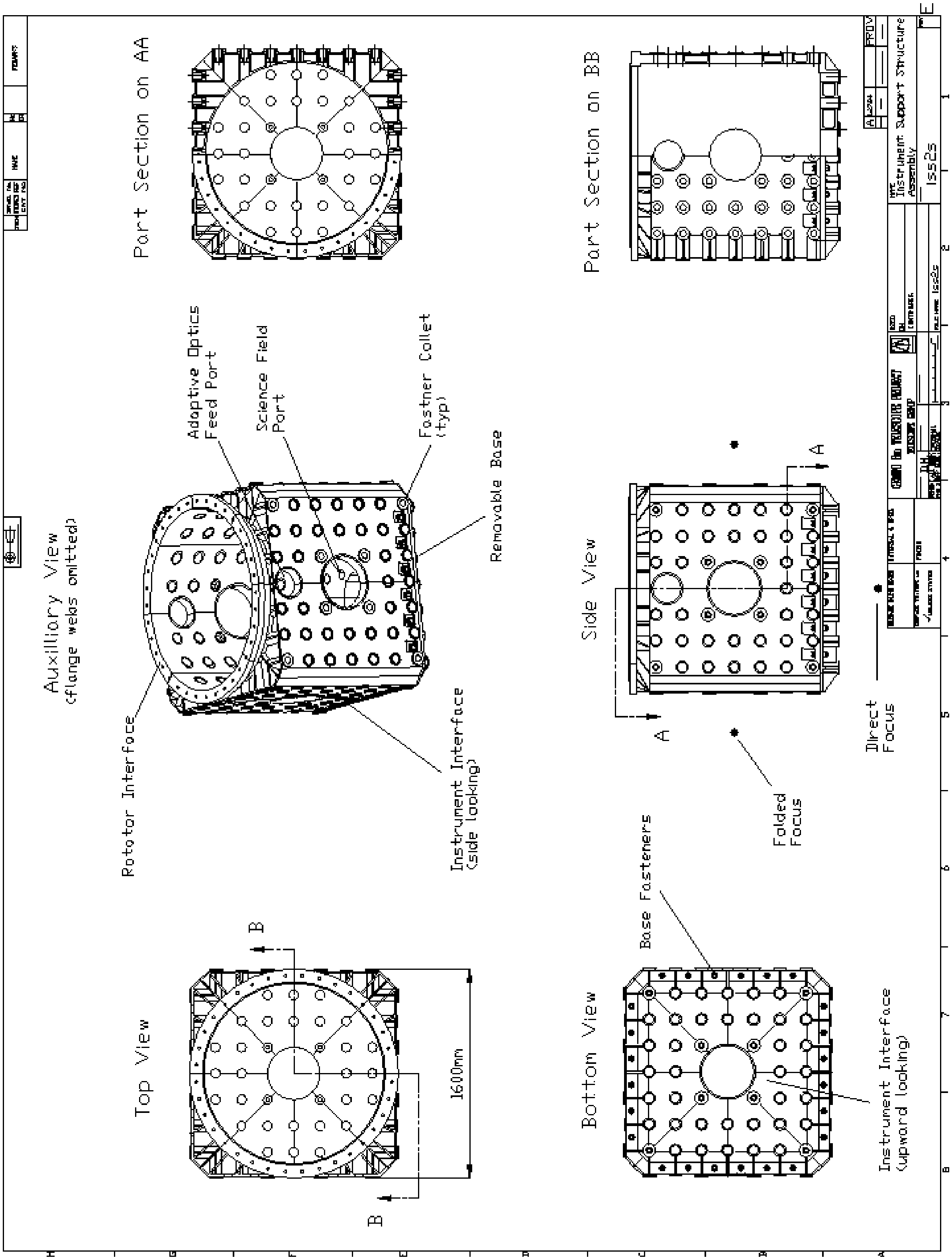

Figure 34. Port Light Baffle Interface Detail

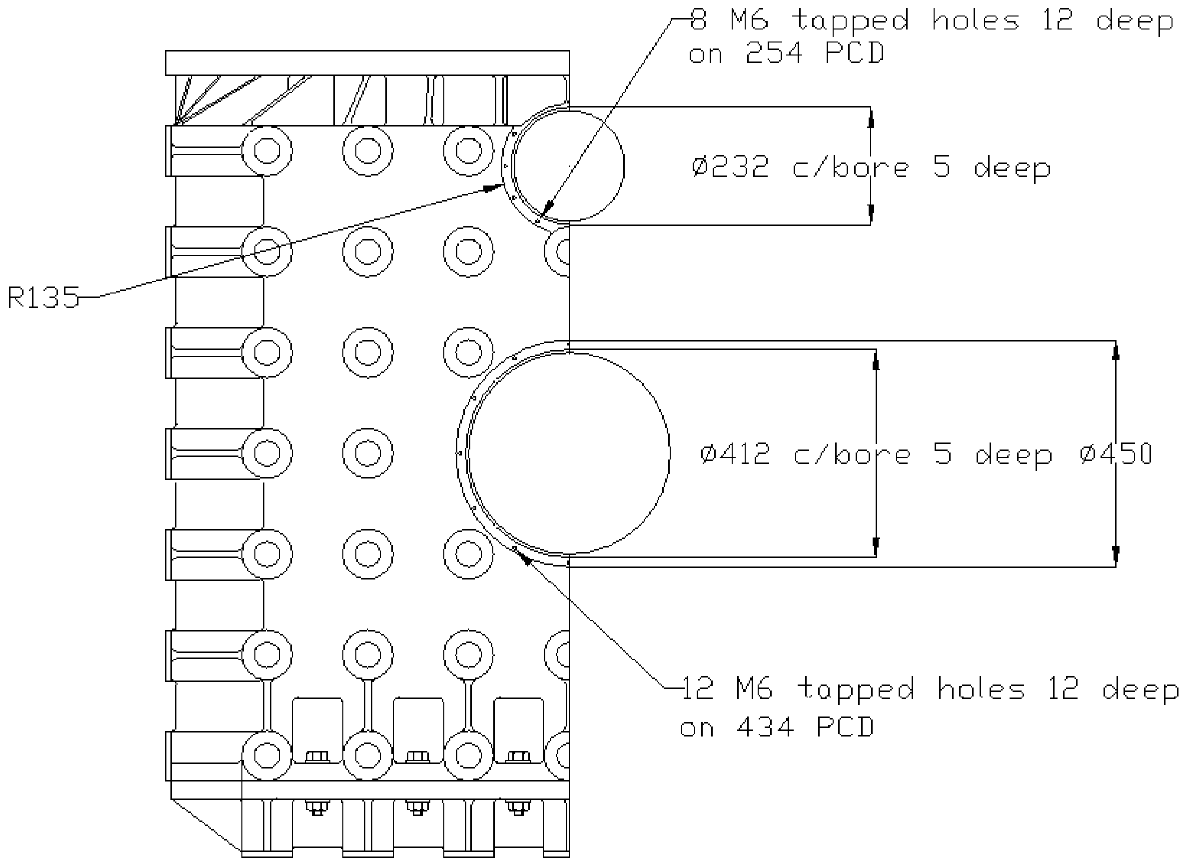

Figure 35. ISS FEA Model

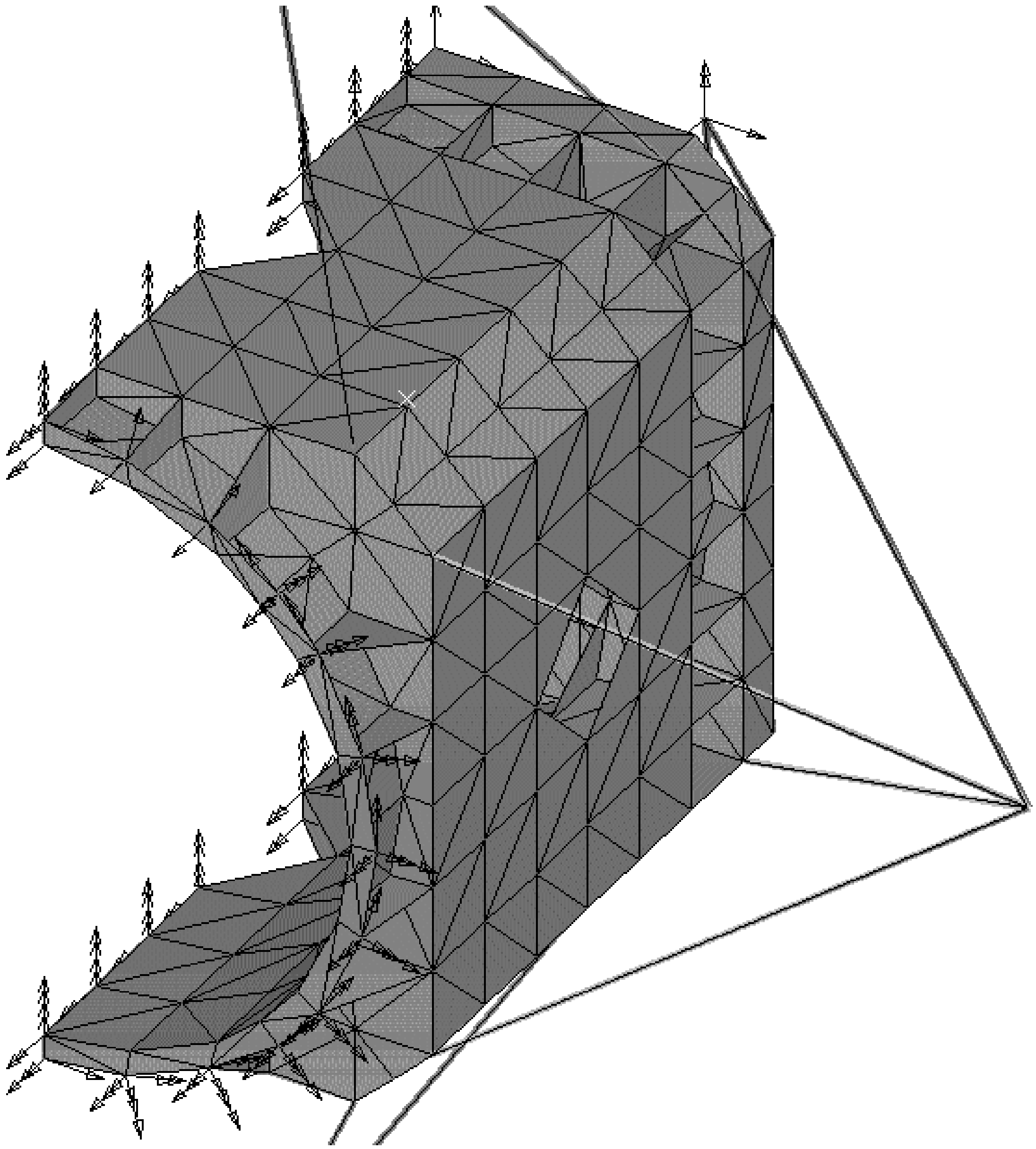

Figure 36. Deformation Plot for ISS Structure

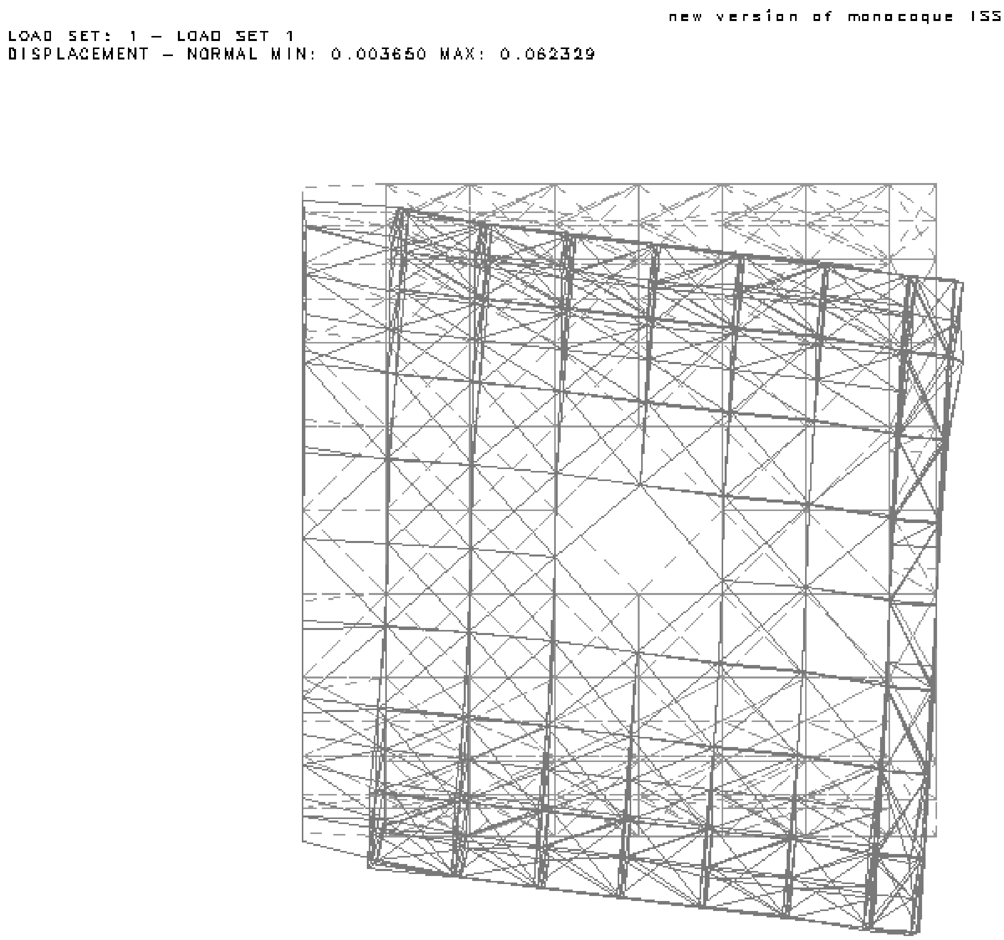

Figure 37. Optimization History of ISS for 50μm Flexure at Base

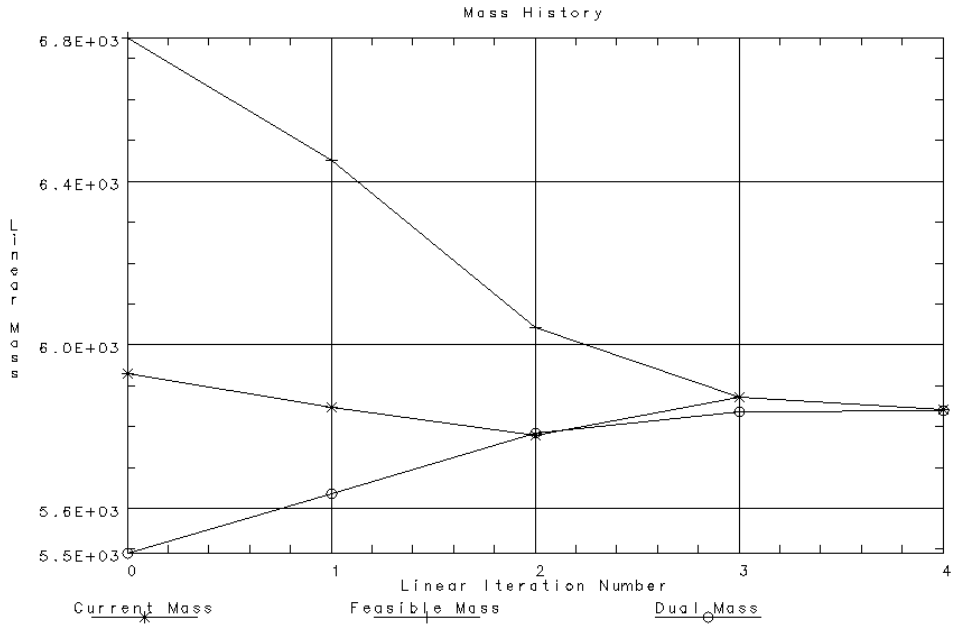

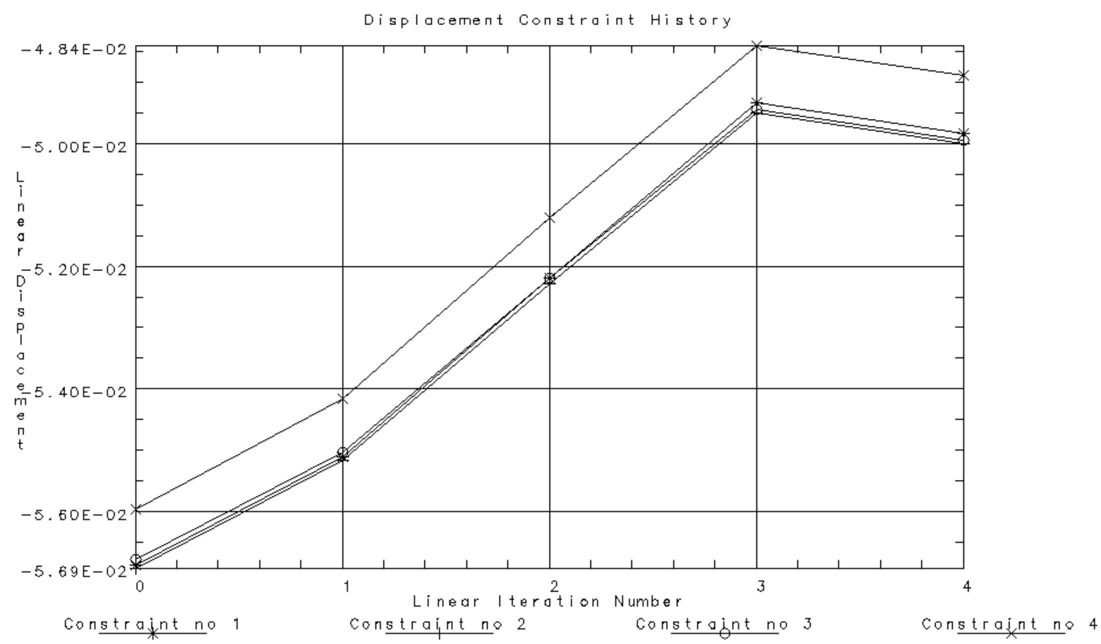

Note. The mass shown is for half of the ISS/Instrument Assembly (this is a half model).

Figure 38. Exploded View of Instrument Mounting Detail

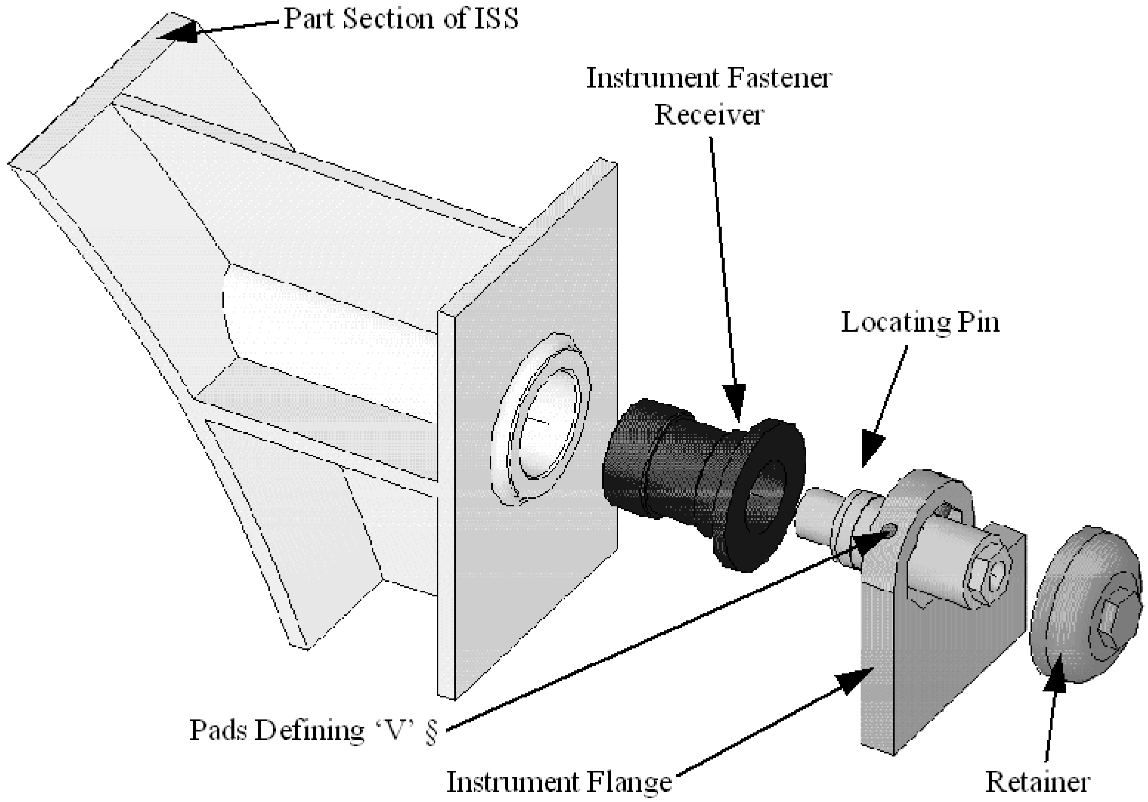

Figure 39. Instrument Fastener Detail - Sectioned View

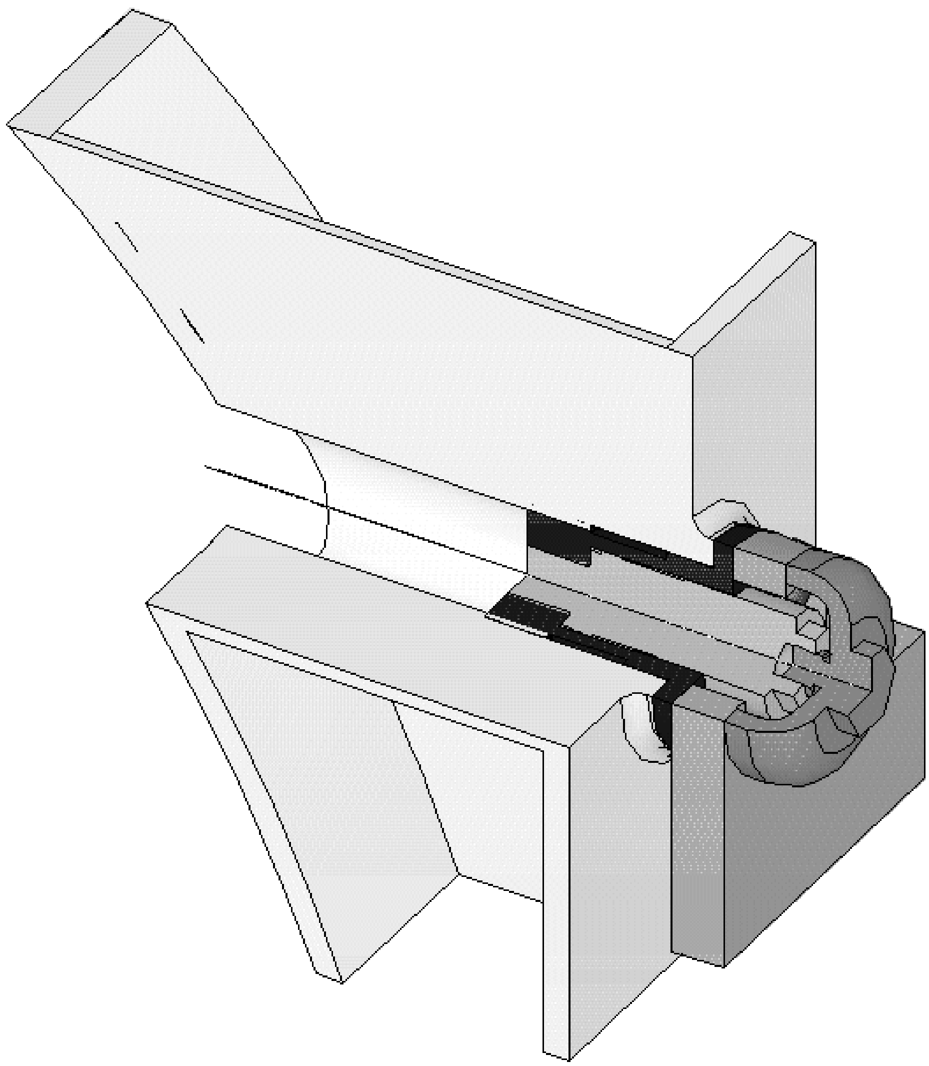

Figure 40. Science Field Fold Mirror Module Layout

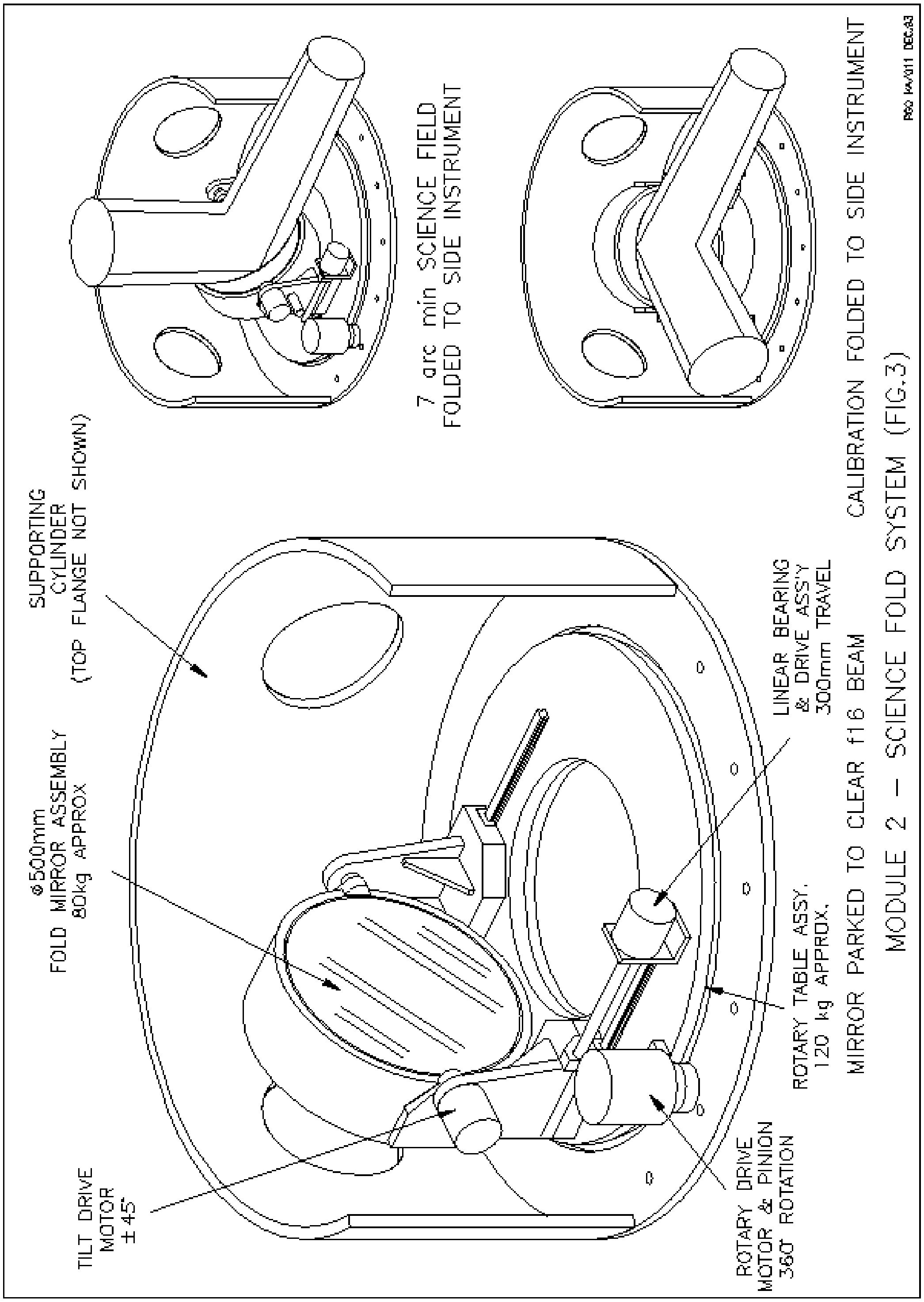

Figure 41. A&G Module Assembly - Exploded View

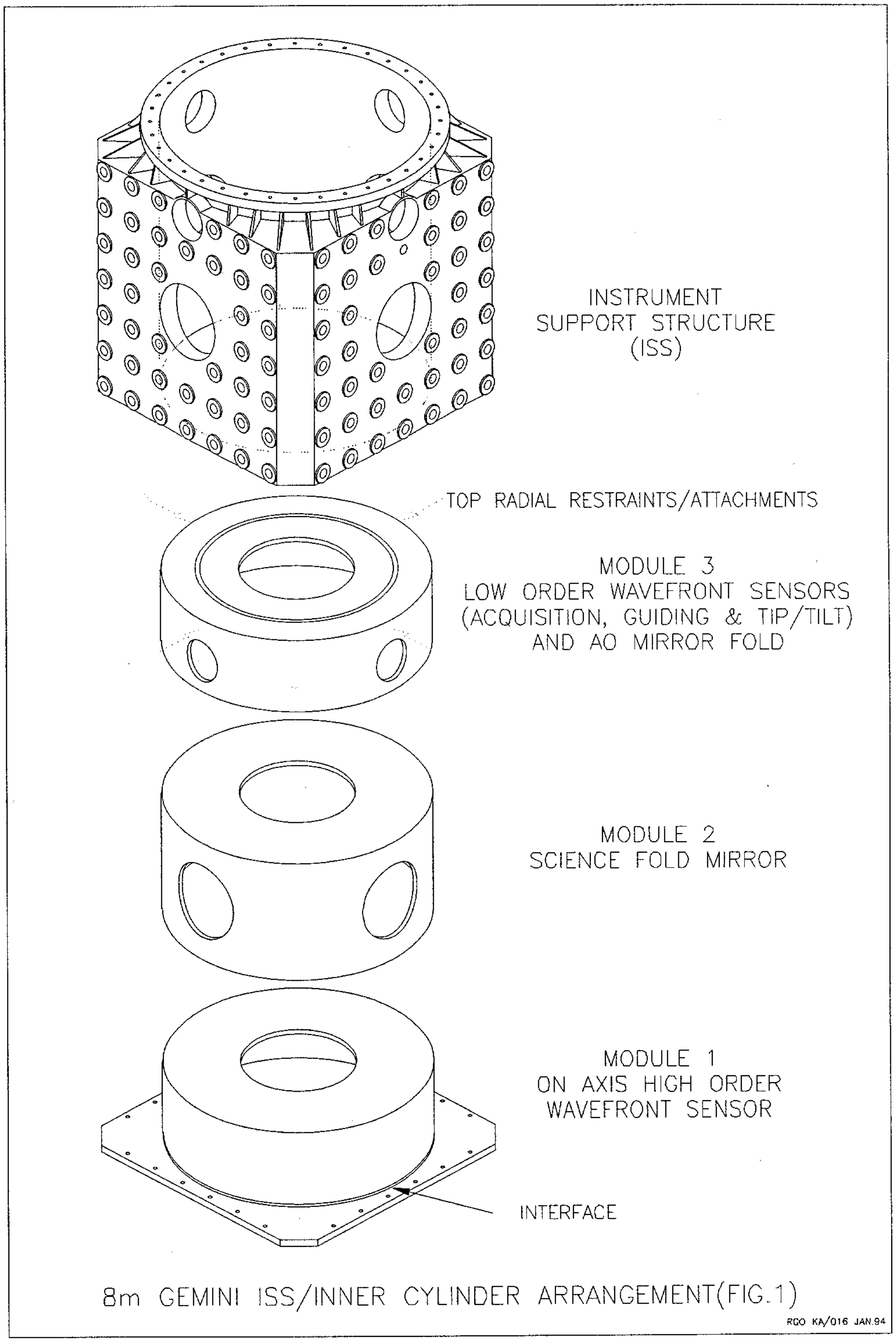

Figure 42. High Resoltion Wavefront Sensor Module Layout

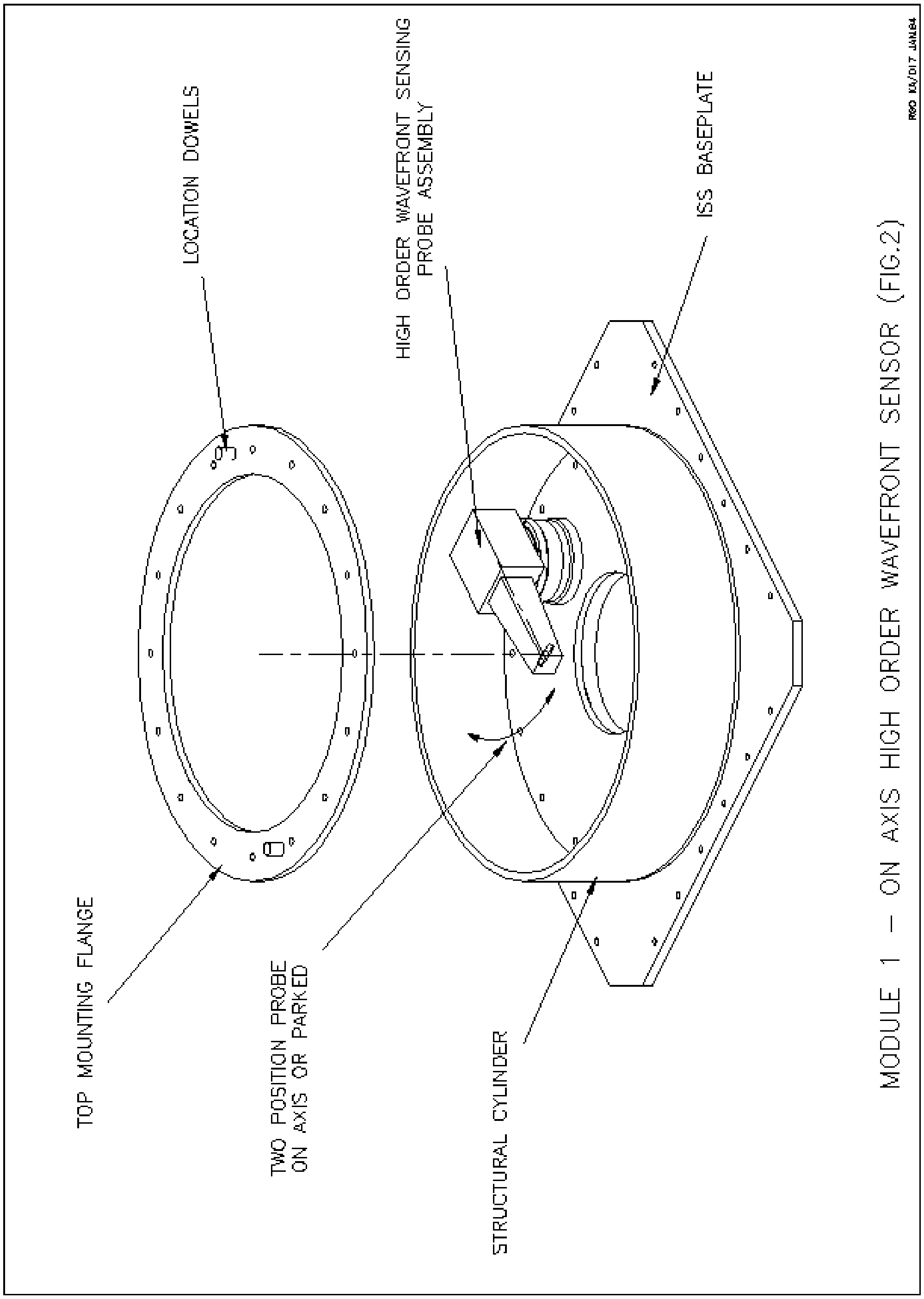

Figure 43. Peripheral Guider/Low Resolution Wavefront Sensor Module Layout

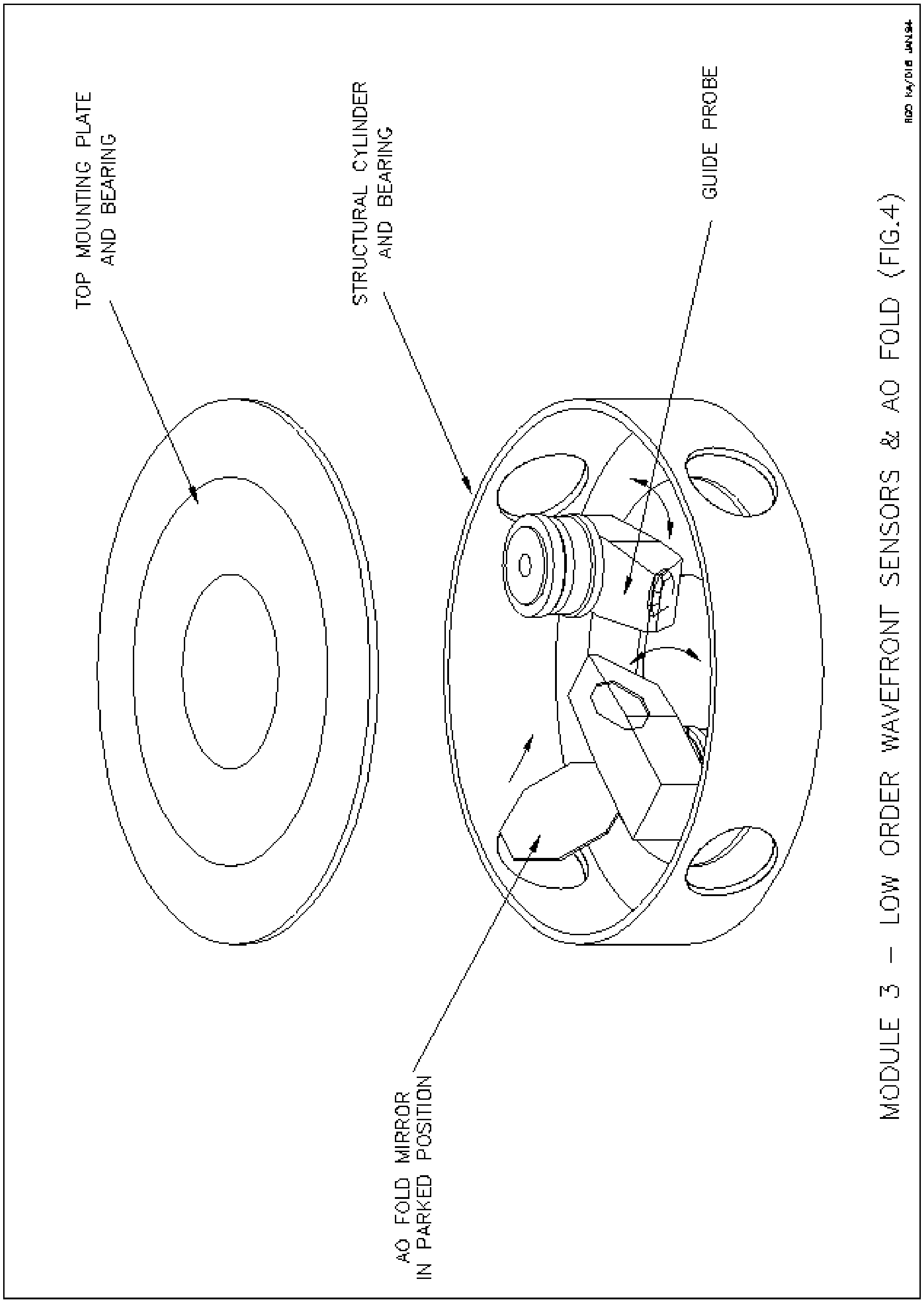

Figure 44. Peripheral Guider/Low Resolution Wavefront Sensor Layout

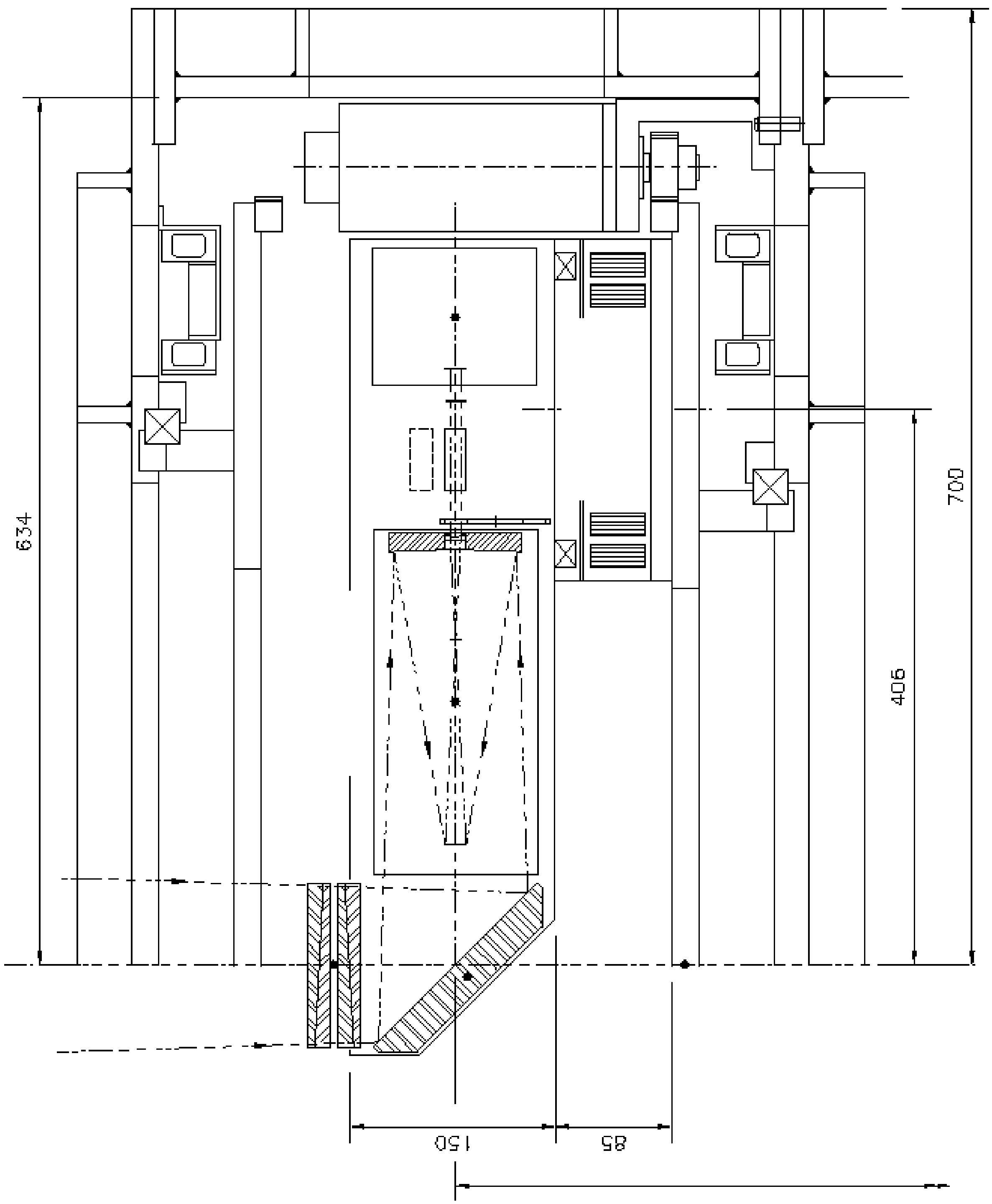

Figure 45. ISS/A&G Assembly Optical Path Schematic

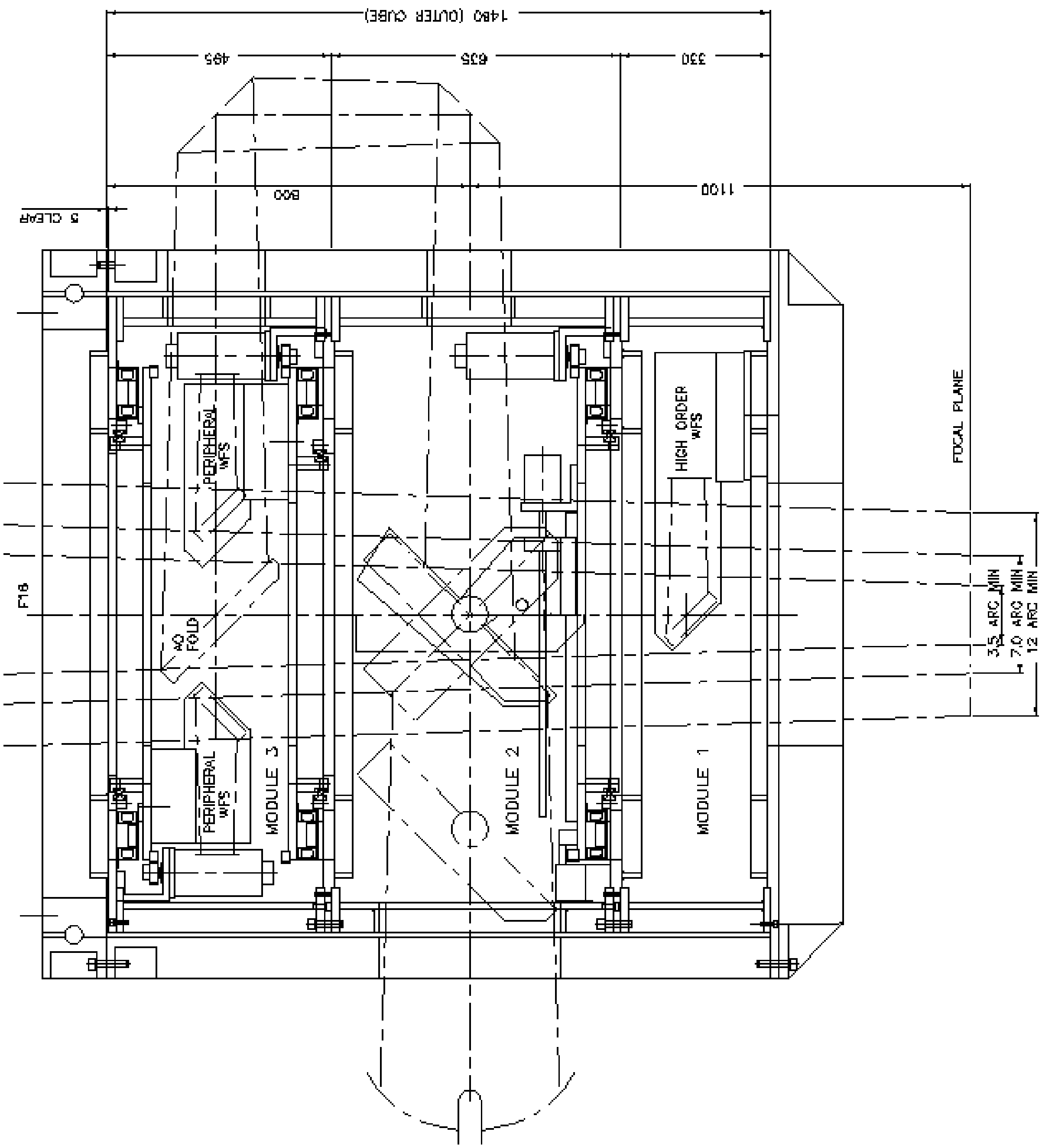

Figure 46. Sketch of Adaptive Optics Unit

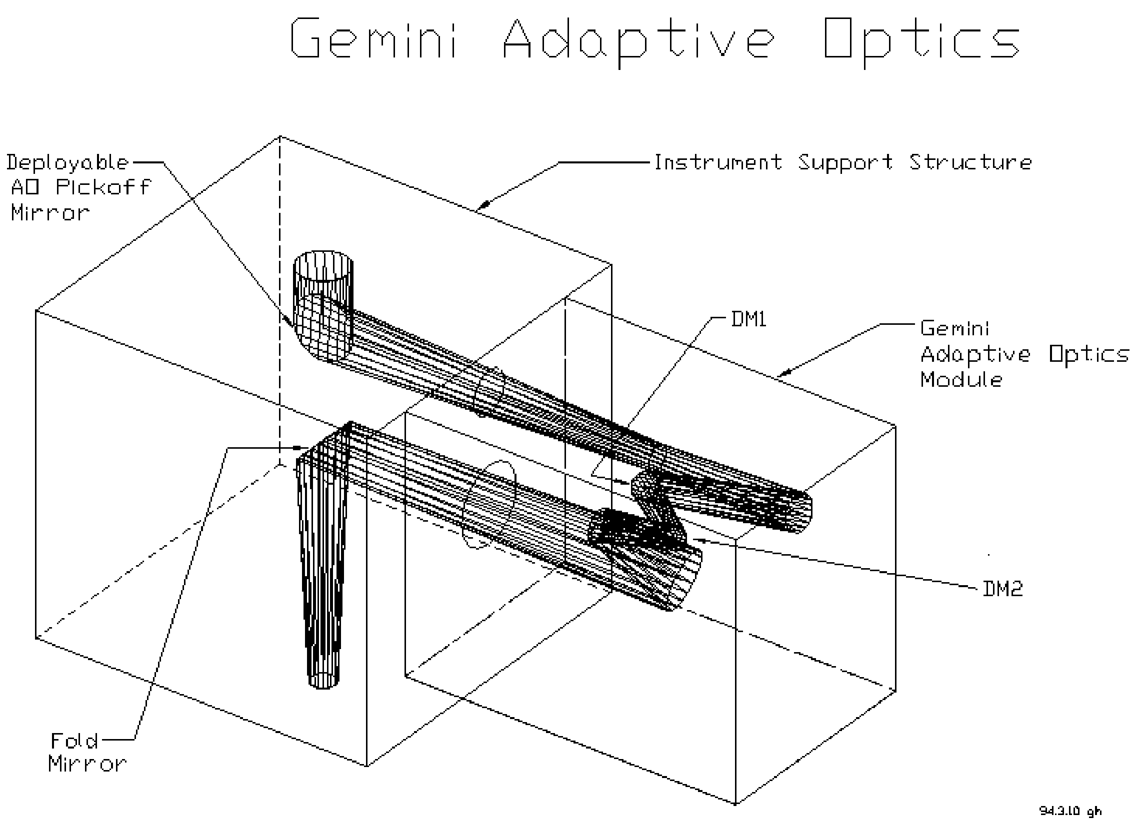

Figure 47. Interface Control Drawing for Cassegrain Area/Telescope

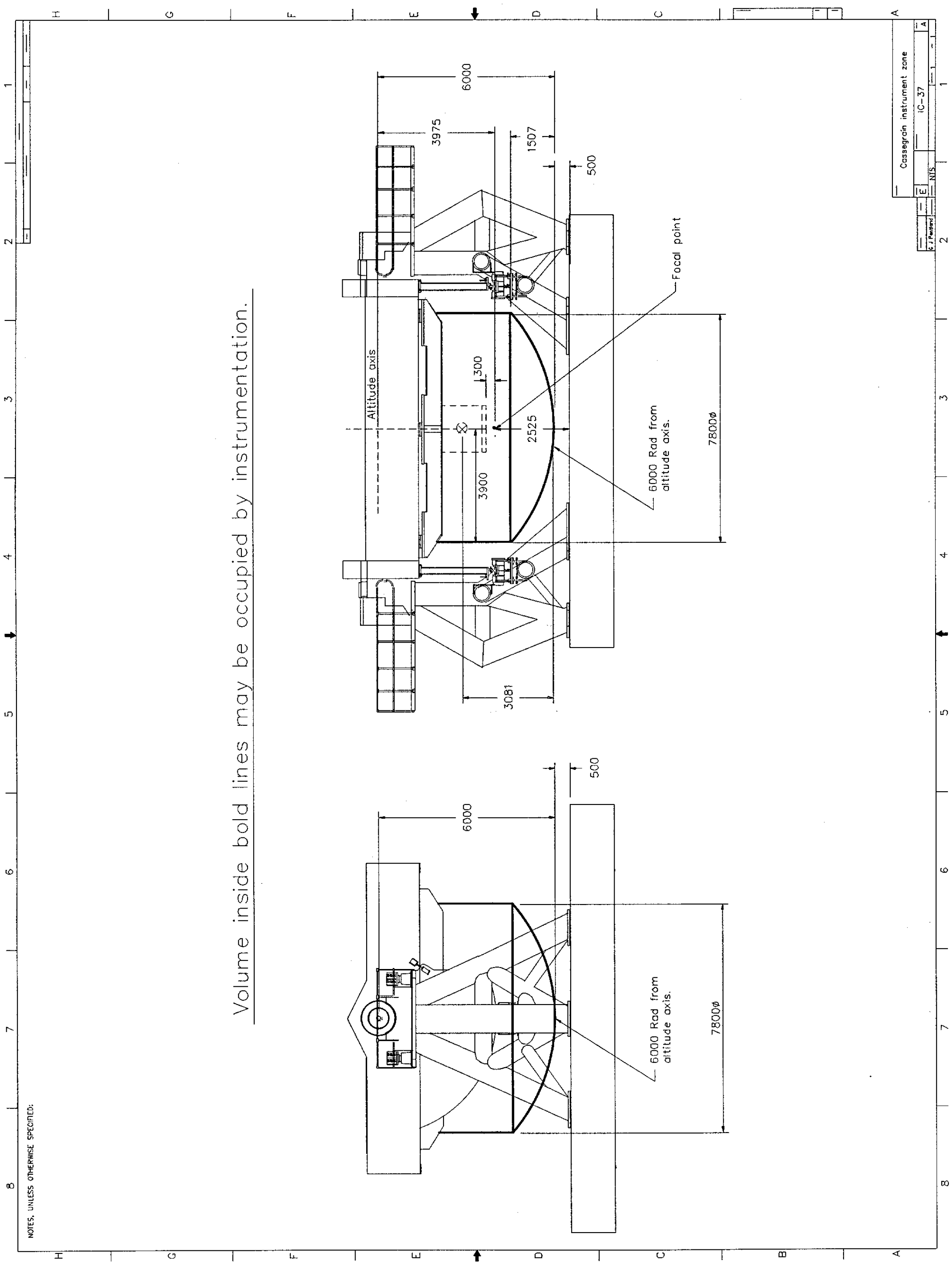

Figure 48. Mauna Kea Facility Floor Plan